USING DECLINE MAP ANALYSIS (DMA) TO TEST WELL COMPLETION INFLUENCE ON GAS PRODUCTION DECLINE CURVES IN BARNETT SHALE (DENTON, WISE, AND TARRANT COUNTIES)

A Thesis

by

IBRAHIM S. ALKASSIM

Submitted to the Office of Graduate Studies of
Texas A&M University
in partial fulfillment of the requirements for the degree of

MASTER OF SCIENCE

August 2009

Major Subject: Petroleum Engineering

USING DECLINE MAP ANALYSIS (DMA) TO TEST WELL COMPLETION INFLUENCE ON GAS PRODUCTION DECLINE CURVES IN BARNETT SHALE (DENTON, WISE, AND TARRANT COUNTIES)

A Thesis

by

IBRAHIM S. ALKASSIM

Submitted to the Office of Graduate Studies of
Texas A&M University
in partial fulfillment of the requirements for the degree of

MASTER OF SCIENCE

Approved by:

Chair of Committee,	David S. Schechter
Committee Members,	Walter Ayers
	Wayne Ahr
Head of Department,	Stephen A. Holditch

August 2009

Major Subject: Petroleum Engineering

ABSTRACT

Using Decline Map Analysis (DMA) to Test Well Completion Influence on Gas Production Decline Curves in Barnett Shale (Denton, Wise, and Tarrant Counties).

(August 2009)

Ibrahim S. Alkassim, B.S., University of New Orleans

Chair of Advisory Committee: Dr. David S. Schechter

The increasing interest and focus on unconventional reservoirs is a result of the industry's direction toward exploring alternative energy sources. It is due to the fact that conventional reservoirs are being depleted at a fast pace. Shale gas reservoirs are a very favorable type of energy sources due to their low cost and long-lasting gas supply. In general, according to Ausubel (1996), natural gas serves as a transition stage to move from the current oil-based energy sources to future more stable and environment-friendly ones.

By looking through production history in the U.S Historical Production Database, HPDI (2009), we learn that the Barnett Shale reservoir in Newark East Field has been producing since the early 90's and contributing a fraction of the U.S daily gas production. Zhao et al. (2007) estimated the Barnett Shale to be producing 1.97 Bcf/day of gas in 2007. It is considered the most productive unconventional gas shale reservoir in Texas. By 2004 and in terms of annual gas production volume, Pollastro (2007) considered the Barnett Shale as the second largest unconventional gas reservoir in the United States.

Many studies have been conducted to understand better the production controls in Barnett Shale. However, this giant shale gas reservoir is still ambiguous. Some parts of this puzzle are still missing. It is not fully clear what makes the Barnett well produce high or low amounts of gas. Barnett operating companies are still trying to answer these questions. This study adds to the Barnett chain of studies. It tests the effects of the following on Barnett gas production in the core area (Denton, Wise, and Tarrant counties):

- Barnett gross thickness, including the Forestburg formation that divides Barnett Shale.
- Perforation footage.
- Perforated zones of Barnett Shale.

Instead of testing these parameters on each well production decline curve individually, this study uses a new technique to simplify this process. Decline Map Analysis (DMA) is introduced to measure the effects of these parameters on all production decline curves at the same time.

Through this study, Barnett gross thickness and perforation footage are found not to have any definite effects on Barnett gas production. However, zone 3 (Top of Lower Barnett) and zone 1 (Bottom of Lower Barnett) are found to contribute to cumulative production. Zone 2 (Middle of Lower Barnett) and zone 4 (Upper Barnett), on the other hand, did not show any correlation or influence on production through their thicknesses.

DEDICATION

This work is dedicated to:

my parents who have inspired me with all the strength I needed throughout my life;

my lovely future wife who has been supportive and patient with me living far away from her… I love you Mashael; and

all my brothers, sisters, and extended family members who have been there for me.

ACKNOWLEDGEMENTS

Praise and gratitude be to the Almighty, Allah, the Creator and Governor of the Universe and his Prophet Mohammed, peace be upon him.

I would like to thank my family for all the support I have been given during my study at Texas A&M. Also, I would like to thank my future wife, Mashael, who has been there all the time for me even though she is far away from me.

Also, I would like to show my sincere appreciation to Saudi Aramco for giving me the chance to pursue my graduate degree in the United States. I am looking forward to going back and paying my dues through hard work.

I would like also to thank my advisor, chairman of the advisory committee, Dr. David S. Schechter. This work would have not been completed without his support and cooperation.

Sincere thanks are extended to:

- Dr. Walter Ayers, for all his thoughts and comments added to this work.
- Dr. Wayne Ahr.
- Dr. Mike Tice.

Last but not least, I thank all my friends and colleagues here in College Station for their support.

TABLE OF CONTENTS

Page

LIST OF FIGURES

FIGURE Page

FIGURE Page

FIGURE Page

CHAPTER I

INTRODUCTION

The Barnett Shale was named after John W. Barnett. During the late 19th century, Mr. Barnett settled in San Saba County, and named a main stream as "The Barnett Stream." In the early 20th century, in a geological mapping of the area, thick black organic-rich shale was found outcropping near the stream. This organic-rich shale formation was named the Barnett Shale (Barnett Shale History, 2009).

Studies show that the Mississippian Barnett Shale formation is the oil-and-gas primary source feeding reservoirs of Paleozoic age in the Bend arch – Fort Worth basin (Hill et al. 2007). These studies were based on correlating oil that was produced from Paleozoic age reservoirs to oil that was produced from the Barnett Shale. This correlation indicates that the Barnett Shale is the primary source of mainly all oil and gas in the basin (Jarvie et al. 2001).

It has been always a question in the gas industry, and yet still not fully solved: what makes many Barnett gas wells produce high? And many others produce low? Finding the answers to these questions would help in optimally planning future wells and developing the field. This study establishes a new method to test the effect of any parameter on production decline curves. Decline Map Analysis (DMA) makes it easy and simple to test the influence of any parameter on all production decline curves, all at once.

_____

This thesis follows the style of *SPE Journal*.

DMA substitutes for testing parameters on each production decline curve individually. In this study, three parameters are tested using this technique to find their effects on Barnett Shale gas production: Barnett gross thickness, total perforation footage, and individual perforated Barnett zones.

Before further discussing work done through this study, the following sections provide general overview on Barnett Shale.

1.1 General Stratigraphy

In the Fort Worth Basin, the sedimentary section has a maximum thickness of around 12,000 ft, in the eastern part. Around 4,000-5,000 ft of this total section consists of Ordovician to Mississippian carbonates and shales. The remaining section consists of Pennsylvanian clastics and carbonates, and a thin Cretaceous layer to the eastern part (Lahti and Huber, 1982).

The basement lies beneath this thick sedimentary section. This Precambrian igneous basement is composed of granite and diorite. Overlying this Precambrian basement is the Cambrian section, which is dominated by carbonate deposition (Pollastro et al. 2007).

During the Early Ordovician, all of Texas was mainly covered by a carbonate platform, known now as the Ellenburger Group carbonate rocks. **Fig. 1.1** shows the top of the Ellenburger Group on a structure contour map. Later on, a significant drop in sea level caused this carbonate platform to be exposed and, consequently, karst features were formed (Montgomery et al. 2005). The erosion process did not stop at this point. A major

erosional incident eroded and removed all Silurian and Devonian formations (Simpson Group and Viola Limestone) presented in this region (Loucks and Ruppel, 2007).

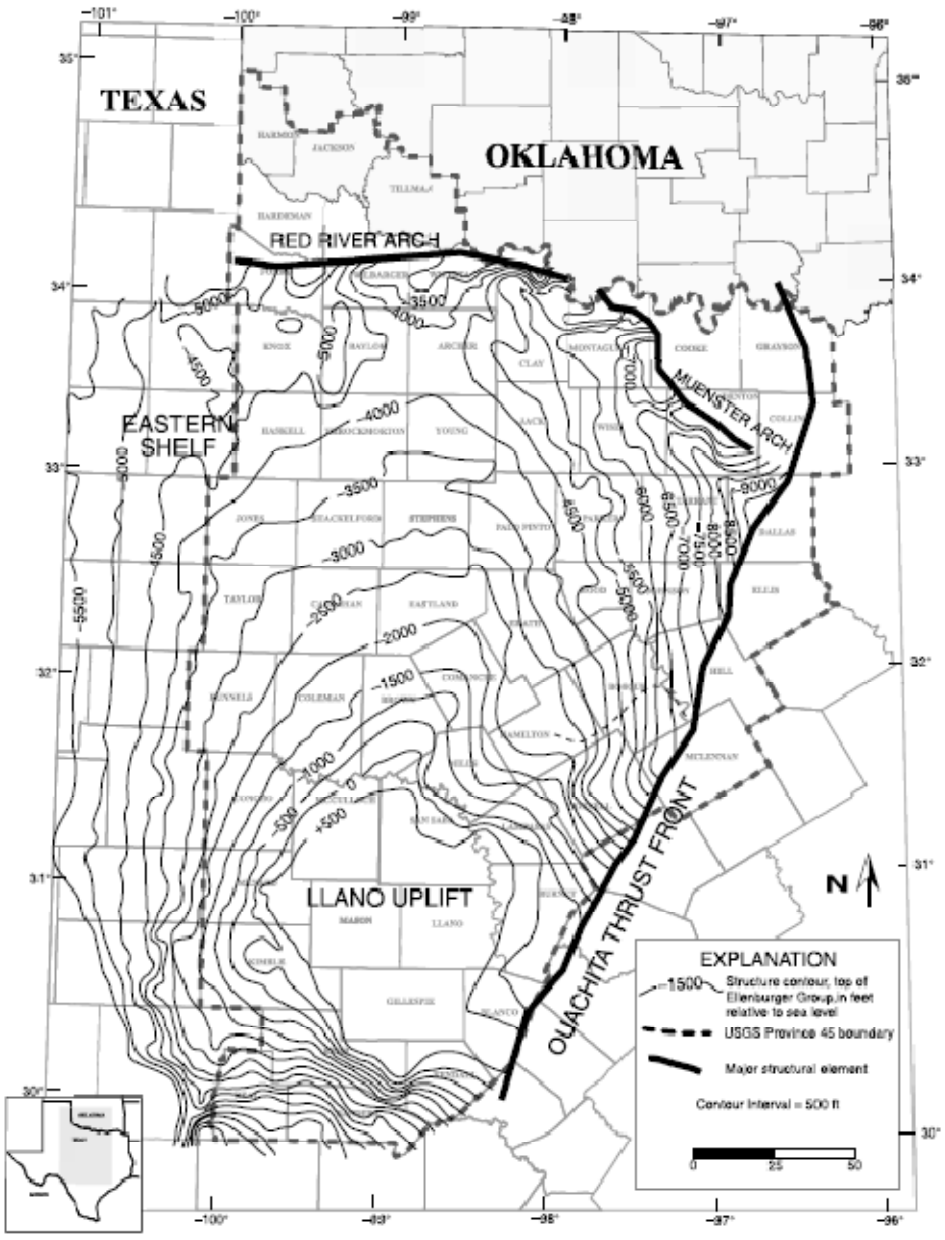

Fig. 1.1: Ellenburger Group top structure map (Pollastro et al. 2007).

The resulting unconformity served as the basement of the Barnett Shale formation. The Barnett Shale was deposited over a large portion of the Fort Worth Basin, which formed due to the collision between North and South American plates (Flippin, 1982; Henry, 1982). To the northwest of the Newark East field, particularly in the Chappel shelf area, Chappel limestone was deposited over the unconformity and the Ellenburger Group. Therefore, by moving toward this direction, northwest, the upper part of the lower Barnett Shale thins out as it drapes over the Chappel limestone, forming a seal for the Chappel limestone reservoirs. The Mississippian rocks are characterized by alternating shallow marine limestones, and black, organic-rich shales, with a lack of distinctive fossils (Pollastro et al. 2007). **Fig. 1.2** shows these formations on a stratigraphic section.

By moving up the stratigraphic section (Fig. 1.2), the Pennsylvanian (Morrowan stage) Marble Falls limestone was deposited over the Barnett Shale formation. This zone is divided into two parts: Upper Marble Falls (limestone zone) and Lower Marble Falls (interbedded dark limestone and black shale). The latter is sometimes known as the Comyn Formation. Although it is used in many cases as a marker bed, the lower shale of the lower Marble Falls is sometimes mistaken on well logs with the Barnett Shale. It is known in the industry as the false Barnett (Pollastro et al. 2007).

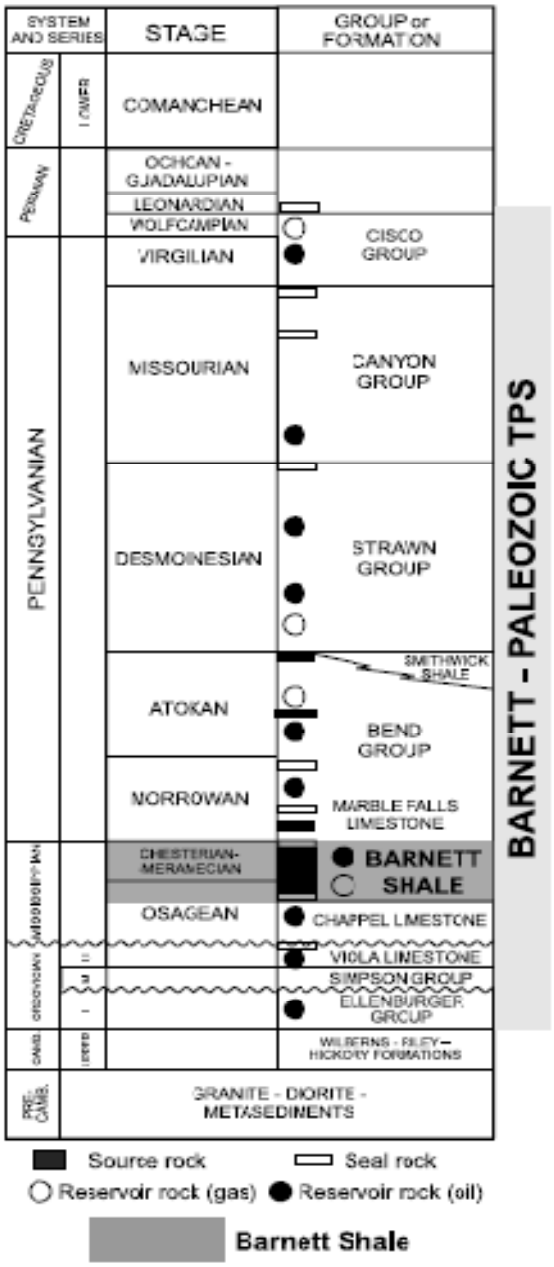

Fig. 1.2: Stratigraphic section of the Fort Worth Basin (Pollastro, 2007).

Permian rocks come next in the column, covering the Pennsylvanian. They exist in some parts of the Fort Worth Basin. After deposition of the Triassic and Jurassic rocks, a major erosion process took place. This Pre-Cretaceous erosion had removed all the

Triassic and Jurassic rocks, in addition to some Paleozoic sections. Therefore, Triassic and Jurassic rocks have never been discovered, in fact, they may not exist at all. The Cretaceous rocks were deposited over the eroded section in the eastern part of the basin. These rocks are not hydrocarbon-productive. However, they hold major groundwater aquifers in the region (Pollastro et al. 2007).

To achieve the final picture of the stratigraphic column and formation lateral continuities, cross sections were constructed by Pollastro et al. (2007). The lines on the map **(Fig. 1.3)** represent the cross section profiles.

The cross section A-A' is shown in **Fig. 1.4.** Top of the Barnett Shale is set as the datum. The point of setting up a datum instead of using sea level is to demonstrate lateral stratigraphic continuities more clearly. As shown in Fig. 1.4, the whole section thins out moving southwest. In the northeastern part, the Forestburg Limestone exists, but then disappears midway through as moving southwest. The Marble Falls shale becomes very thin as well by moving southwest.

As could be seen on cross section B-B' **(Fig. 1.5),** the Marble Falls shale bed disappears by moving from southeast to northwest. Also, the Upper Mississippian Lime disappears in the opposite direction. In general, Barnett Shale is thick on the northeastern part of the basin, but then it starts to thin by moving in any other direction within the basin (Chaouche, 2006).

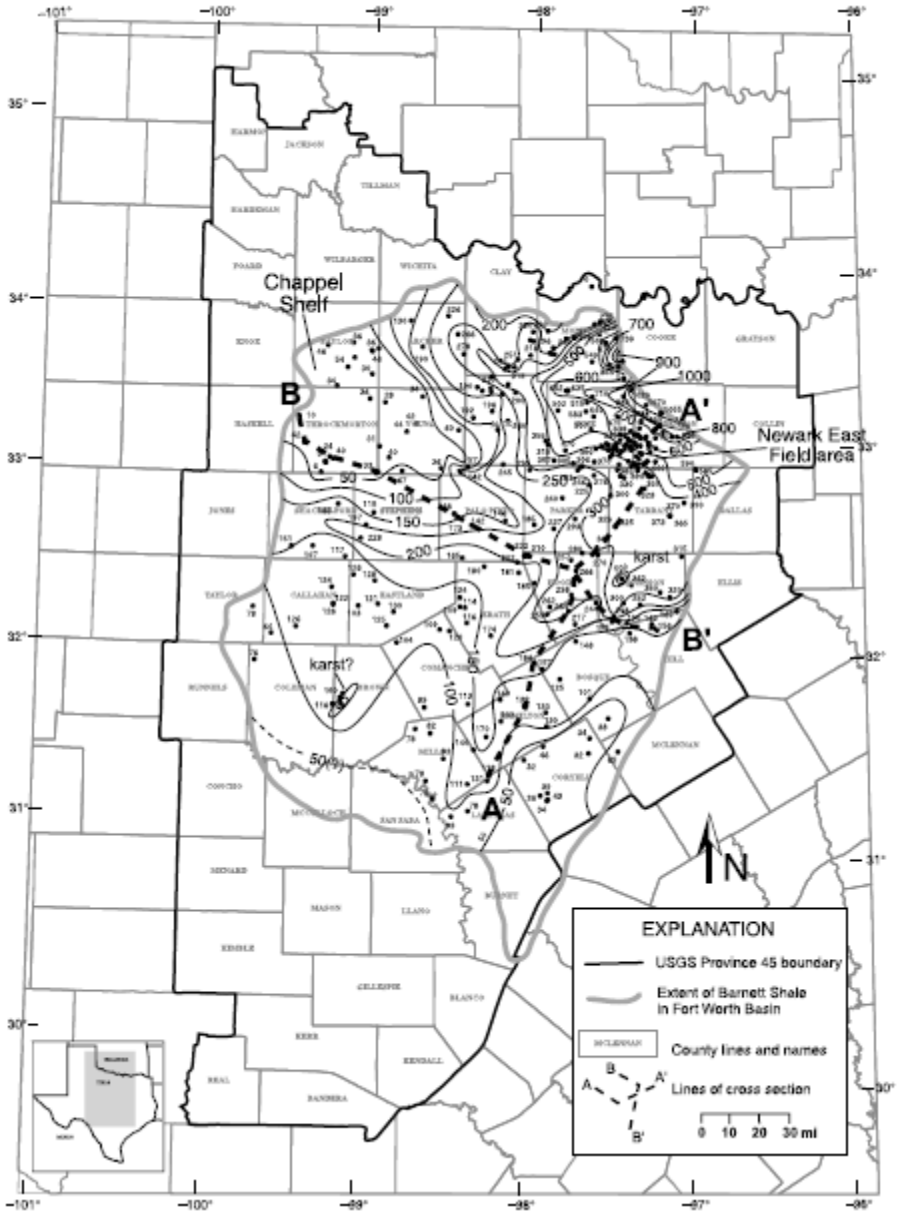

Fig. 1.3: Fort Worth Basin map. A-A' and B-B' are cross section profiles created by Pollastro et al. (2007).

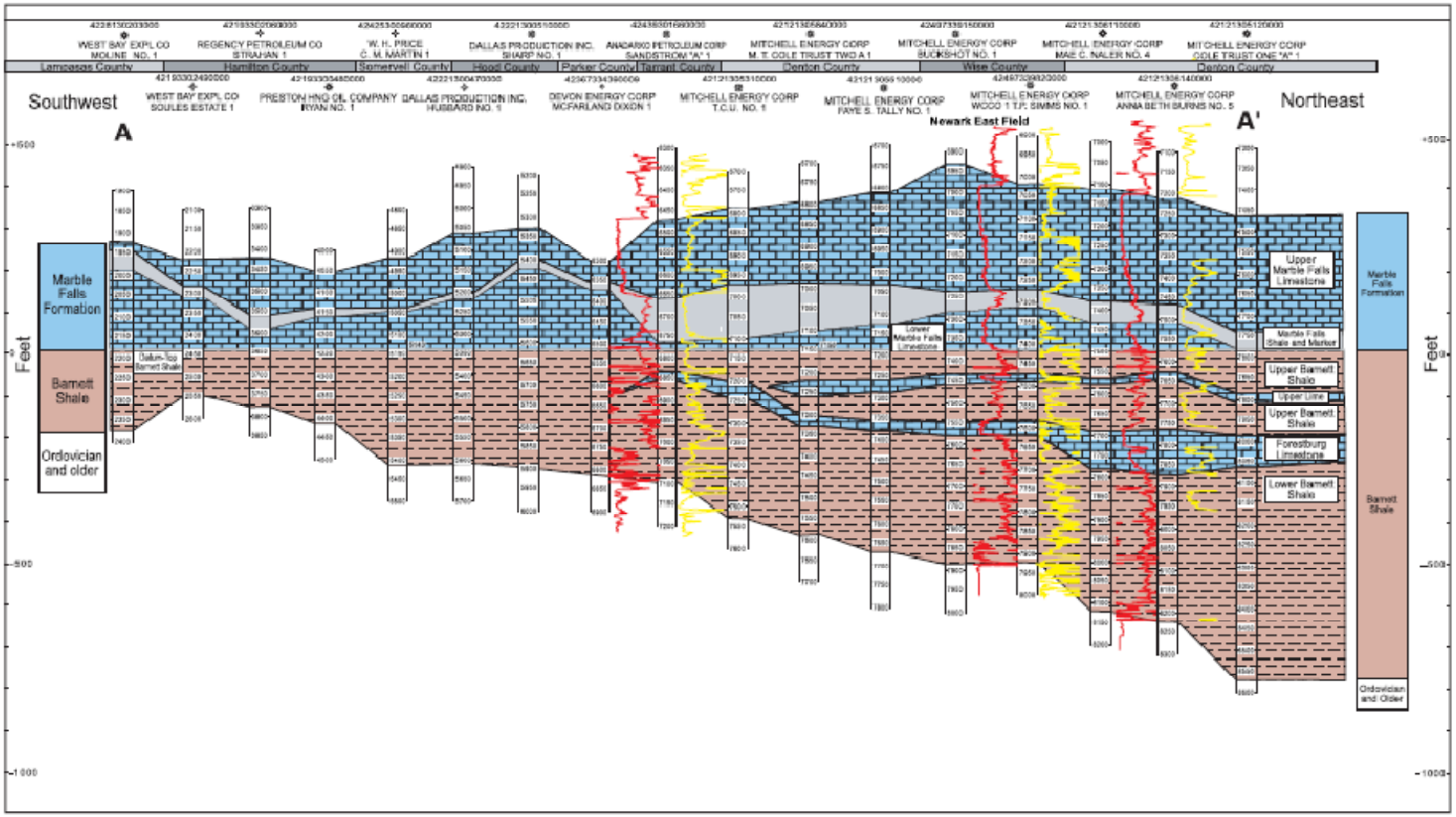

Fig. 1.4: A-A’ (SW-NE) cross section profile created by Pollastro et al. (2007) (Barnett Shale in pink, Marble Falls in blue).

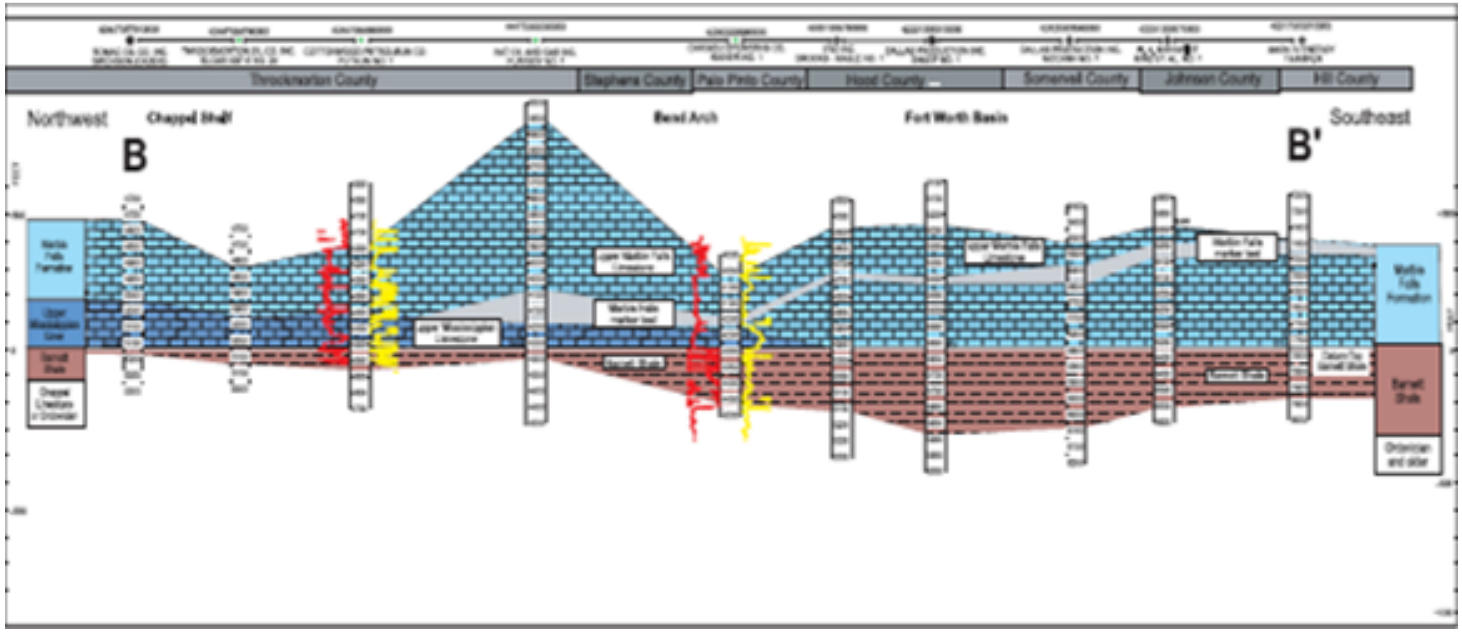

Fig. 1.5: B-B’ (NW-SE) cross section profile created by Pollastro et al. (2007).

1.2 Production History

The Bend arch – Fort Worth Basin is a mature petroleum region. Oil and gas exploration and production in this region has been there since the early 20th century. However, until the end of the 20th century, hydrocarbons were mainly produced from Ordovician-to-Permian conventional reservoirs (Bowker, 2003).

A giant unconventional gas accumulation has been explored. This huge accumulation existed in the Mississippian Barnett Shale formation. In year 2000, annual gas production from the Barnett Shale pushed the Newark East field up the ranking as the largest producing gas field in Texas (Rach, 2004).

Newark East field is considered among its kind as the largest shale gas field in the world in lateral extent (Zhao et al. 2007). Barnett Shale has a lateral estimated area of 6,000 mi² (15,500 km²). Its daily production rate is estimated to be 1.97 Bcf of gas and 6000 barrels of oil or condensate, with a cumulative production of 2.2 Tcf of gas and 7.5 MMbbl of oil or condensate (Zhao et al. 2007). U.S. Geological Survey (USGS) studies estimate 26 Tcf of undiscovered and technically recoverable gas in Barnett Shale formation within the Fort Worth Basin (Pollastro et al. 2007).

Fig. 1.6 shows yearly gas production rates of the major gas plays in the United States: Ohio, Antrim, New Albany, Barnett, and Lewis. As seen clearly, Barnett gas production had been notably increasing since early 90's. It reached a significant production rate in year 1999. Since then, Barnett Shale gas production has increased dramatically **(Fig. 1.7).** This figure was generated using HPDI software. Beginning in Jan 1999, number of Barnett gas wells significantly increased resulting in a significant jump

in gas production. More and more wells have been drilled since then, increasing gas well count, and consequently, increasing Barnett gas production.

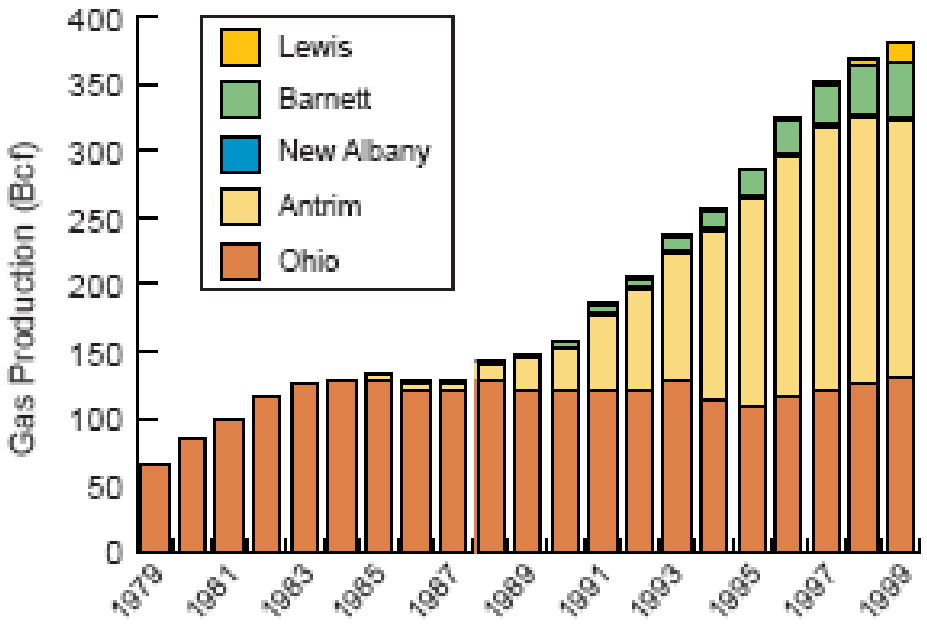

Fig. 1.6: Yearly gas production rates of the major gas plays in the United States (Hill and Nelson, 2000).

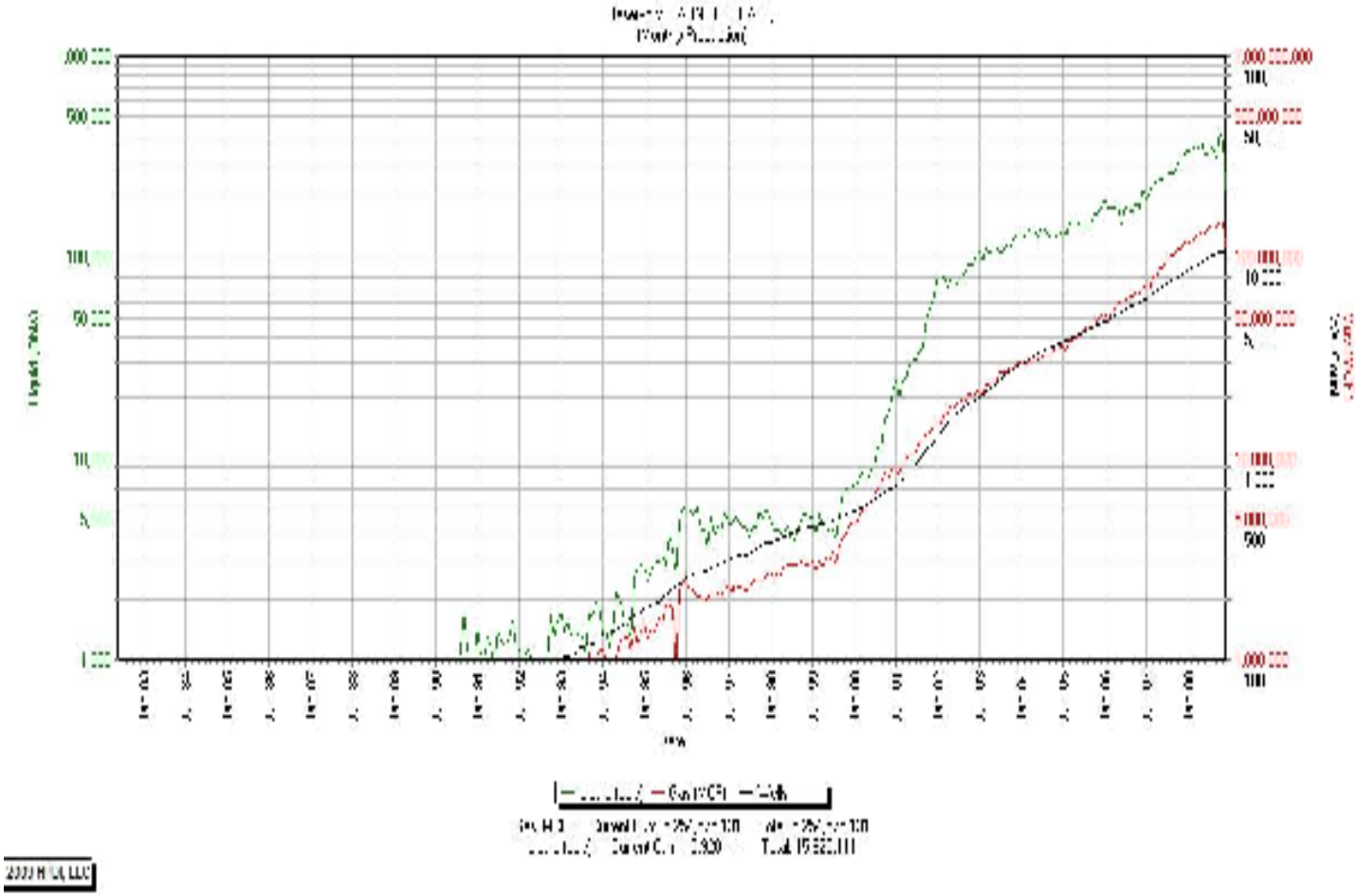

Fig. 1.7: Monthly Barnett gas (red line) and liquid (green line) production rates plot. Monthly Barnett well count (black line). This figure generated using HPDI software.

CHAPTER II

METHODS

2.1 Data Screening

A database file was provided by IHS Energy Inc. This database included a wide data spectrum for 5119 Newark East Field wells. This database spectrum involved, but not only: location coordinates, targeted formation (reservoir), formation tops, and hole direction (vertical, horizontal, or deviated). This file was used along with Scout Tickets that were provided by IHS Energy Inc. too.

These 5119 wells were filtered to a smaller field-representative number. The following criteria were used to carry out the filtration process:

- All wells must be vertical gas wells. (since horizontal gas wells surveys were not available)
- All wells must be targeting Barnett Shale reservoir. (to limit the study to Barnett Shale only)
- All wells must include Barnett Shale top and bottom depths. (to create Barnett Shale gross thickness map)

560 wells were filtered out of this process. So, an Area of Interest (AOI) was automatically created, enclosing these 560 vertical wells in the core area (Denton, Wise, and Tarrant counties) **(Fig. 2.1).**

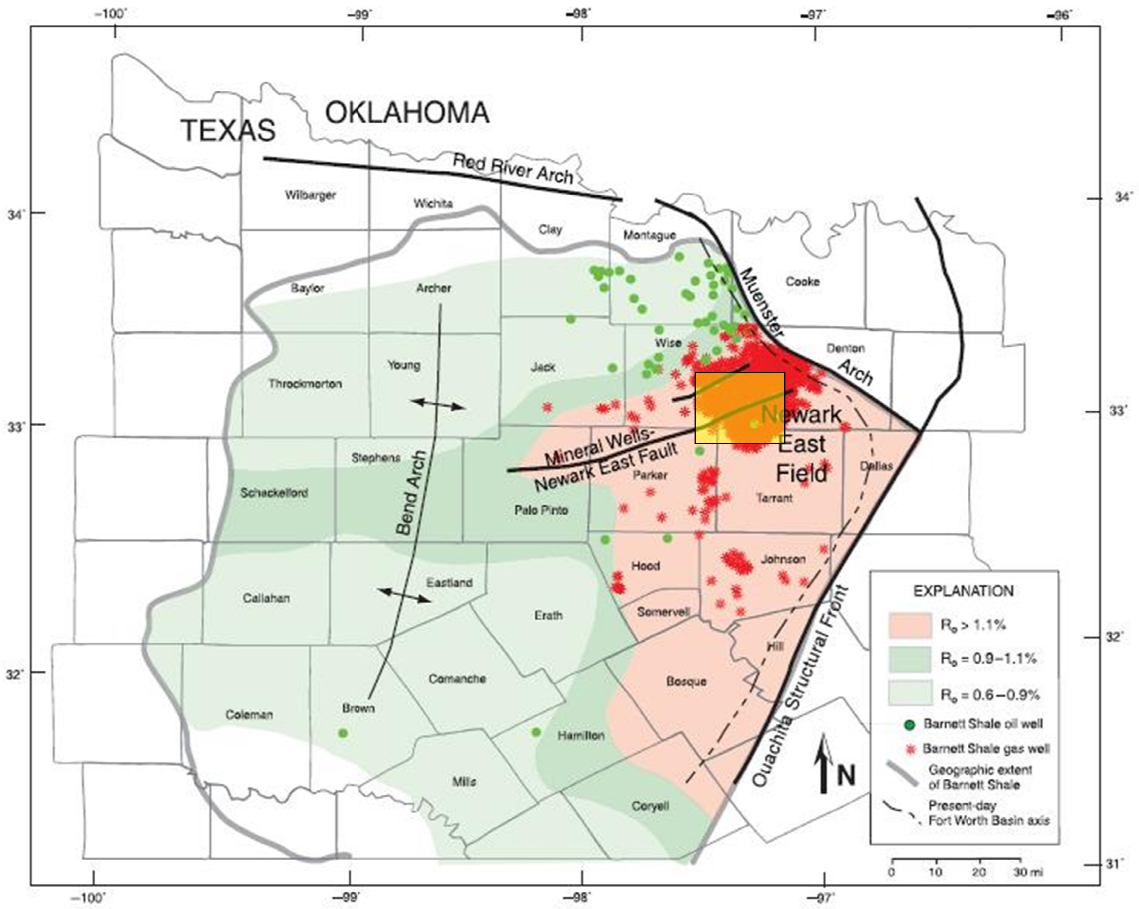

Fig. 2.1: Fort Worth Basin map with the study AOI highlighted (Map from Deshpande, 2007).

These wells were then imported into mapping software (Geographix). Using Barnett Shale top and bottom True Vertical Depths (TVD), Barnett Shale gross thickness map was generated and contoured **(Fig. 2.2),** which represents the highlighted rectangle in Fig. 2.1. As shown in Fig. 2.2, Barnett Shale formation mainly thickens in the NE direction, matching the topography mentioned in literature in the introduction of this thesis. This thickness map includes the Forestburg formation dividing the upper and lower Barnett. Its top and bottom depths were not available in the database, so it was impossible to remove its effect from the map.

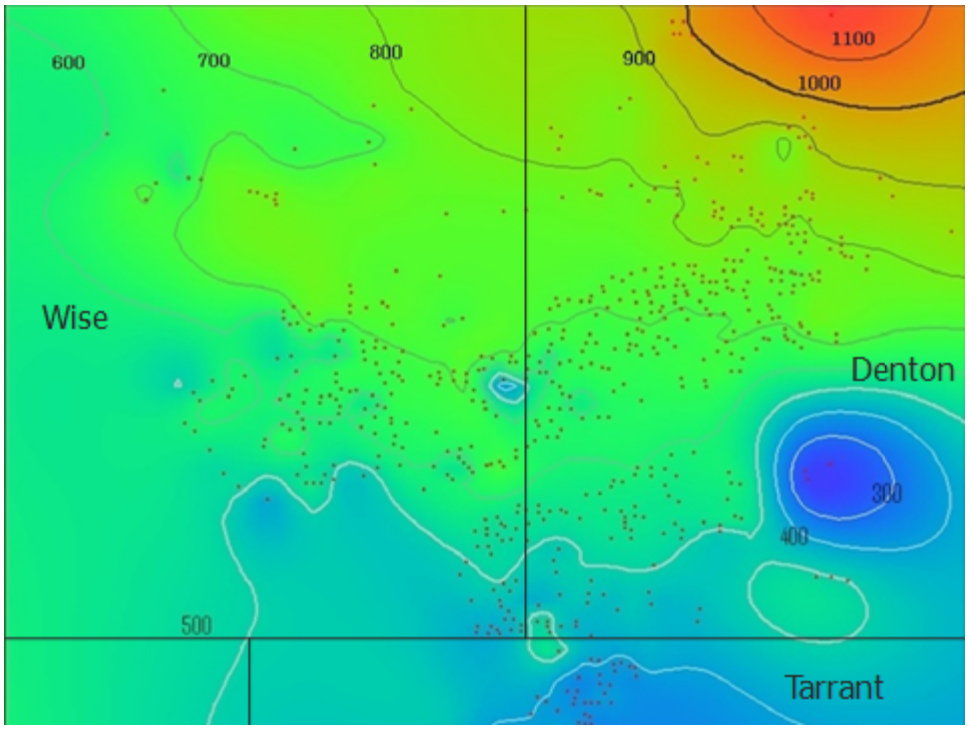

Fig. 2.2: Barnett gross thickness map (Isochore map) of current AOI.

As mentioned earlier, vertical wells were filtered out to easily generate Barnett Shale thickness (Isochore) map since horizontal wells surveys were not available. Then, horizontal wells were added to the AOI highlighted in Fig. 2.1. All Barnett Shale horizontal wells enclosed in this AOI were added, increasing the total number of wells from 560 to 781. These 781 Barnett Shale gas wells complete the final well list carried out through the remainder of this study.

2.2 Production Forecast

In any production forecast process, historical production data is an essential element to complete the process. In this study, historical production data was obtained

from U.S Historical Production Database (HPDI). Each well API number was imported into the HPDI software. To have a general idea of their production history, **Fig. 2.3** represents a historical production plot of these wells, along with a trendline demonstrating the increase in number of wells through time.

Each well historical production data was extracted from HPDI. This data then was copied into an Excel sheet exclusively built for production forecast purposes. This sheet used Arp's equations to forecast data. Arp's equations are favored over other models for their simplicity; they do not require any well or reservoir parameters (Mohaghegh et al., 2005). These equations are as follows (Lee and Wattenberger, 1996):

- Exponential Decline:

$$b = 0 \rightarrow Q_t = Q_i \times e^{\frac{-D_i}{12} \times t} \quad \ldots\ldots\ldots\ldots\ldots\ldots\ldots\ldots\ldots\ldots \quad \text{Eq. 1}$$

$$b = 0 \rightarrow N_p = \frac{Q_i - Q_t}{\frac{D_i}{12}} \times 30.4375 \quad \ldots\ldots\ldots\ldots\ldots\ldots\ldots\ldots \quad \text{Eq. 2}$$

- Harmonic Decline:

$$b = 1 \rightarrow Q_t = \frac{Q_i}{1 + \frac{D_i}{12} t} \quad \ldots\ldots\ldots\ldots\ldots\ldots\ldots\ldots\ldots\ldots\ldots\ldots\ldots\ldots \quad \text{Eq. 3}$$

$$b = 1 \ \rightarrow \ N_p = 2.303 \frac{Q_i}{\frac{D_i}{12}} \times [\log Q_i - \log Q_t] \times 30.4375 \quad \ldots \quad \text{Eq. 4}$$

- Hyperbolic Decline:

$$Q_{t=} \frac{Q_i}{(1 + b(\frac{D_i}{12})t)^{\frac{1}{b}}} \ldots\ldots\ldots\ldots\ldots\ldots\ldots\ldots\ldots\ldots\ldots\ldots\ldots\ldots\ldots\ldots\ldots\ldots \quad \text{Eq. 5}$$

$$N_p = \frac{{Q_i}^b}{\frac{D_i}{12}(b-1)} ({Q_t}^{1-b} - {Q_i}^{1-b}) \times 30.4375 \quad \ldots\ldots\ldots\ldots\ldots \quad \text{Eq. 6}$$

Where Q_i is the initial daily gas flow rate, D_i is the initial decline rate, and b is the decline exponent. **Fig. 2.4** shows the Excel sheet interface

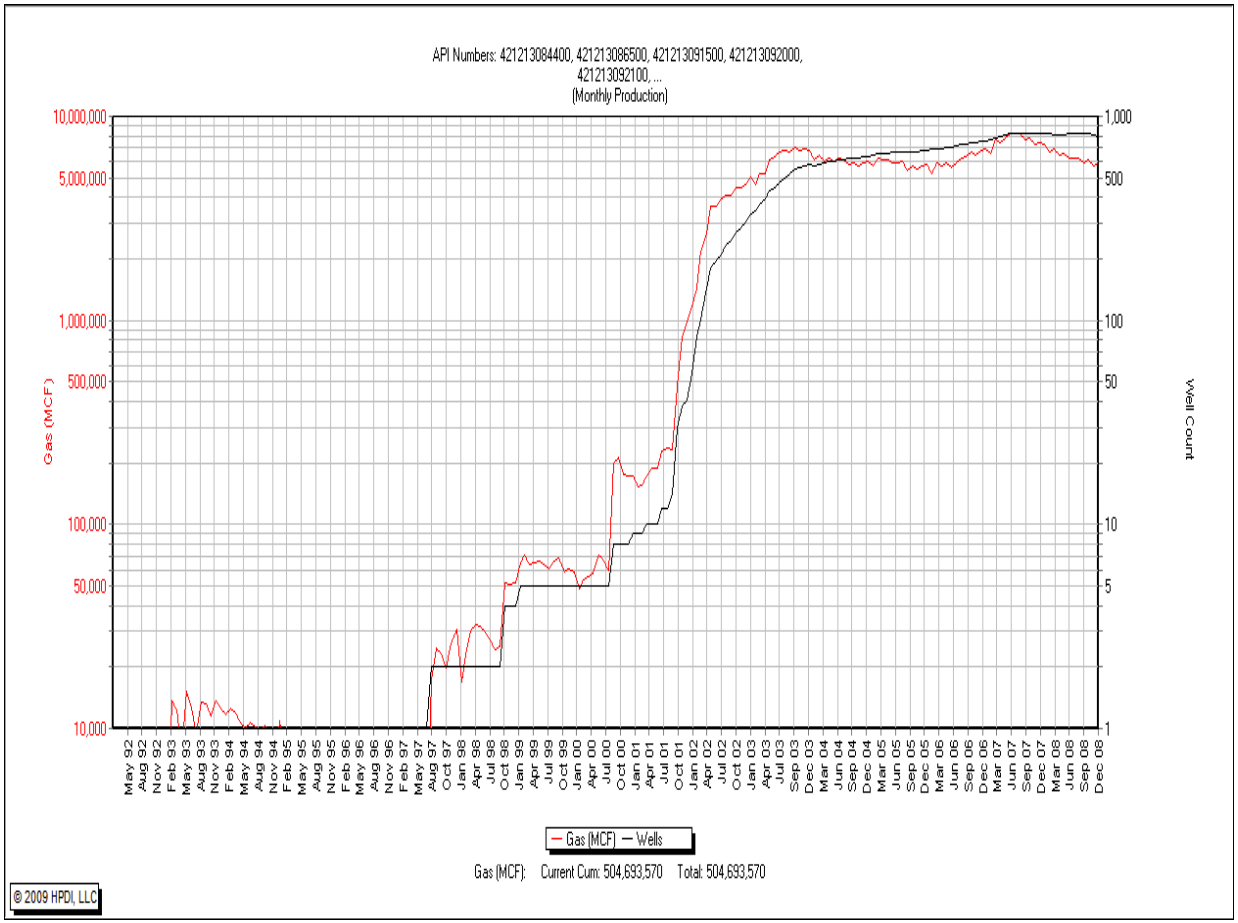

Fig. 2.3: Monthly Barnett gas (red line) production rates of the selected 781 wells plot. Monthly Barnett well count (black line). This figure generated using HPDI software

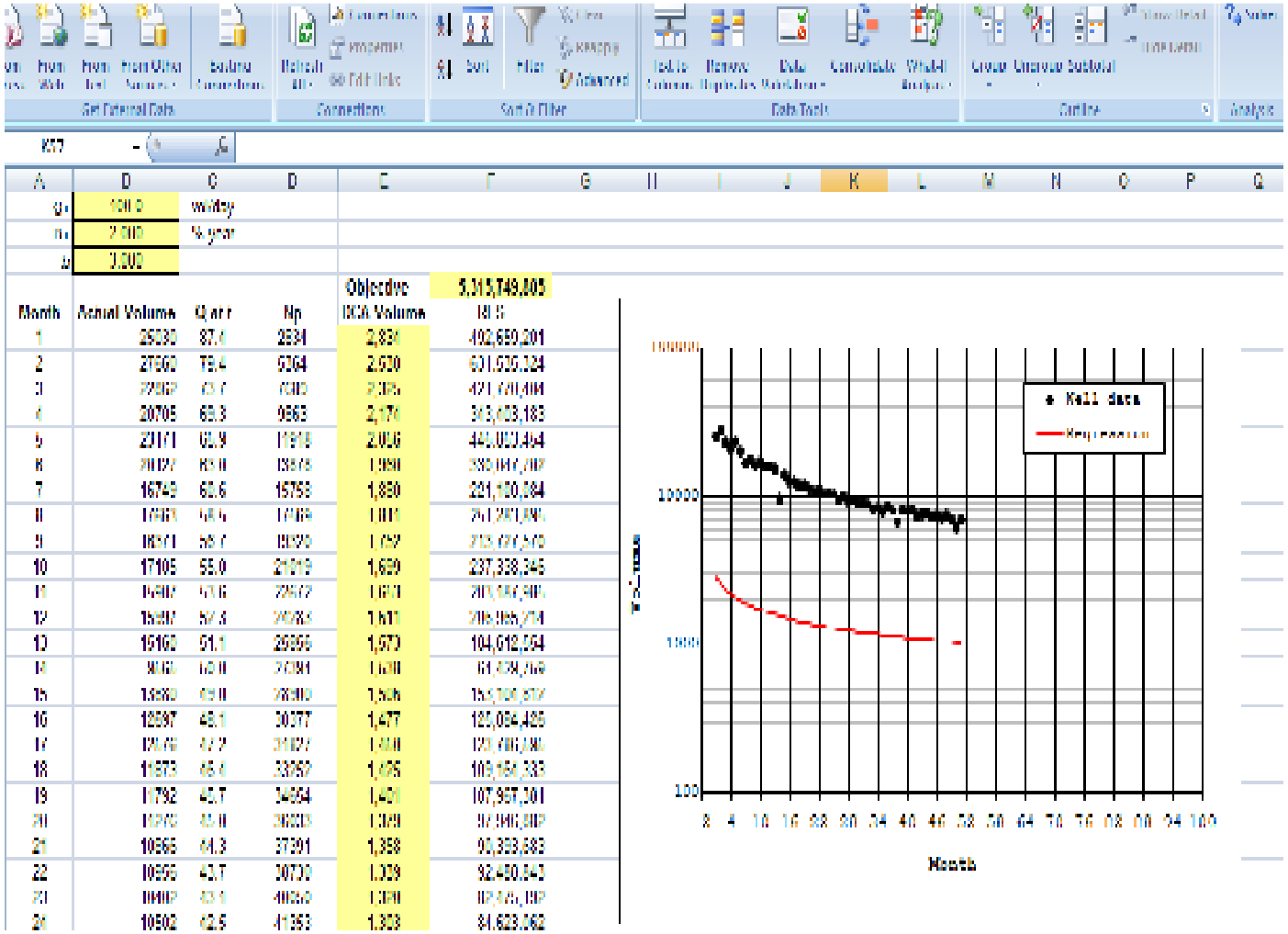

Month	Actual Volume	Qarr	Np	IDCA Volume	IRR
1	25033	87.4	2834	2,834	402,650,201
2	27560	79.4	5394	2,560	601,525,324
3	22869	83.7	7810	2,416	421,620,488
4	20705	80.3	9863	2,053	313,623,183
5	23171	82.9	11978	2,116	443,023,464
6	20027	85.0	13878	1,900	335,184,787
7	16743	82.6	15753	1,850	221,150,284
8	17461	84.4	17489	1,737	261,281,840
9	18171	86.7	19329	1,839	213,424,240
10	17105	85.0	21019	1,689	237,338,345
11	16487	87.6	22617	1,598	203,184,980
12	15887	87.3	24083	1,467	208,185,714
13	15162	91.1	25556	1,473	104,012,564
14	14661	92.0	27001	1,445	61,458,268
15	13983	91.0	28310	1,309	153,700,512
16	12597	48.1	30377	1,477	125,054,425
17	12176	47.7	31827	1,450	123,486,240
18	11573	45.4	33767	1,675	103,154,335
19	11792	45.7	34654	1,421	107,957,201
20	13272	51.0	36333	1,679	97,946,849
21	10566	54.3	37291	1,358	90,353,683
22	10555	43.7	38730	1,329	92,480,842
23	10402	43.1	40050	1,320	87,545,182
24	10502	42.5	41383	1,333	84,623,062

Fig. 2.4: Production forecast excel sheet.

To start the forecast process for each well individually, the following steps were followed:

- Historical monthly gas production data was copied from HPDI, pasted into "Actual Volume" column, and plotted as black points on the graph.
- Forecast parameters (Q_i, D_i, and b) were entered manually and arbitrarily.
- Q_t and N_p columns were calculated automatically using Arp's equations, and based on the arbitrary parameters.
- Each cell in "DCA Volume" column equaled the difference between the corresponding and previous N_p's. This column was plotted as a red line on the graph.
- "RES" column was created, where each cell was the difference of squares between corresponding "Actual Volume" and "DCA Volume".
- All the "RES" cells were then summed into "Objective" cell.

Now, the sheet is set up and ready to start the forecast process. The goal now is to fit the red line (DCA Volume) into the black points (Actual Volume). This step is achieved by adjusting the parameters (Q_i, D_i, and b). However, adjusting these parameters manually would not fit the data accurately.

Setting up Excel to perform the parameters adjustment is the preferred method in this study. This is done by minimizing difference of squares between "Actual Volume" and "DCA Volume". As mentioned earlier, the "Objective" cell is the sum of all difference of squares in "RES" column. By using "Solver" feature in Excel, shown on the top right corner of Fig. 2.4, the "Objective" cell is minimized by changing the forecast

parameters. **Fig. 2.5** shows the new parameters values, and how suitably "DCA Volume" red line fits into "Actual Volume" black points.

Regression step: the initial step in production forecast procedure is now complete. The next step is to use the current parameters to forecast production for the desired amount of time. In this study, data is forecasted for 480 months (40 years). Forecast parameters are copied and pasted into another sheet **(Fig. 2.6).** The same Arp's equations used in the previous sheet are used here. "Volume" column is the difference between the corresponding and previous N_p's. This sheet is built to calculate forecasted production to month 480.

From Fig. 2.6, "Volume" column is plotted vs. months. The resulting plot represents the final forecast. "Actual Volume" black points are plotted too to see how they are matched to the "Volume" curve. Out of the forecasted 781 wells, below are examples of four cases, initial (Regression) and final forecast plots **(Figs. 2.7a, 2.7b, 2.8a, 2.8b, 2.9a, 2.9b, 2.10a, and 2.10b).**

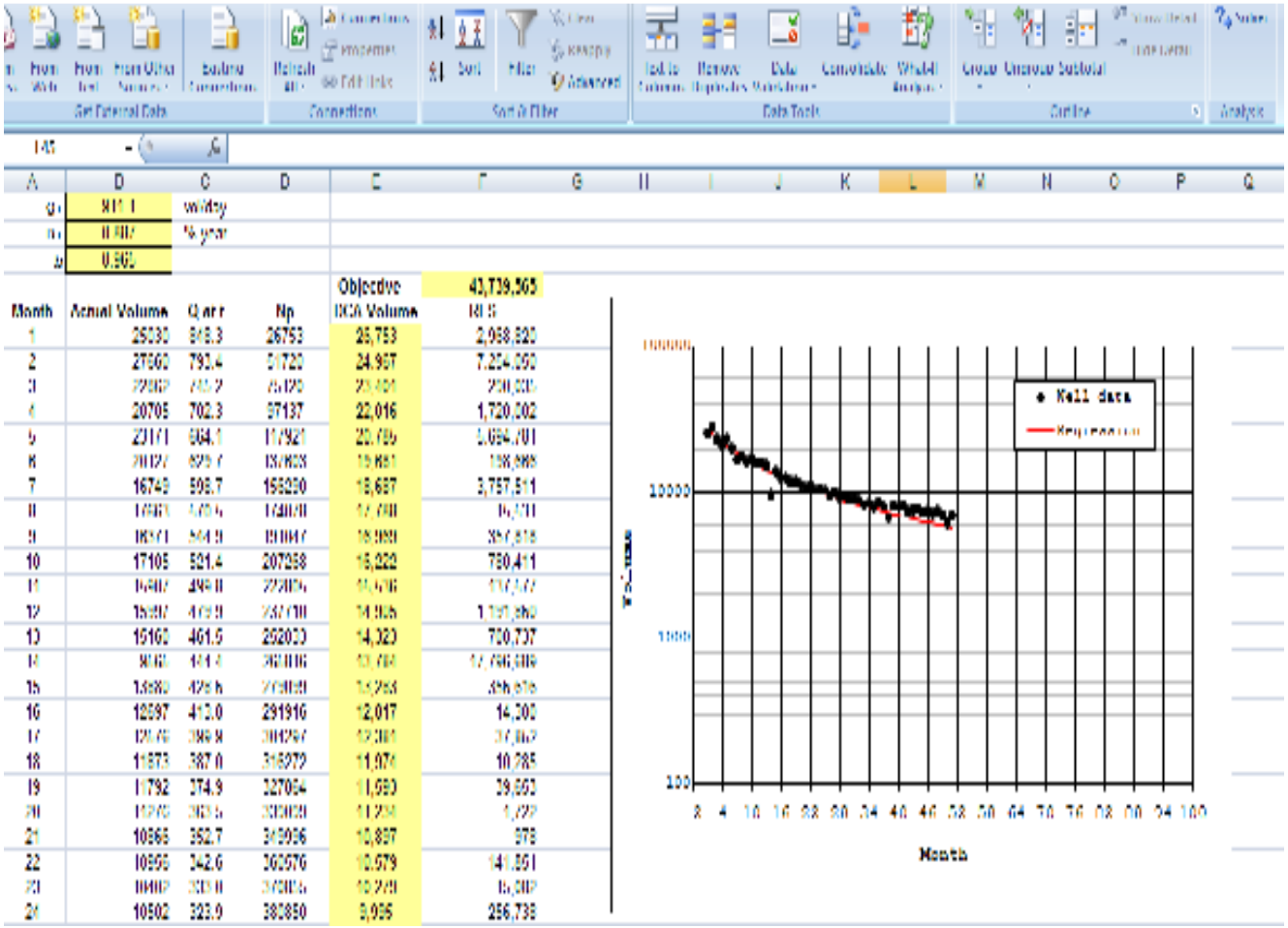

Fig. 2.5: Production forecast excel sheet after fitting the regression line into the actual monthly production rates.

Qi	911.1	vol/day		
Di	0.887	% year		
b	0.965			
	From DCA Equation			
				Nominal
Month				Decline
(t)	q at t	Np	Volume	/year
0	911.1	0	0	
1	848.3	26753	26,753	0.857
2	793.4	51720	24,967	0.802
3	745.2	75120	23,401	0.753
4	702.3	97137	22,016	0.710
5	664.1	117921	20,785	0.672
6	629.7	137603	19,681	0.637
7	598.7	156290	18,687	0.606
8	570.5	174078	17,788	0.578
9	544.9	191047	16,969	0.552
10	521.4	207268	16,222	0.529
11	499.8	222804	15,536	0.507
12	479.9	237710	14,905	0.488
13	461.5	252032	14,323	0.469
14	444.4	265816	13,784	0.452
15	428.6	279099	13,283	0.436
16	413.8	291915	12,817	0.421
17	399.9	304297	12,381	0.408
18	387.0	316271	11,974	0.395
19	374.9	327864	11,593	0.383
20	363.5	339099	11,235	0.371

Fig. 2.6: Production forecast excel sheet built to predict monthly production rates for 480 months (40 years).

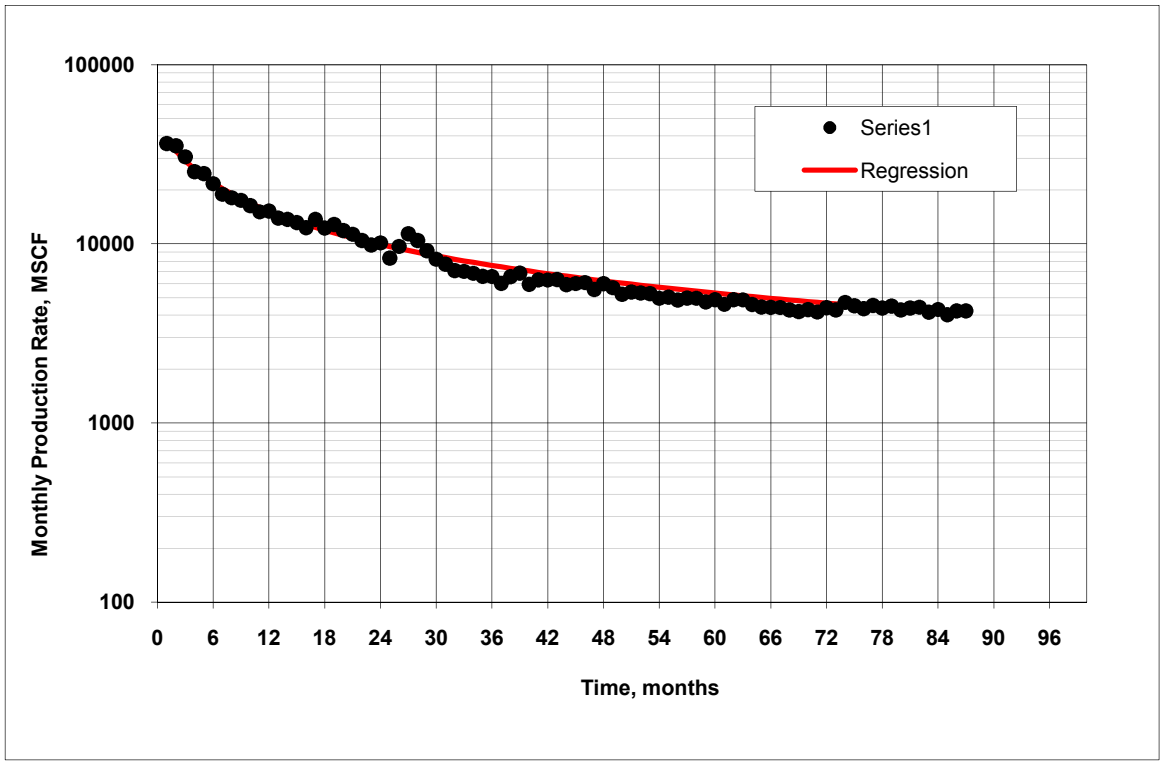

Fig. 2.7a: Example 1 regression plot.

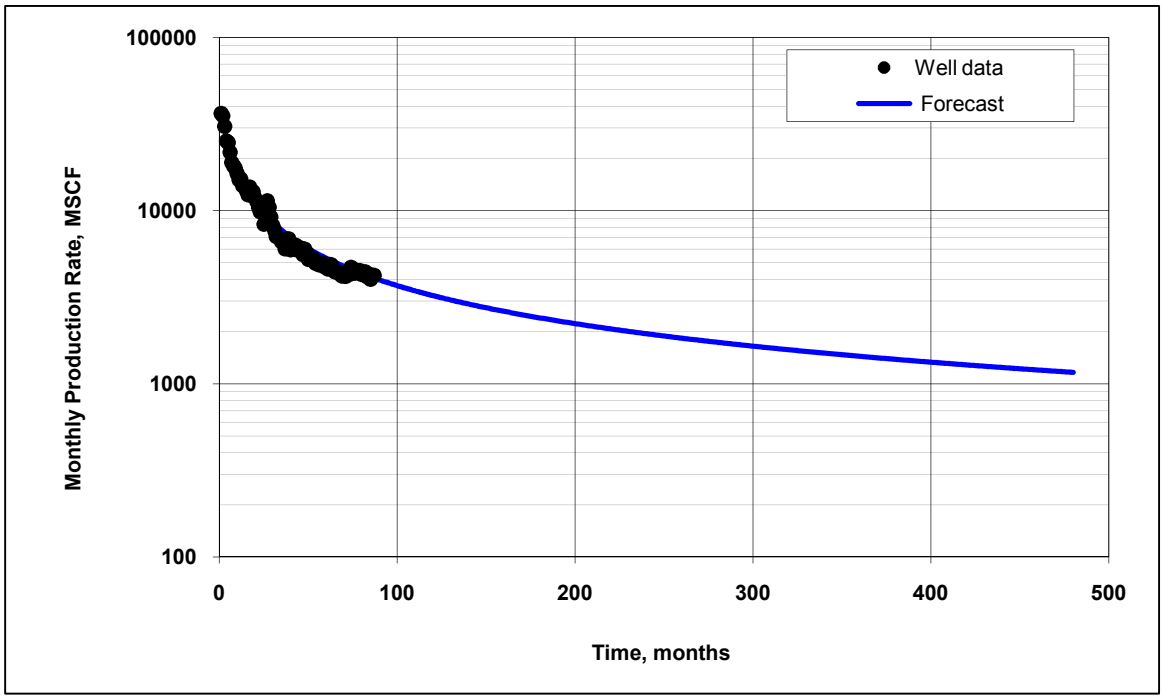

Fig. 2.7b: Example 1 final production decline curve.

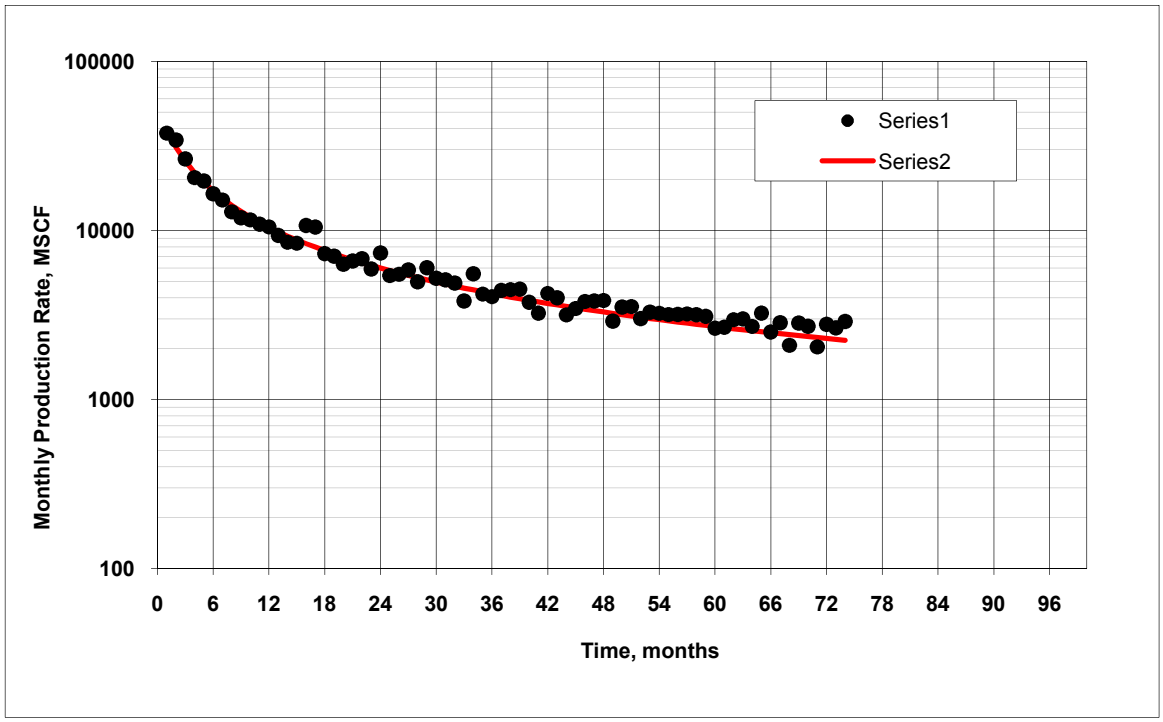

Fig. 2.8a: Example 2 regression plot.

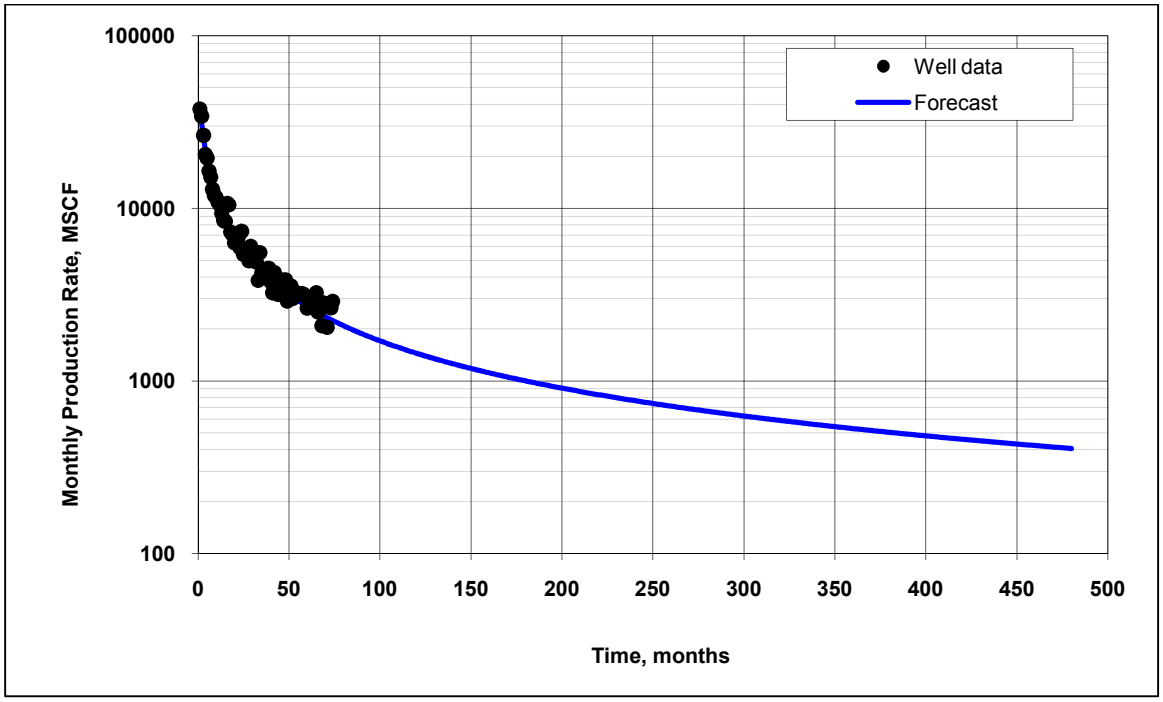

Fig. 2.8b: Example 2 final production decline curve.

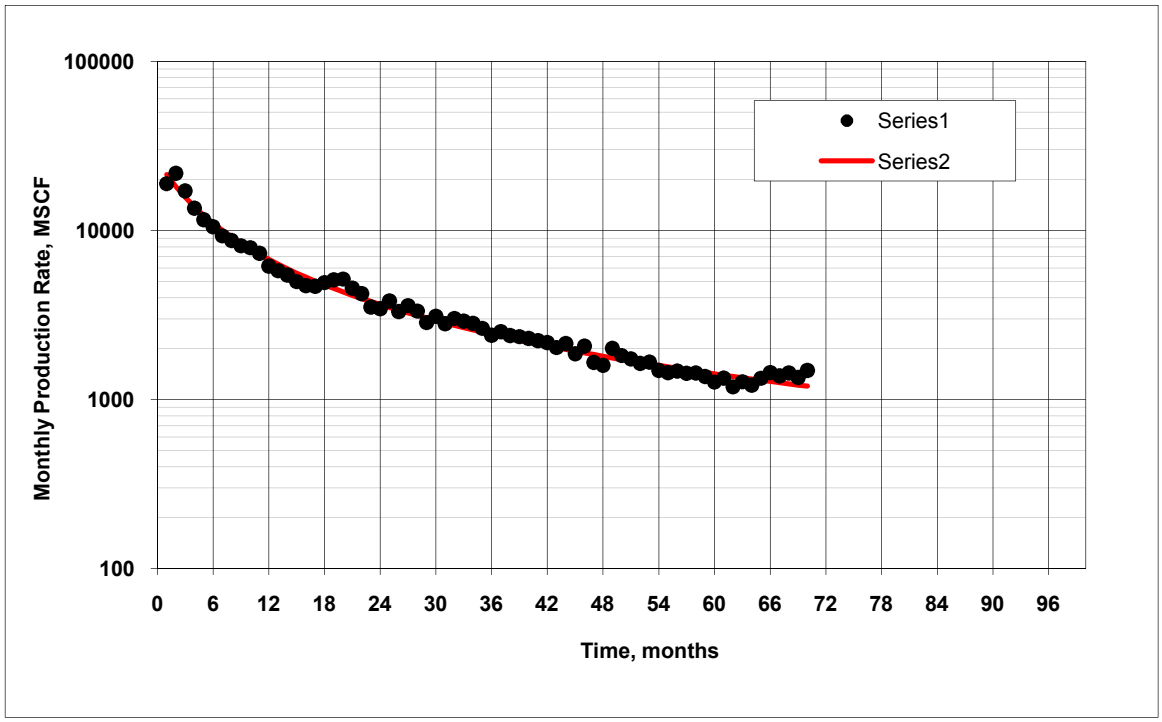

Fig. 2.9a: Example 3 regression plot.

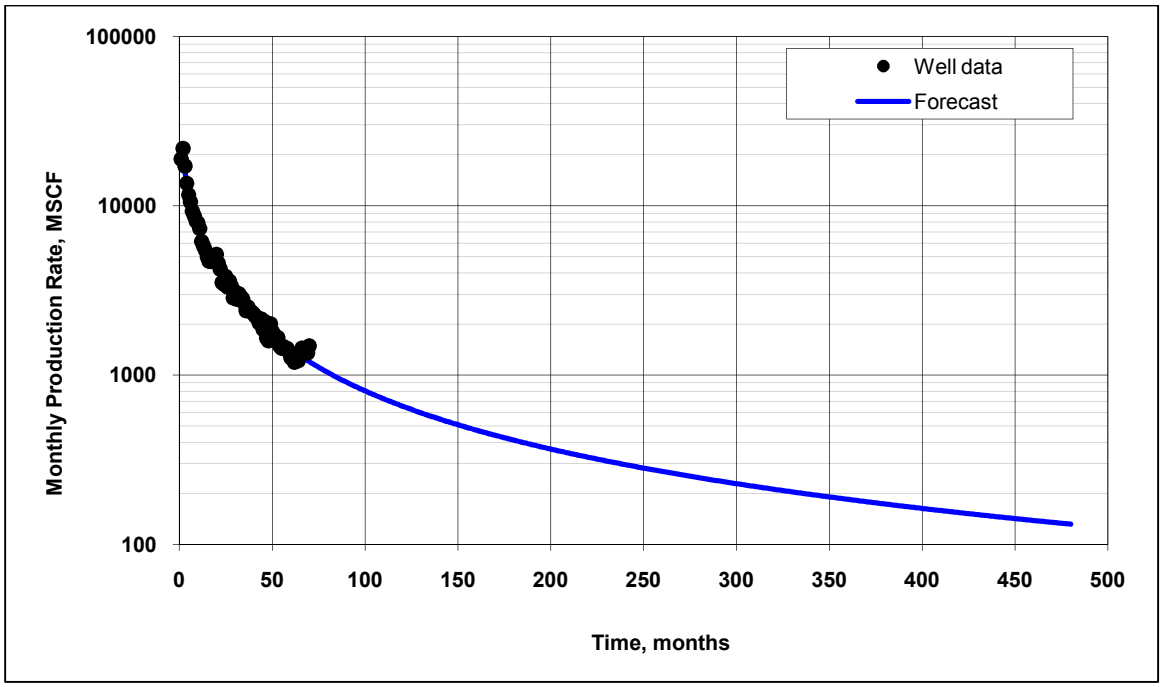

Fig. 2.9b: Example 3 final production decline curve.

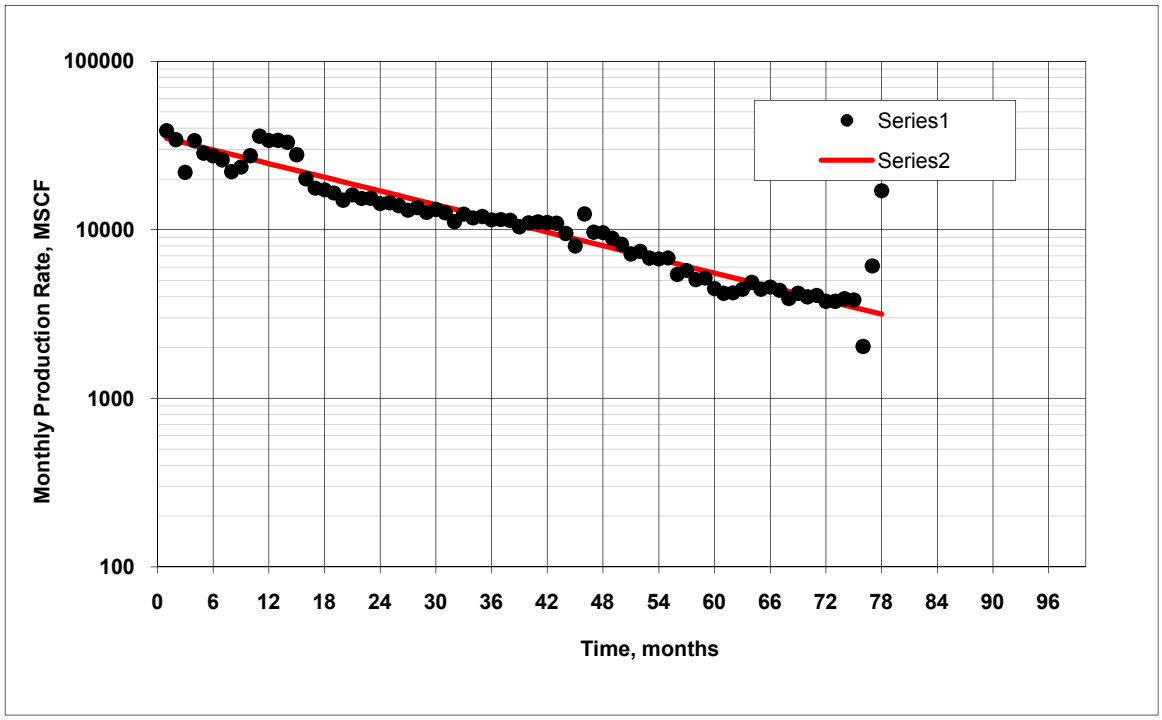

Fig. 2.10a: Example 4 regression plot.

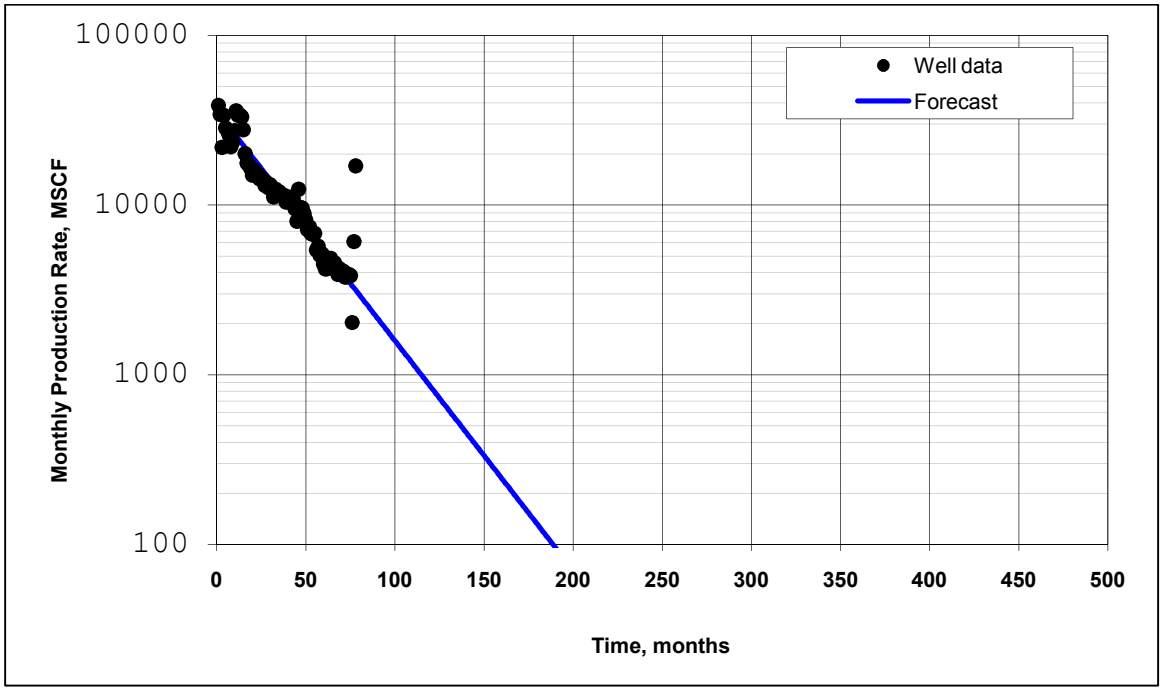

Fig. 2.10b: Example 4 final production decline curve.

By now, the forecast process is complete and a total of 781 decline curves are available. However, using these decline curves to compare between production forecasts is very difficult, if not impossible. By using conventional methods, two ways are available:

- Arranging all the decline curves next to each other and going through them one by one. As seen earlier, four decline curves were attached. It is difficult to use these four curves to compare between their forecasts. Therefore, it is even way more difficult and time consuming to use decline curves to compare between 781 forecasts.
- Combining all the curves into one plot. This method is effective only when few curves are combined. However, it is very complicated to combine 781 curves in one plot.

Furthermore, these two methods are ineffective and time consuming when it comes to testing a parameter's influence on production decline curves. A new simple way is introduced here: Decline Map Analysis (DMA) simplifies this process. It simply plots these Decline Curves on maps. The next section discusses this new technique in details.

2.3 Decline Map Analysis (DMA)

A question might rise at this point: how a decline map is different from a regular production map? The answer is basically as follows:

A production map is a visual expression of production values on a specific date. In other words, it maps out the production rates collected on a specific day, month, or

year. To illustrate this point, **Fig. 2.11** shows an example of three production plots. Each plot is set to its original production start point on the year (x) axis. To create a 1995 production map, for example, each value from the production (y) axis corresponding to the 1995 time line would be collected and plugged into the map. In this way, all the rates produced in 1995 would be collected and mapped out, no matter how old or young the well is.

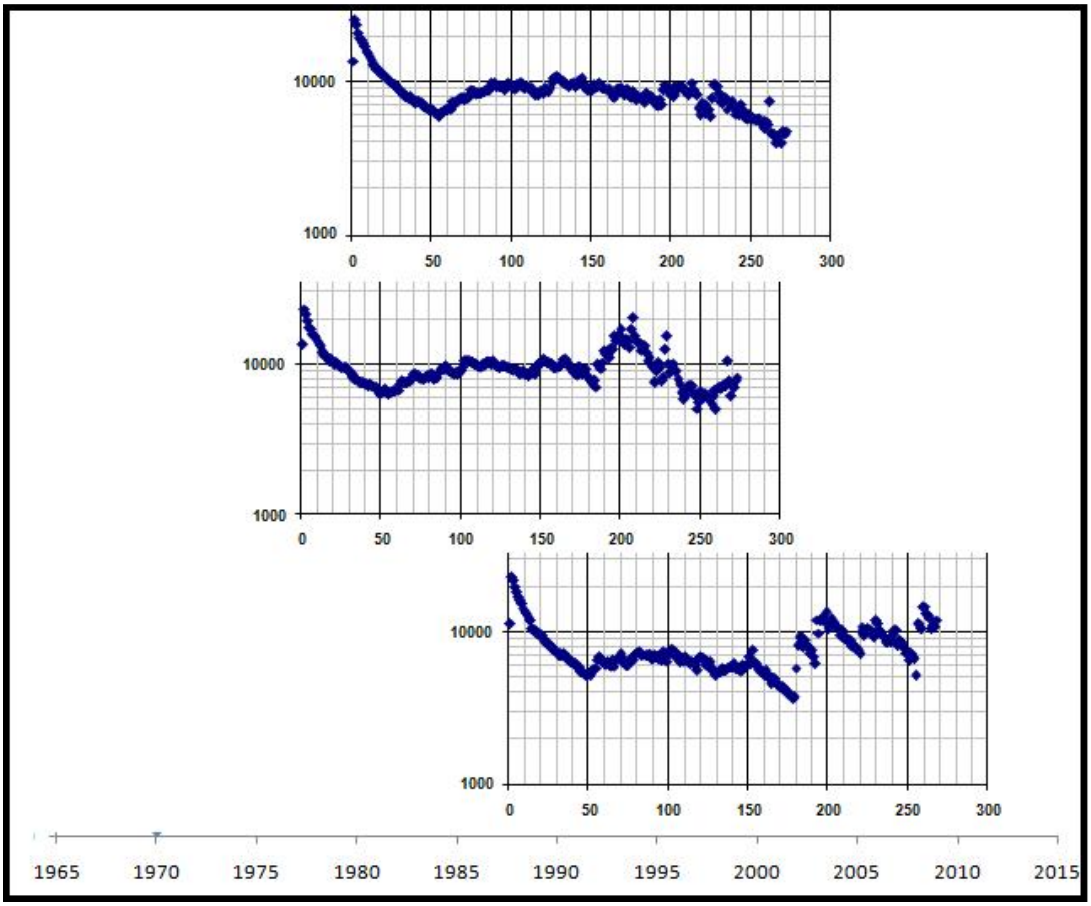

Fig. 2.11: Three production curves set to their original production start points to illustrate production mapping (Data from Deshpande, 2008).

On the other hand, a Decline Map assumes that all wells have started production at the same point of time. In other words, all the Decline Curves are zero-timed. The reason for this step is to reference all the production data to the same time line. As shown in **Fig. 2.12,** the same three plots used earlier are normalized to the same start point. Now, instead of mapping the production on a specific date, production in a specific month is mapped. For example, to create a map for the 50th month, the production value in the 50th month of each well is collected and plugged into the map. This 50th month map shows how each well production behaved in its 50th month compared to other wells. So, on each x'th month decline map, the production of each well in its x'th month is displayed and color coded to visualize its x'th month production behavior compared to others. In this way, all the decline curves are compared at the same time.

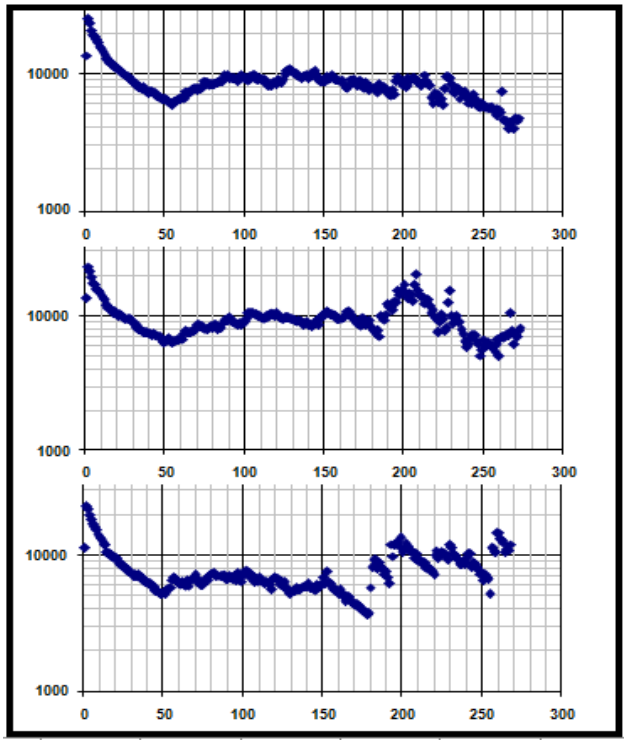

Fig. 2.12: Same production plots used in Fig. 2.11 normalized to same start point to illustrate decline mapping (Data from Deshpande, 2008).

To create Decline Maps for the current Area of Interest, all the 781 decline curves are normalized to the zero time line. Therefore, all the 781 wells are assumed to have started production at the same time. These production values are then imported into Geographix mapping software. **Fig. 2.13** shows the decline map created for month one. Since each well is forecasted for 480 months, decline maps are created until month 480 too. However, to save storage memory, these maps are chosen for this study (all figures are available in the Appendix page 65):

- Months one, five, and 10.
- Months 20, 40... 100.
- Months 120, 140, 160… 300.
- Months, 330, 360, 390… 480.

These maps are then tied to some parameters to see how these parameters influence decline curves, and consequently decline maps. These parameters include: Barnett gross reservoir thickness (including Forestburg formation), total perforation footage, and perforated Barnett zones.

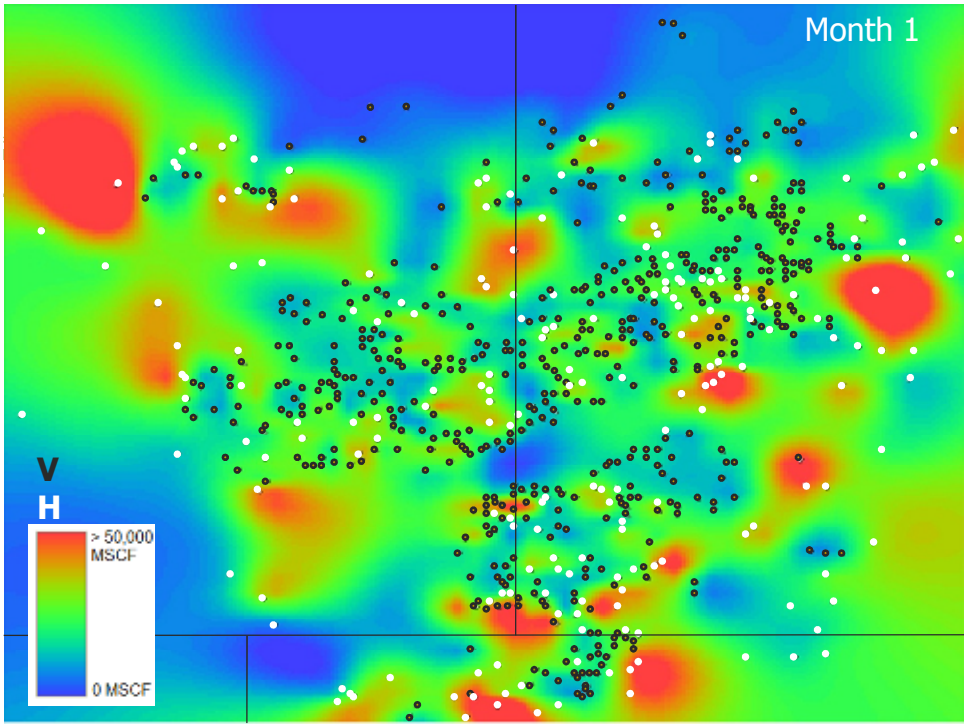

Fig. 2.13: First month decline map of the current AOI.

Tian (2009), in her ongoing M.S. research at Texas A&M, divided Barnet shale into four zones, from bottom to top: 1, 2, 3, and 4. Zone 4 represents Upper Barnett, where 1, 2, and 3 divide the Lower Barnett. In between Upper and Lower Barnett exists the Forestburg formation. Tian divided these zones based on Gamma Ray responses **(Fig. 2.14).**

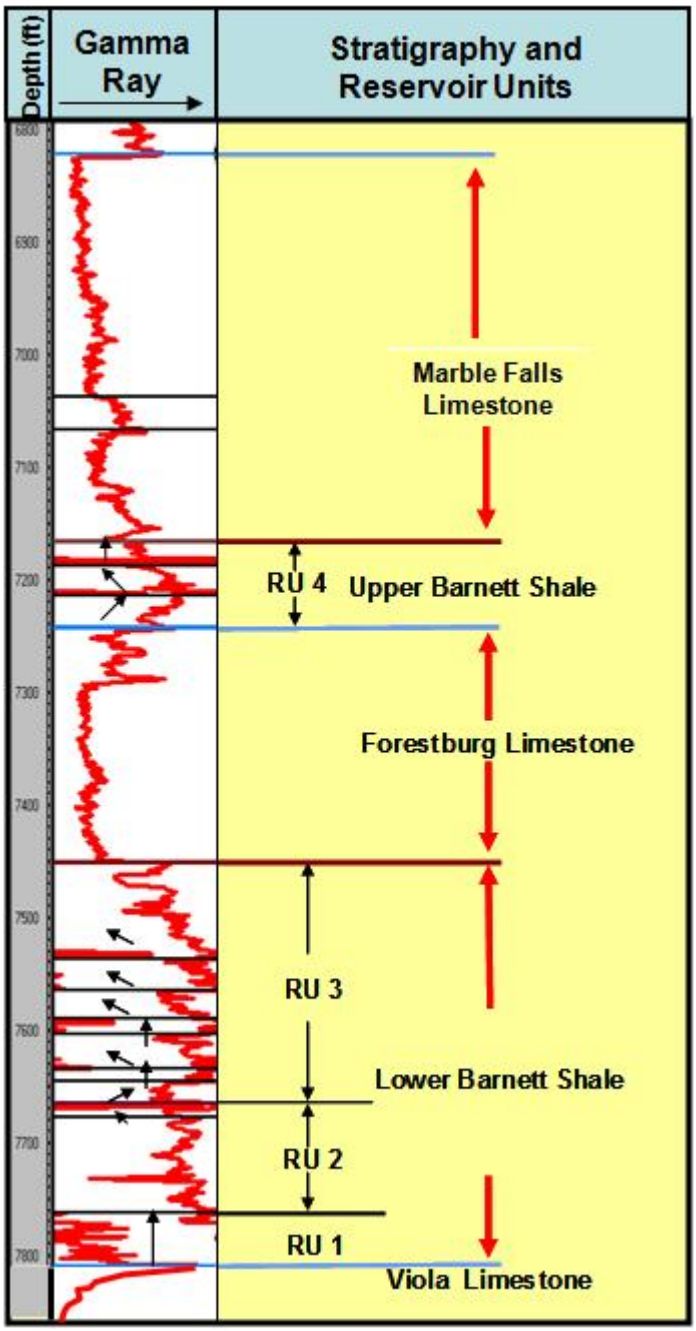

Fig. 2.14: Barnett zones divided by Tian (2009).

Out of the 560 vertical wells and 221 horizontal wells included in this study, only 35 well logs became available. These 35 well logs represent 35 vertical wells scattered

throughout the field: 4 wells in Denton, 13 wells in wise, and 18 wells in Tarrant counties **(Fig. 2.15).**

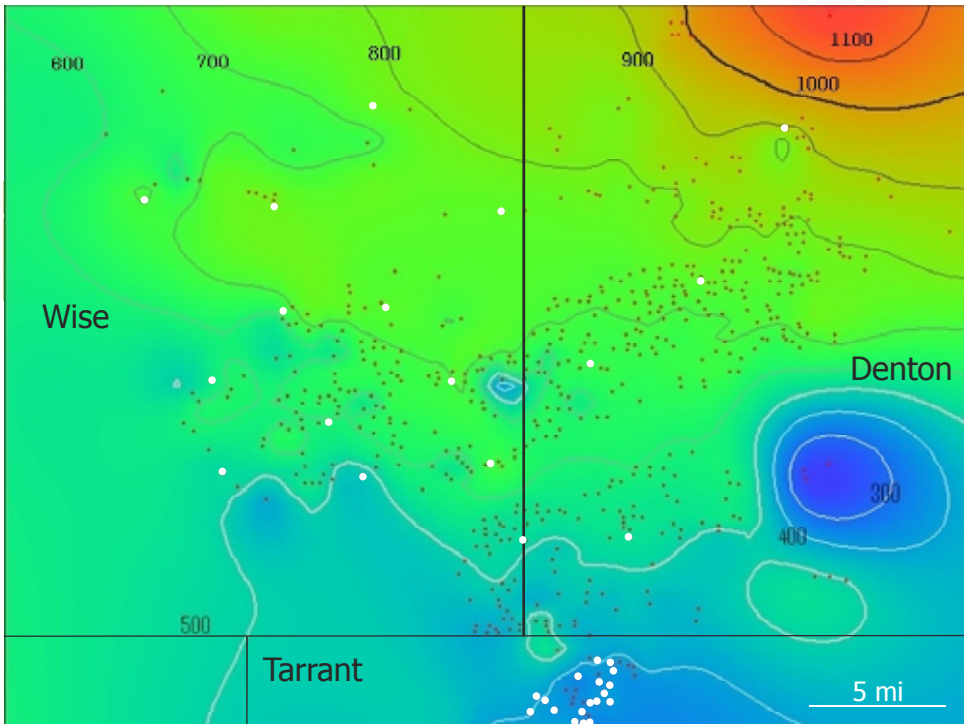

Fig. 2.15: 35 wells with logs pointed out (white points) on the Barnett gross thickness map.

Barnett zones which Tian (2009) divided are correlated through these 35 logs. The objective of this step is to match these zones with the perforation footage (from Scout Tickets) and see how this match correlates to each well production.

CHAPTER III

RESULTS AND DISCUSSIONS

3.1 Decline Curve Analysis

As mentioned in the previous chapter, 781 decline curves are generated. Each Decline Curve represents the past and the predicted future production data of a specific well. Since each well has a different production history, each well's decline curve looks different. In other words, each well's future production is forecasted with different parameters (Q_i, D_i, and b), resulting in a unique declining curve.

Each of the forecast parameters (Q_i, D_i, and b) has a particular effect on the curve. Q_i is the initial flow or production. On the curve, it is the point where the curve starts. D_i is the initial decline rate. It determines the degree of decline in the first 12 months. In other words, it decides how steep or gentle the slope of the curve is during the first 12 months. b, decline exponent, determines the decline curvature passed the first 12 months. That is: a zero b value leads to a straight line, and as the value increases, the curve is curved upward more and more.

Fig. 3.1 shows how relevant the first month production rates in decline curves to the actual first month production rates. Exhibiting a 45º line, this correlation indicates that these values are very close and, therefore, the decline curve first month values could be used instead in the correlations coming later. **Fig. 3.2** plots the "decline" versus actual first 12 month production rates averages. As could be seen on the plot, room of error in the forecast process is very small since the correlation exhibits a 45º line.

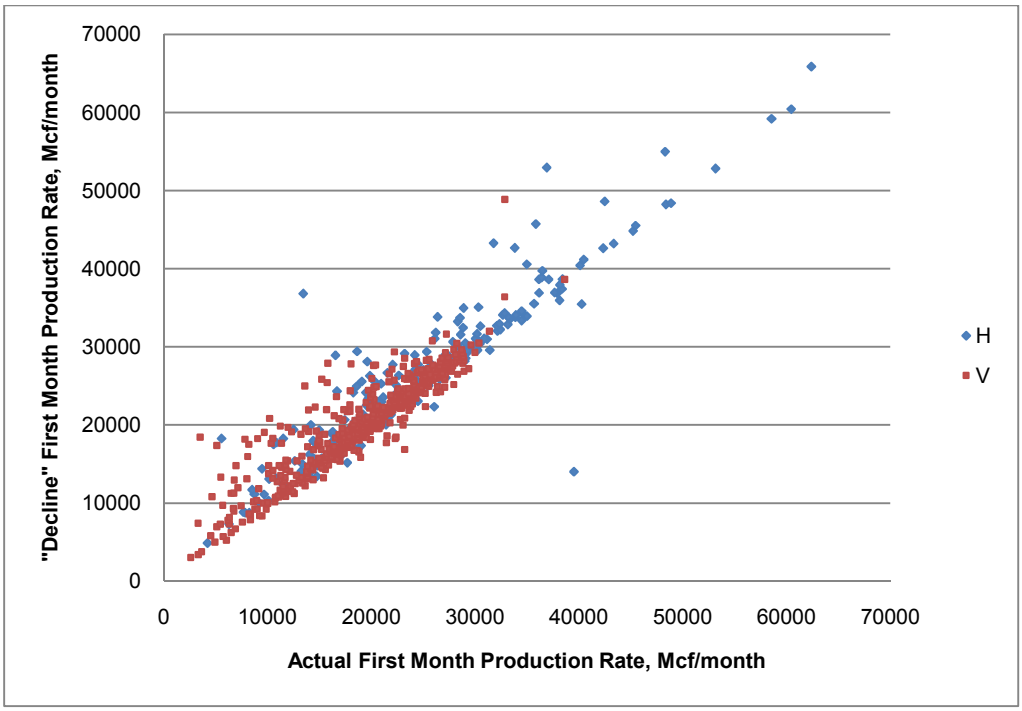

Fig. 3.1: Decline vs. actual first month production rates.

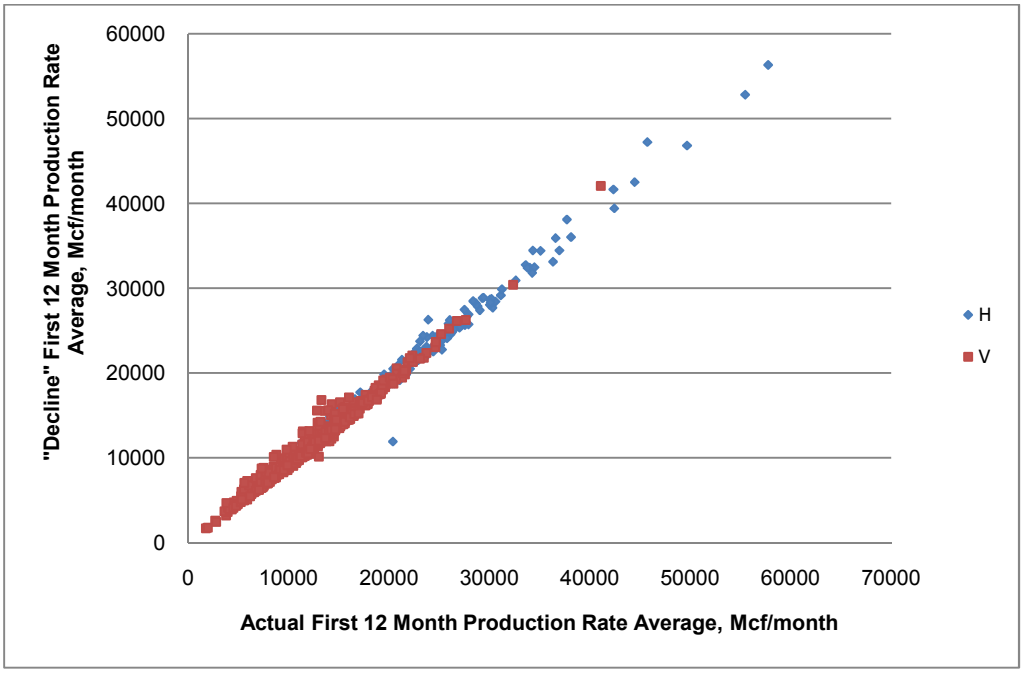

Fig. 3.2: Decline vs. actual first 12 month production rate averages.

In **Fig. 3.3,** first month production rates in the decline curves are plotted versus their corresponding actual first 12 month production rate averages. The correlation from this plot shows how reliable the first month production rates from decline curves are. Therefore, again, first month production rates from decline curves are used in correlations throughout this study.

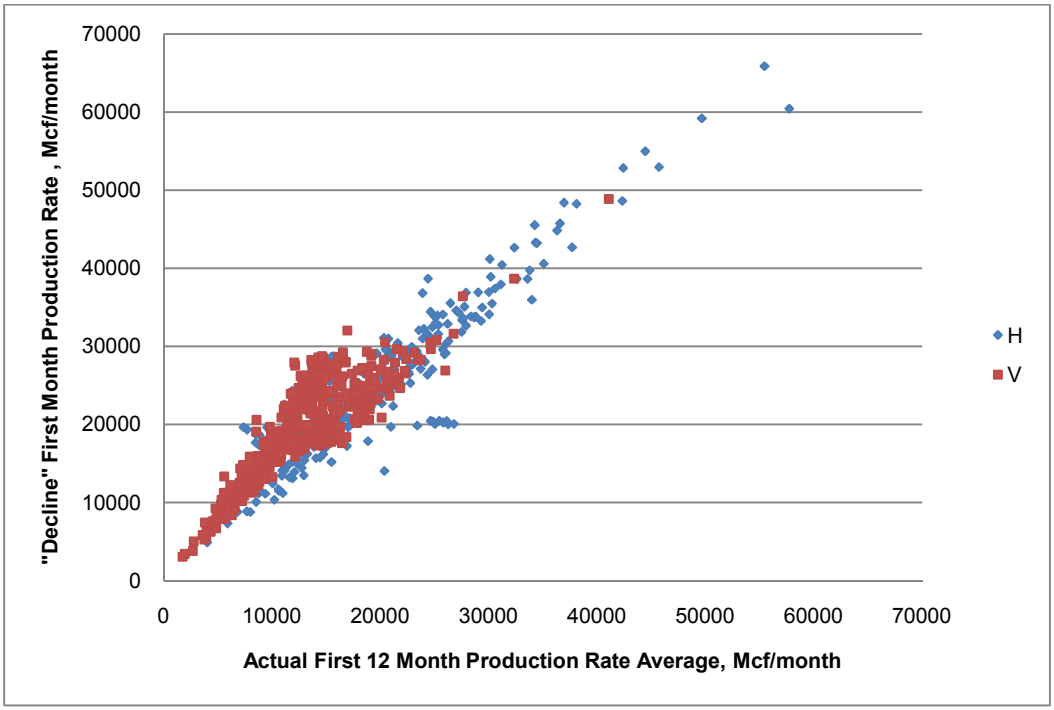

Fig. 3.3: Decline first month production rates vs. actual first 12 month production rate averages.

3.2 Vertical vs. Horizontal

Horizontal wells are more favorable over vertical wells in Barnett Shale. Reasons from production perspective include: more wellbore-reservoir contact, and higher production rates. In fact, according to The U.S. Department of Energy, horizontal wells

generally produce 3.2 times higher than vertical wells (Directional and Horizontal Drilling, 2009). Therefore, in terms of production rates, horizontal wells Decline Curves must be higher as well. Average horizontal well (221 horizontal wells production rates averaged) and average vertical well (560 vertical wells production rates averaged) decline curves are shown in **Figs 3.4 and 3.5,** respectively. As could be seen on the plots, the curve starts with a higher initial flow rate (Monthly production rate) in the horizontal well case. However, it initially declines fast with D_i=27% during the first 12 months. On the other hand, for the same amount of time, vertical well curve declines with D_i=11.2%. It then speeds up the decline with b=1.902, while the horizontal case slows down with b=2.228. As mentioned earlier, smaller b value means low curvature and faster decline toward low production rates. At the end, after 40 years, the horizontal well produces with a monthly rate 76.4% less than the first month, where it is 69.4% less than the first month in the vertical case. Therefore, Barnett horizontal wells would decline faster than vertical wells but they would mainly still produce with higher monthly production rates.

In terms of Estimated Ultimate Recovery (EUR), the average Barnett horizontal well would have an EUR of 7,230,541 Mcf in 40 years. On the other side, the average Barnett vertical well is estimated to recover 3,150,817 Mcf in 40 years, which is only 56.4% of the horizontal well EUR. Considering their costs, Barnett horizontal well and vertical well cost about $2 million and $1 million, respectively (Hayden and Pursell, 2005). These costs include drilling and completion. Although a vertical well would cost 50% less than a horizontal well, an EUR ratio of 2.3:1 Mcf makes the horizontal well more efficient.

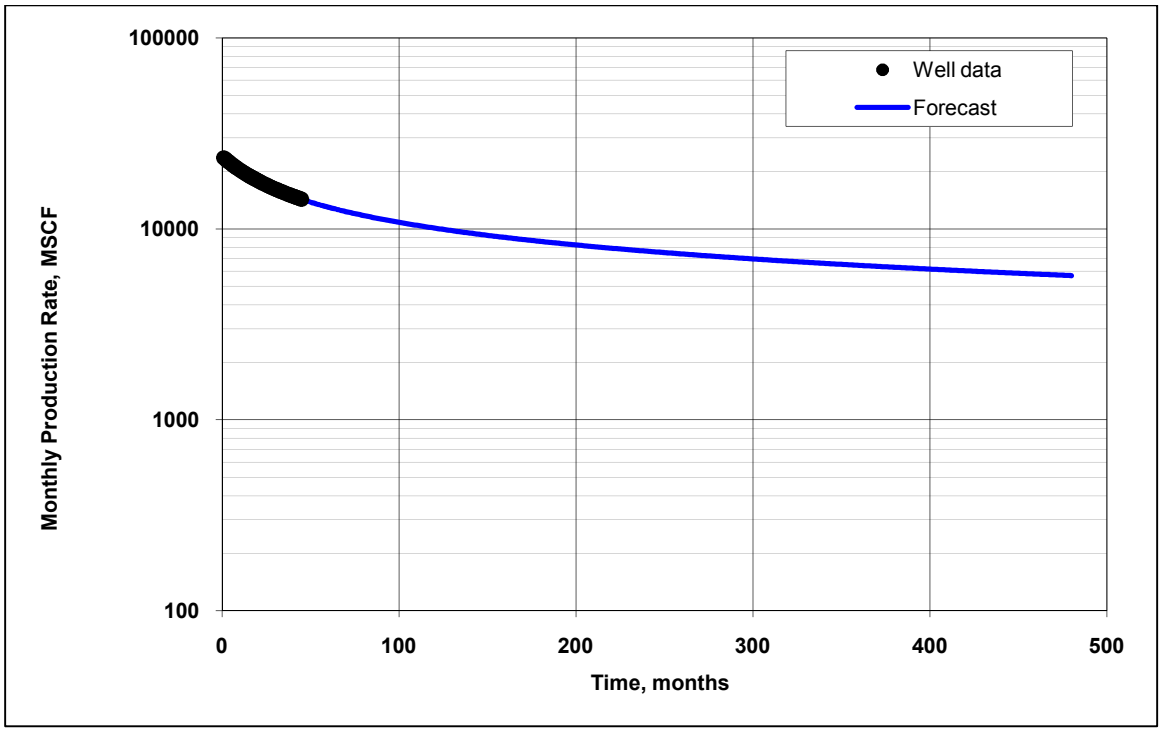

Fig. 3.4: Average horizontal well decline curve.

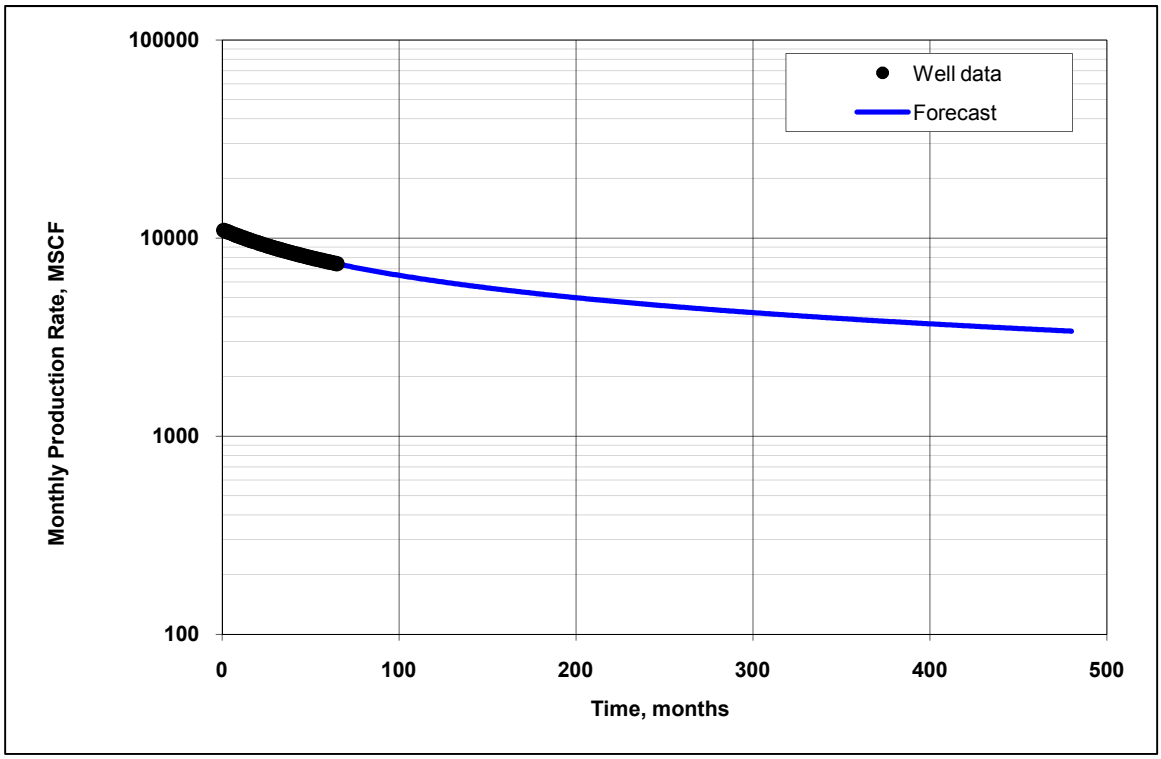

Fig. 3.5: Average vertical well decline curve.

3.3 Gross Reservoir Thickness on DMA

One of the parameters influencing original gas in place (OGIP) is gross reservoir thickness. A thick reservoir would have more reserves than a thin reservoir with the same parameters (area, porosity, and fluids saturation). This section studies the influence of gross reservoir thickness on production by using DMA.

Fig. 3.6 shows the first month decline map of the current study area. By correlating this map with the gross reservoir thickness map of the same area **(Fig. 3.7),** no clear correlation is indicated. As mentioned earlier, note that this gross reservoir thickness includes the Forestburg formation.

Vertical-wells-only decline map is created and shown in **Fig. 3.8.** The reason for generating this map is to see the influence of gross reservoir thickness on vertical well production only. By correlating the vertical wells decline and gross reservoir thickness maps, correlation could not be established either. Months one, 100, 200, 300, and 480 decline maps are attached **(Figs. 3.8, 3.9, 3.10, 3.11, and 3.12, respectively)** to see the influence of gross reservoir thickness. **Fig. 3.13** represents the scale-shifted version of Fig. 3.12. However, no clear definite influence is spotted. This poor correlation could be seen in **Fig. 3.14** where the production of each well through time is averaged and plotted versus the gross reservoir thickness. Estimated Ultimate Recovery (EUR) at month 480 versus gross reservoir thickness plot **(Fig. 3.15)** has no clear correlation either. Therefore, Barnett gross thickness, including Forestburg formation, has no definite influence on production through time in Barnett Shale.

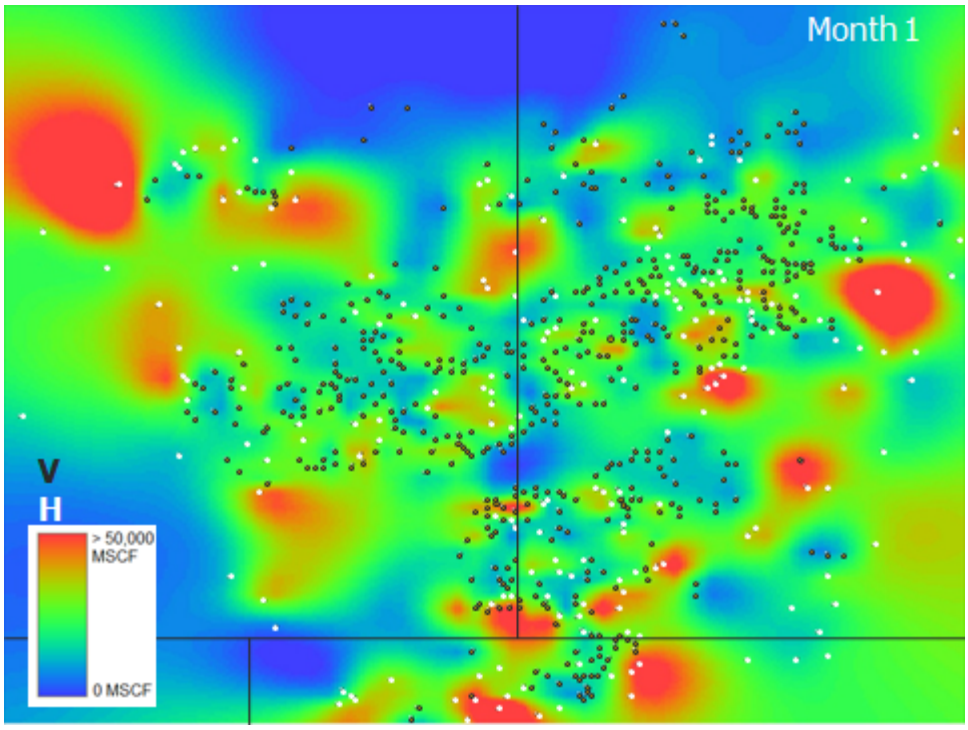

Fig. 3.6: First month decline map of the current AOI to test Barnett gross thickness influence.

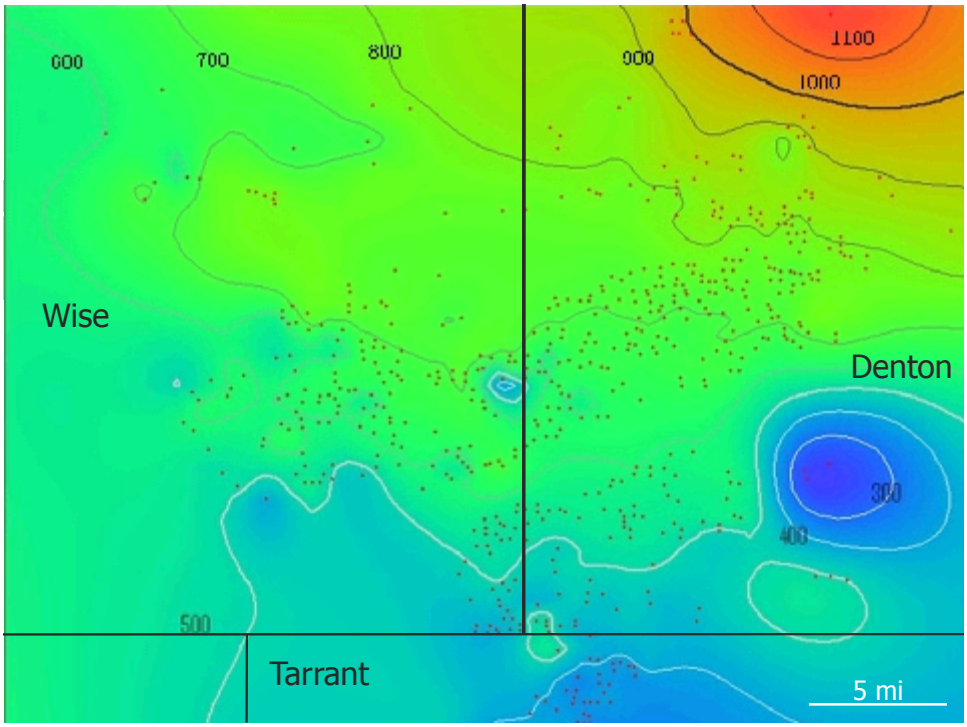

Fig. 3.7: Barnett gross thickness map of the current AOI to correlate with decline maps.

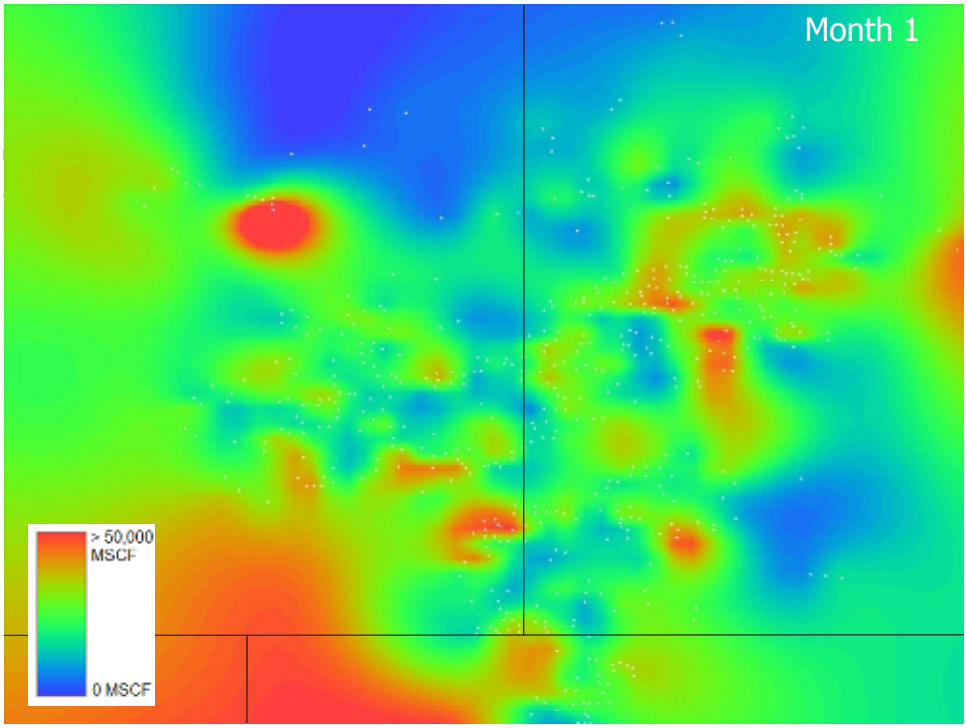

Fig. 3.8: First month vertical wells only decline map of the current AOI.

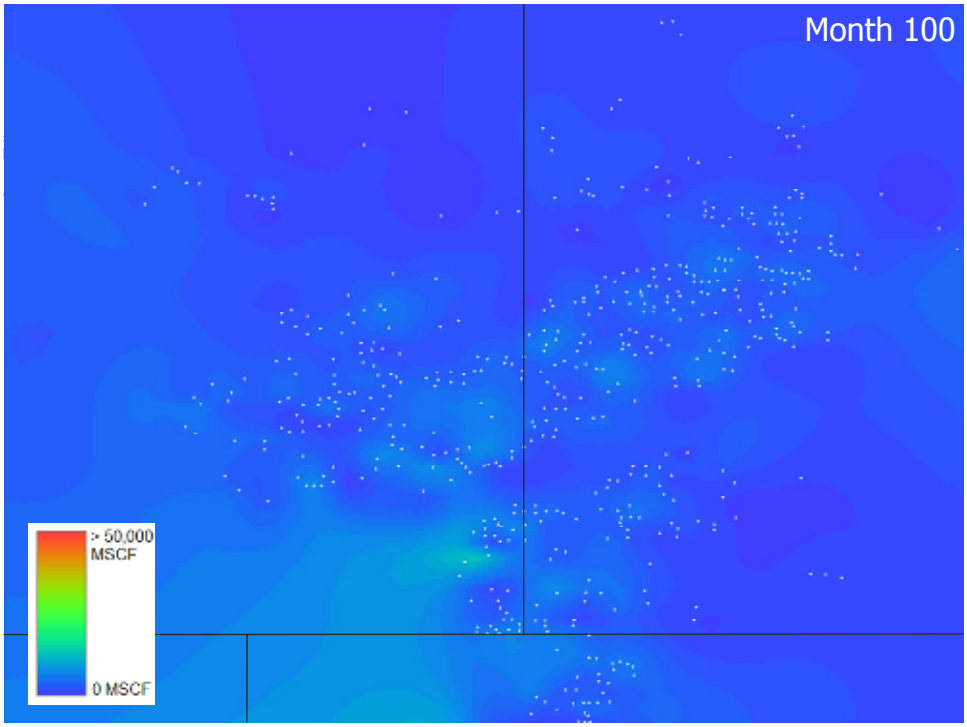

Fig. 3.9: 100th month vertical wells only decline map of the current AOI.

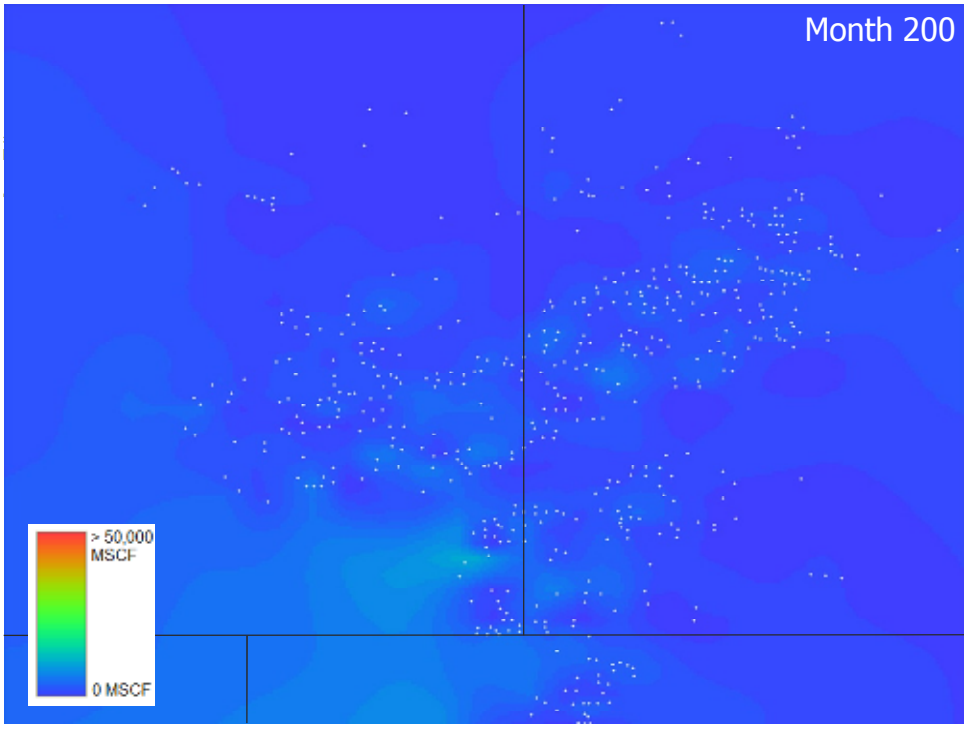

Fig. 3.10: 200th month vertical wells only decline map of the current AOI.

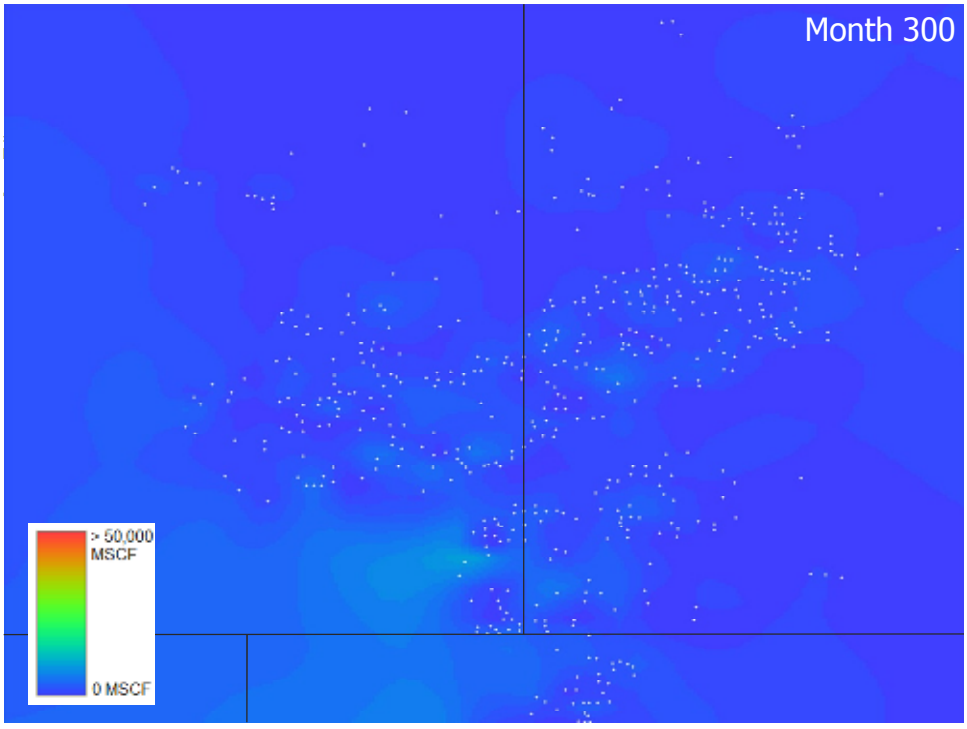

Fig. 3.11: 300th month vertical wells only decline map of the current AOI.

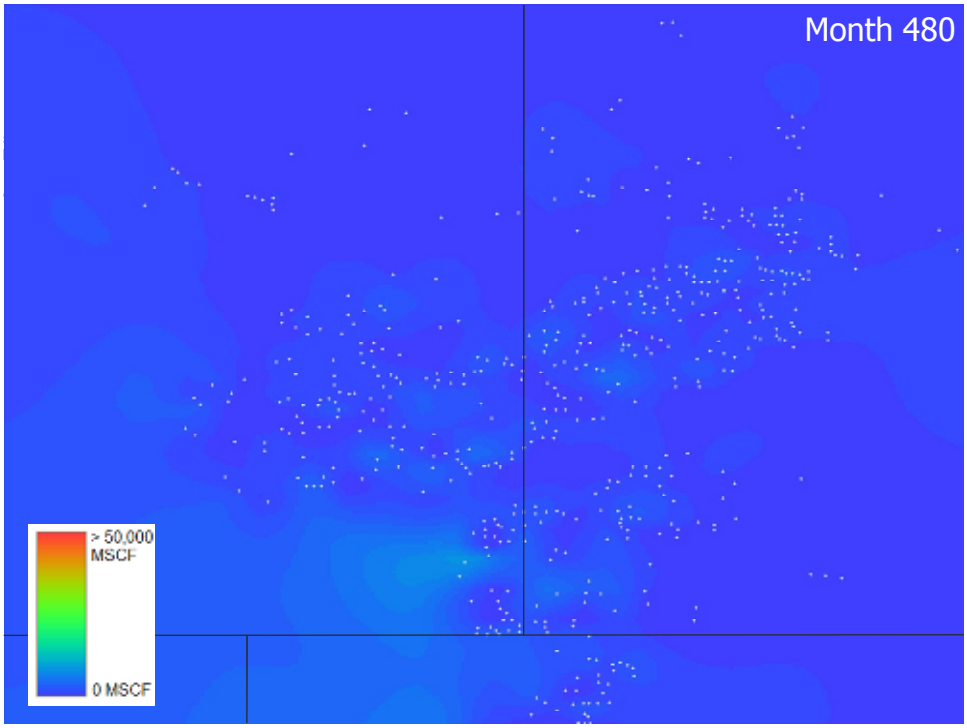

Fig. 3.12: 480th month vertical wells only decline map of the current AOI.

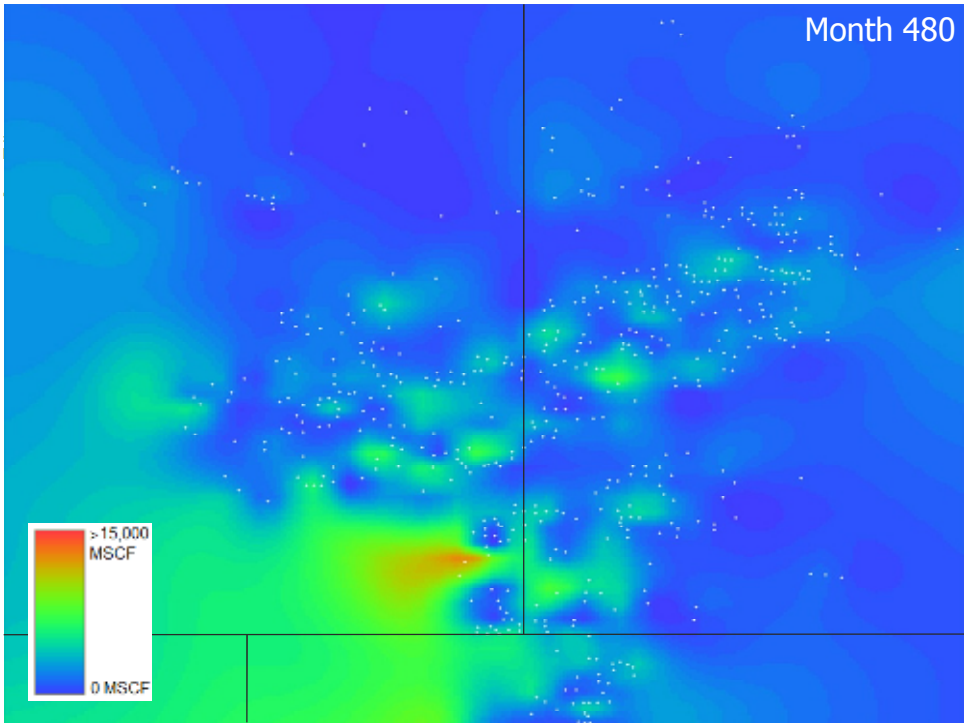

Fig. 3.13: 480th month vertical wells only decline map of the current AOI (shifted scale).

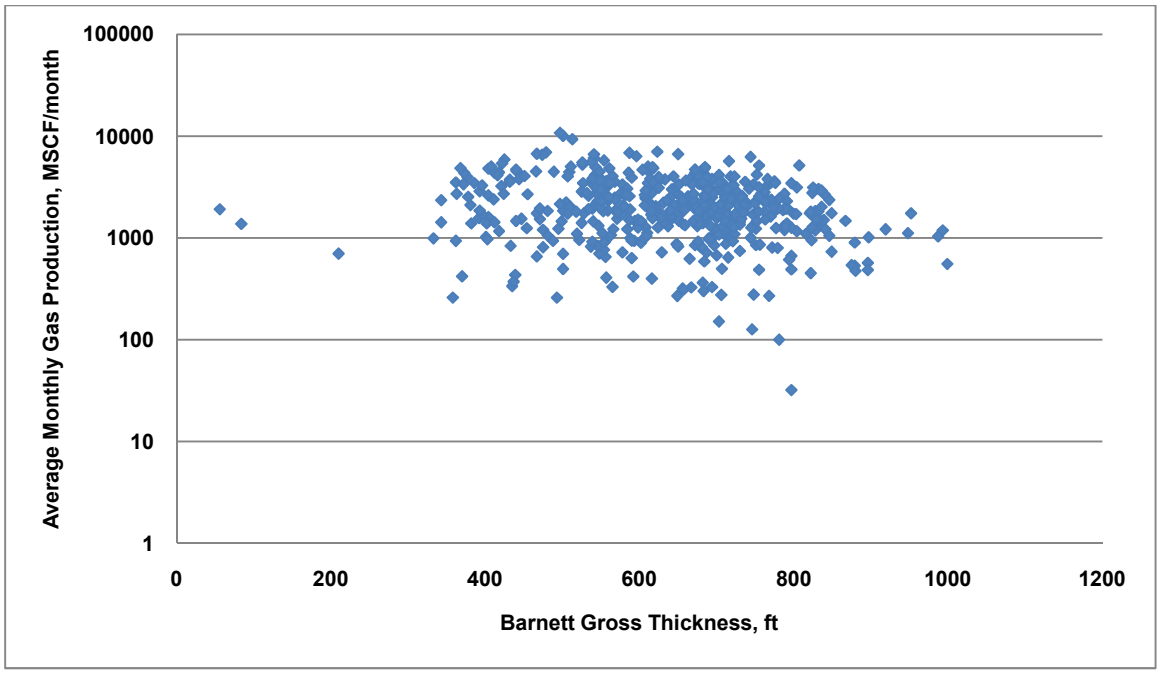

Fig. 3.14: Average monthly gas production of each vertical well vs. Barnett gross thickness (including Forestburg formation) plot.

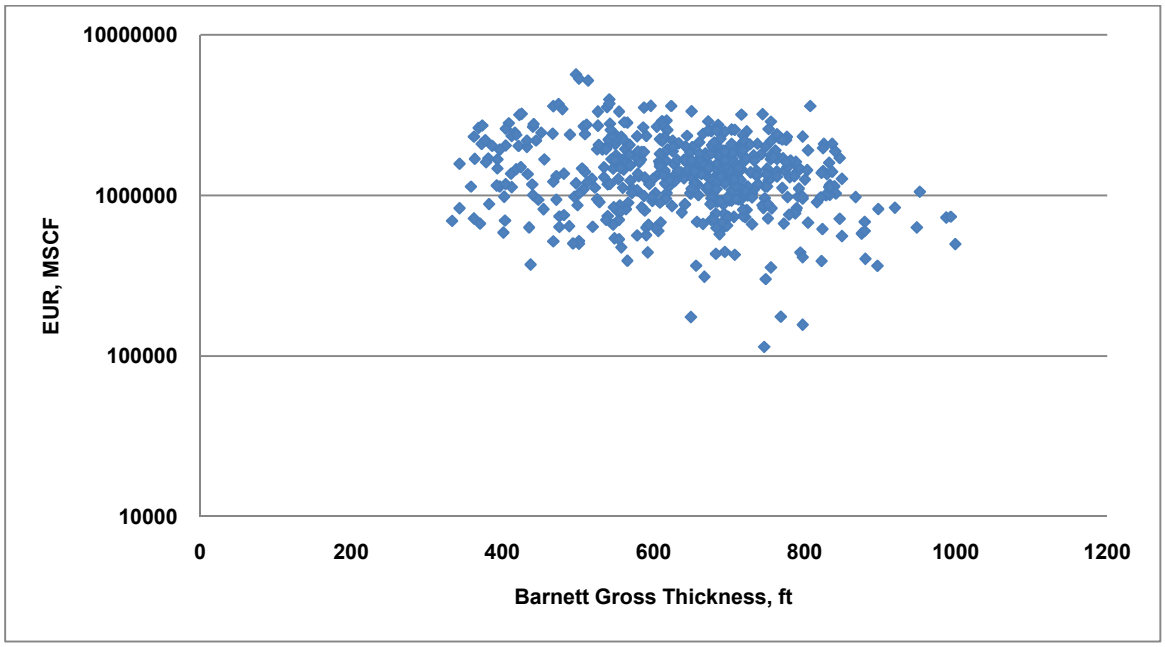

Fig. 3.15: EUR in month 480 vs. Barnett gross thickness (including Forestburg formation) plot.

3.4 Perforation Footage on DMA

Another factor to possibly influence production rate and EUR is the perforation footage. Perforation footage is the sum of lengths of perforated zones in each well. The total perforation footage of each well is copied from Scout Tickets and plugged into a map, generating a perforation footage map **(Fig. 3.16).** This contour map shows the perforation length of each vertical well included in this study. By correlating this map to the same decline maps used in the previous section, no definite correlation could be established. Assuming higher production rates along with higher perforation footage, or vice versa, is not correct here. This poor correlation is illustrated in **Fig. 3.17:** average monthly production rate of each well is plotted versus the corresponding perforation footage. As seen on the plot, no clear correlation could be found; neither could it be found in the EUR vs. perforation footage plot **(Fig. 3.18).** Therefore, perforation footage has no noticeable influence on Barnett Shale production.

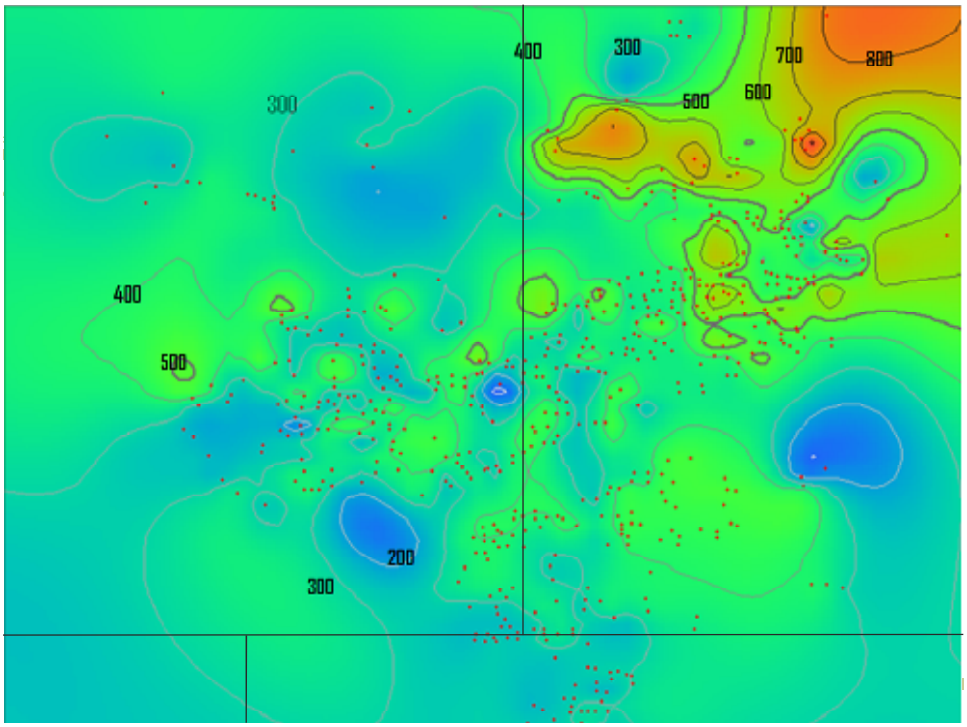

Fig. 3.16: Perforation footage contour map of the current AOI.

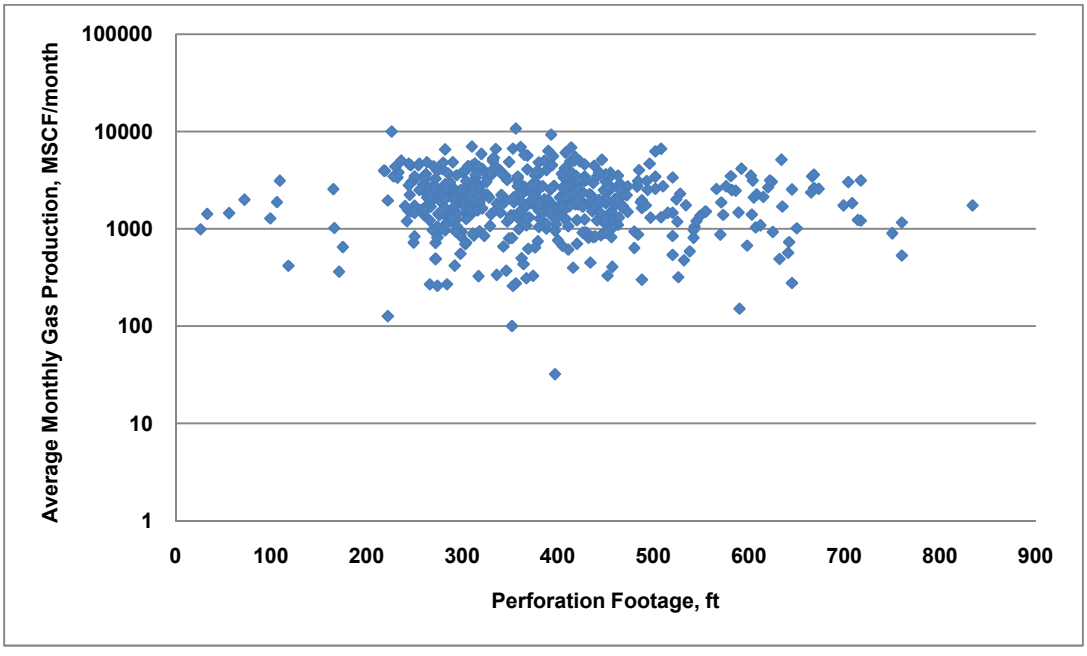

Fig. 3.17: Average monthly gas production of each vertical well vs. perforation footage plot.

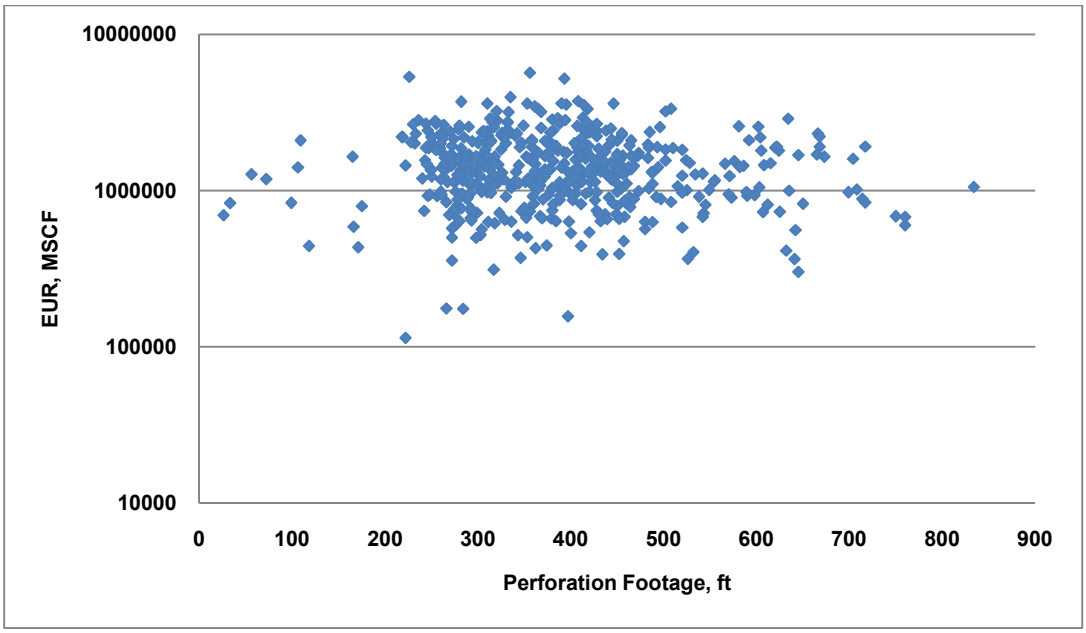

Fig. 3.18: EUR in month 480 vs. perforation footage plot.

3.5 Perforated Barnett Zones on DMA

According to the Scout Tickets, HPDI, and IHS excel sheet, perforation in Barnett Shale mainly starts from top of Upper Barnett to bottom of zone 2 in Lower Barnett. In general, most of the wells have their perforation zones reported as one slot covering that section. **Fig. 3.19** shows the general perforation zone on the type log. The dark blue section on the side indicates the perforated zone.

Although all data sources used in this study: Scout Tickets, HPDI, and IHS excel sheet report same perforated zones, some perforation details seem to be missing. It seems that these data sources provide information on the major perforated zones but do not include the minor ones. It is uncertain to say whether this whole section is perforated or some zones within are selectively perforated. However, completion of zone 1 is the only

visible difference between wells. It is perforated in some wells, and not in others. This section studies the influence of perforating zone 1 on gas production.

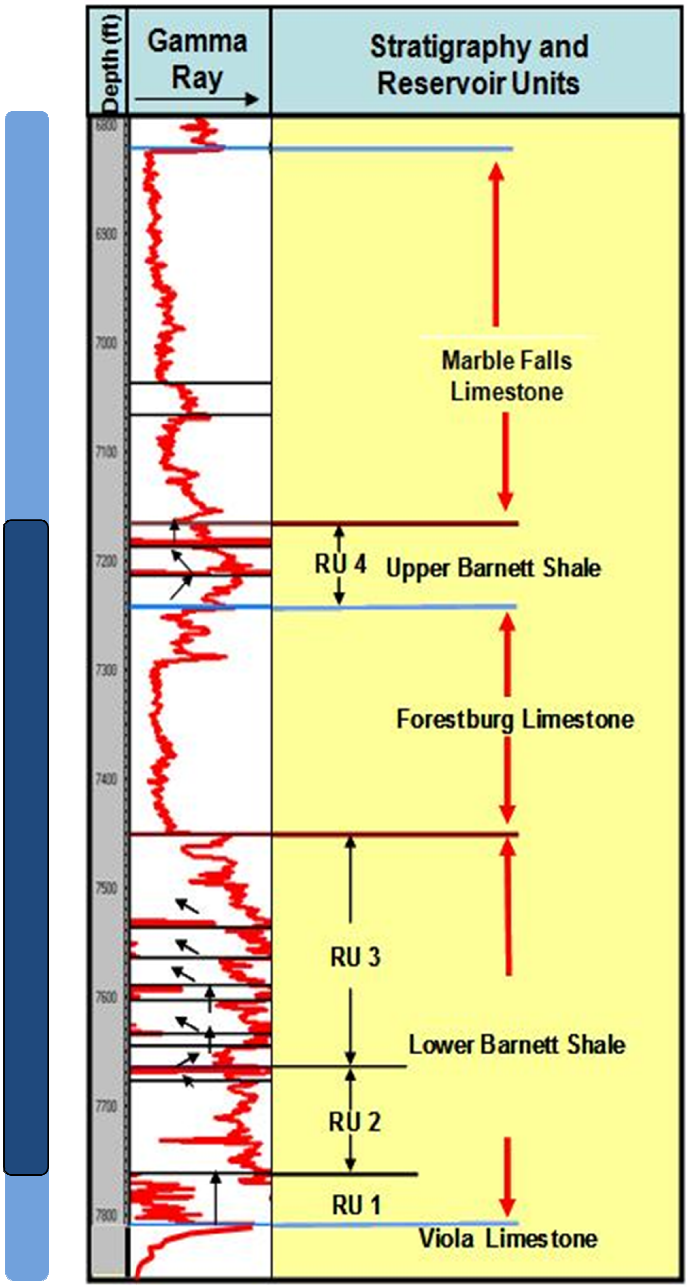

Fig. 3.19: Common Barnett perforated section (dark blue) (Type log from Tian, 2007)

Estimated Ultimate Recovery (EUR) at month 480 for each well of the 35 wells is plotted versus its corresponding first month production rate **(Fig. 3.20).** Data points are plotted representing wells perforating and not perforating zone 1, as indicated by the plot's legend. Wells perforating zone 1 tend to produce more in the first month of production than wells that are not. Perforating zone 1 seems to be one of the factors contributing to higher production rates.

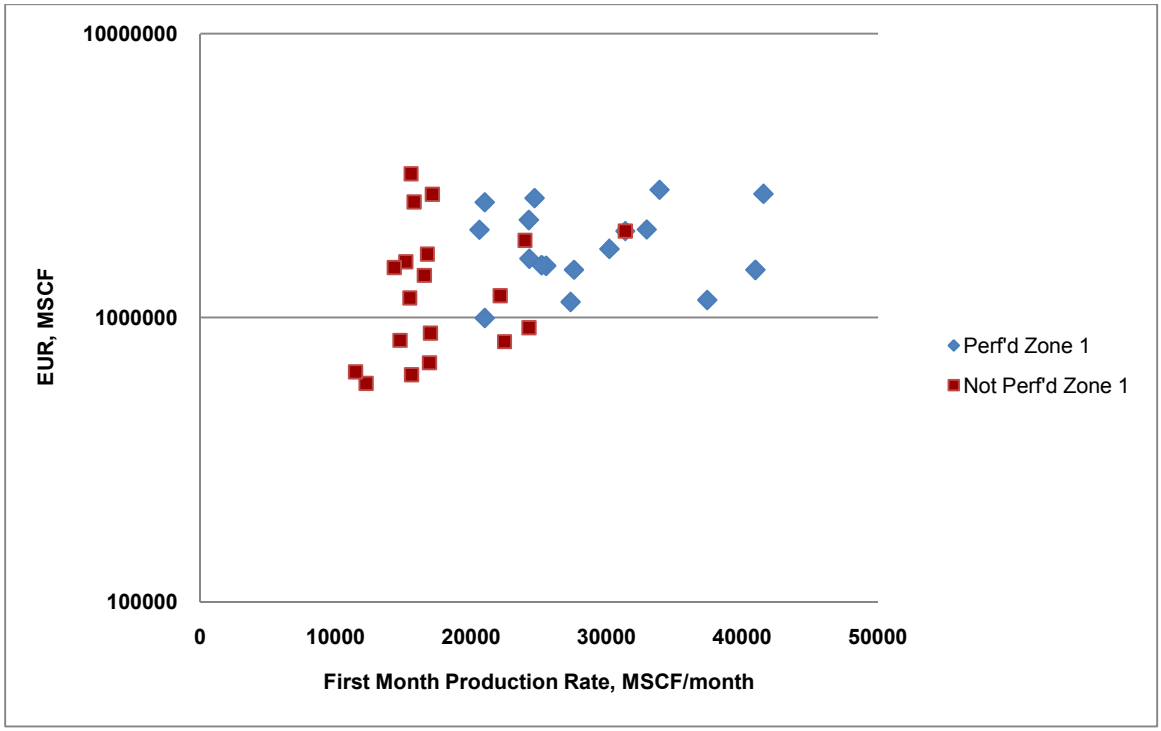

Fig. 3.20: EUR in month 480 vs. first month production rate plot for the 35 wells.

As seen in Fig. 3.20, some wells not perforated in zone 1 produce higher in the first month than wells with zone 1 perforated. This is due to the large distance separating those wells and difference in reservoir thicknesses. In other words, one well with a thick reservoir but not perforated in zone 1 might still produce more than another well with less

thick reservoir and perforated in zone 1. Therefore, to see results of zone 1 perforation more clearly, it is better to compare between wells that are close to each other and within a close range of reservoir thickness. By looking at the thickness map in **Fig. 3.21,** wells in Tarrant county seem to be the right choice since they are close in distance and gross reservoir thickness.

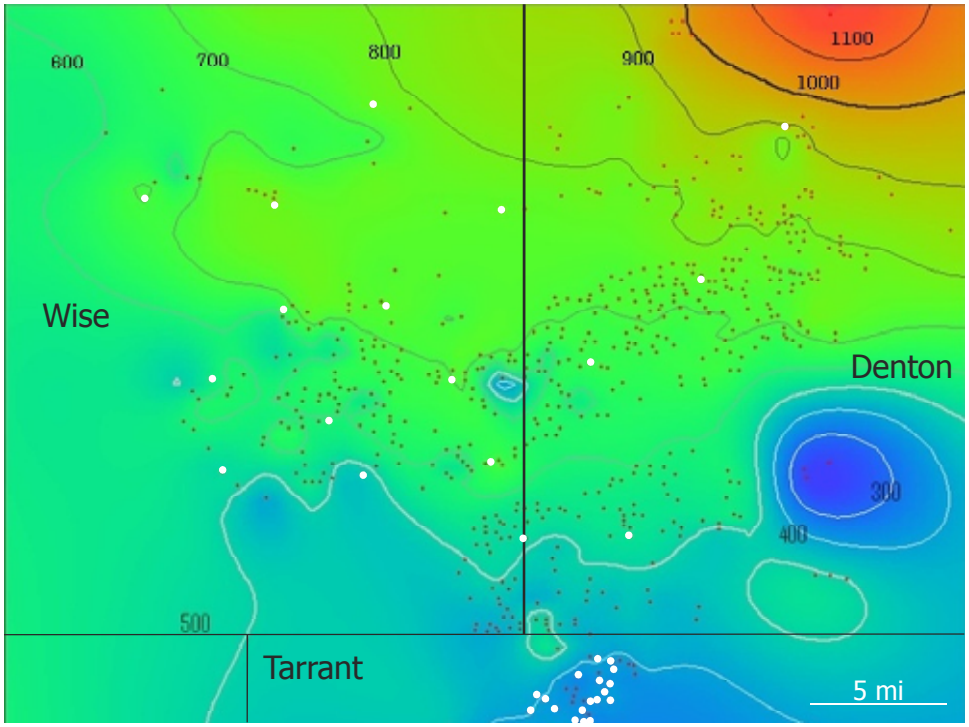

Fig. 3.21: Difference in Barnett thickness between the 35 wells with logs.

Fig. 3.22 is a well log of one of the 18 wells in Tarrant county. The red marks indicate the perforated section in this well. This well did not perforate zone 1. It produced 15,148.78 Mcf of gas in the first month of production. Another Tarrant well is shown in **Fig. 3.23.** This well perforated zone 1 and produced 41,531.69 Mcf of gas in the first month. The only visible difference between these two wells in terms of perforated zones

is zone 1. The latter well perforating zone 1 produced higher in the first month than the first well that did not perforate the same zone.

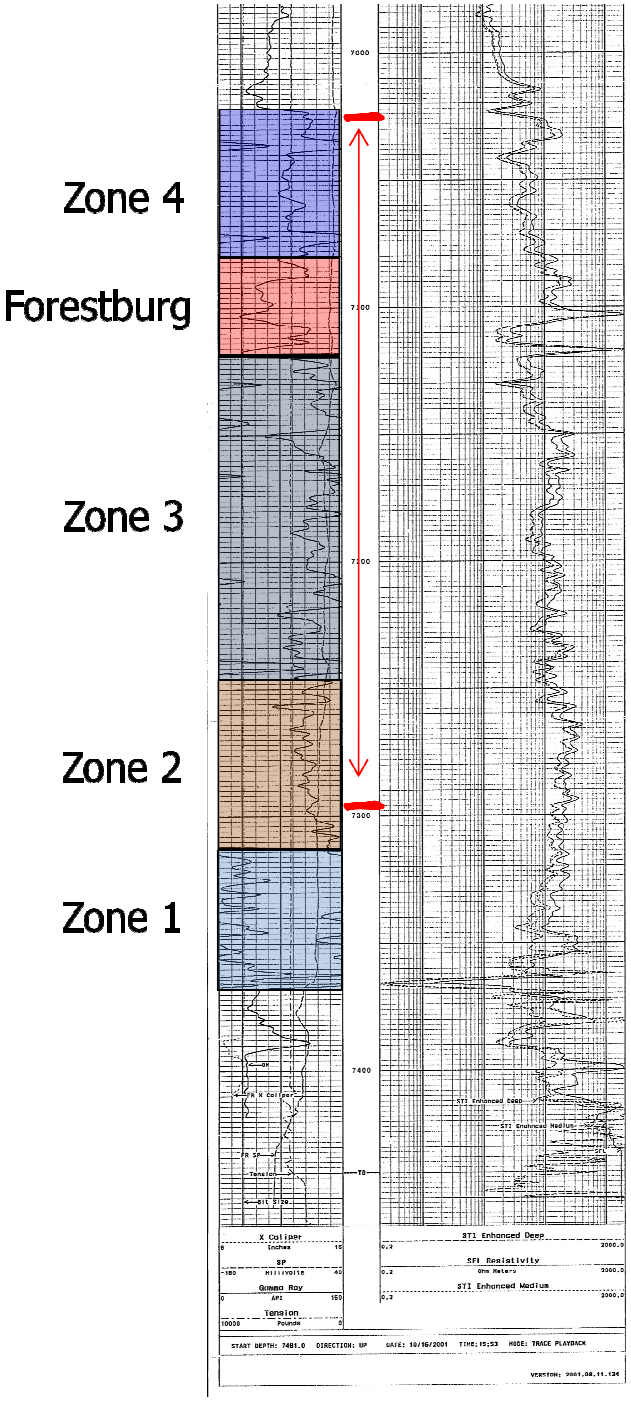

Fig. 3.22: Well log from Tarrant county with zone 1 not perforated.

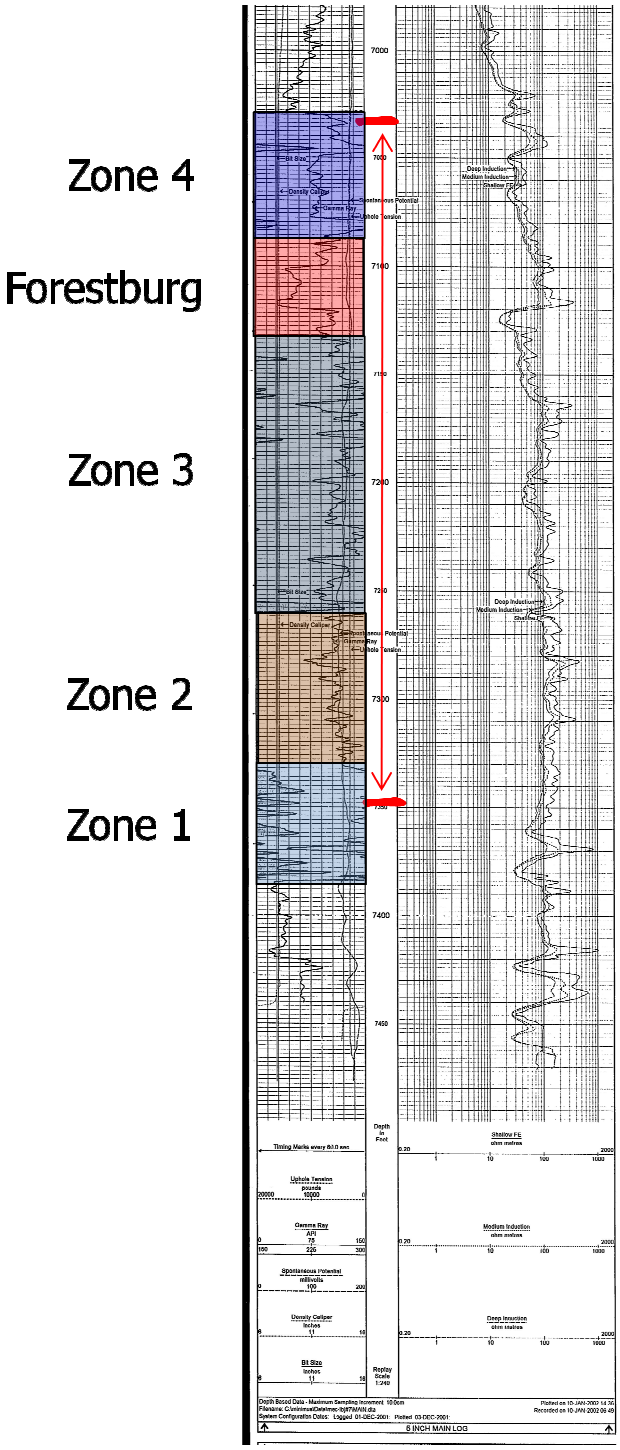

Fig. 3.23: Well log from Tarrant county with perforated zone 1.

In **Fig. 3.24,** Tarrant wells perforating zone 1 tend to produce more in the first month than wells that did not perforate zone 1. Also, they tend to have higher EUR's in month 480. However wells not perforating zone 1 but have high EUR's could be considered exceptions caused by either forecast process uncertainty or reasons beyond the data sources included in this study.

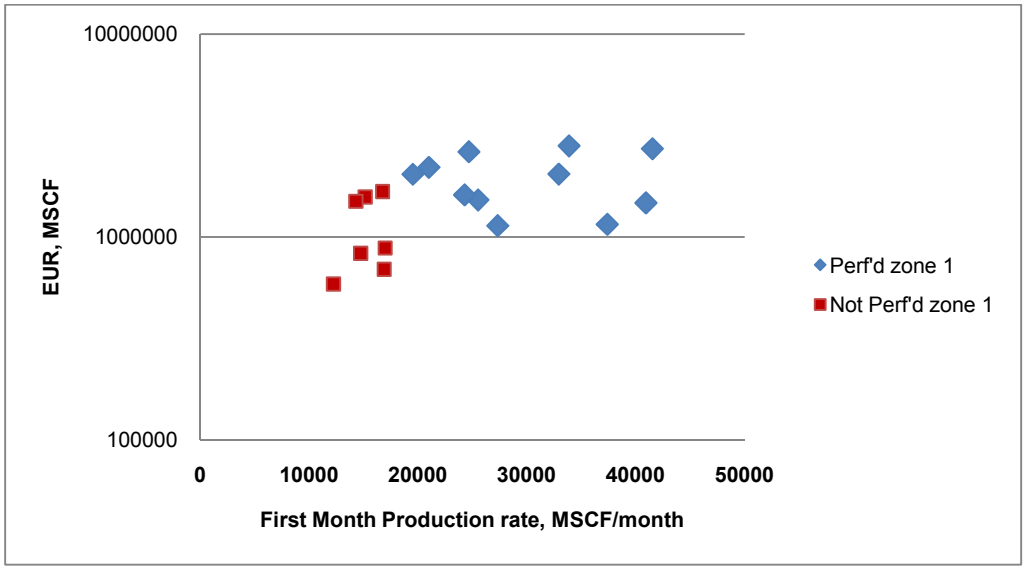

Fig. 3.24: EUR in month 480 vs. first month production rate plot (18 wells in Tarrant county).

Figs. 3.25, 3.26, 3.27, 3.28, 3.29, and 3.30 show these 18 Tarrant wells on the decline maps. As could be seen on month 1 decline map (Fig. 3.25), white wells (perforating zone 1) are producing higher than black wells (not perforating zone 1). Moving through time, by going through the decline maps, white wells are mainly still producing higher than black wells. It could be said now that zone 1 contributes to the total gas produced from Barnett Shale.

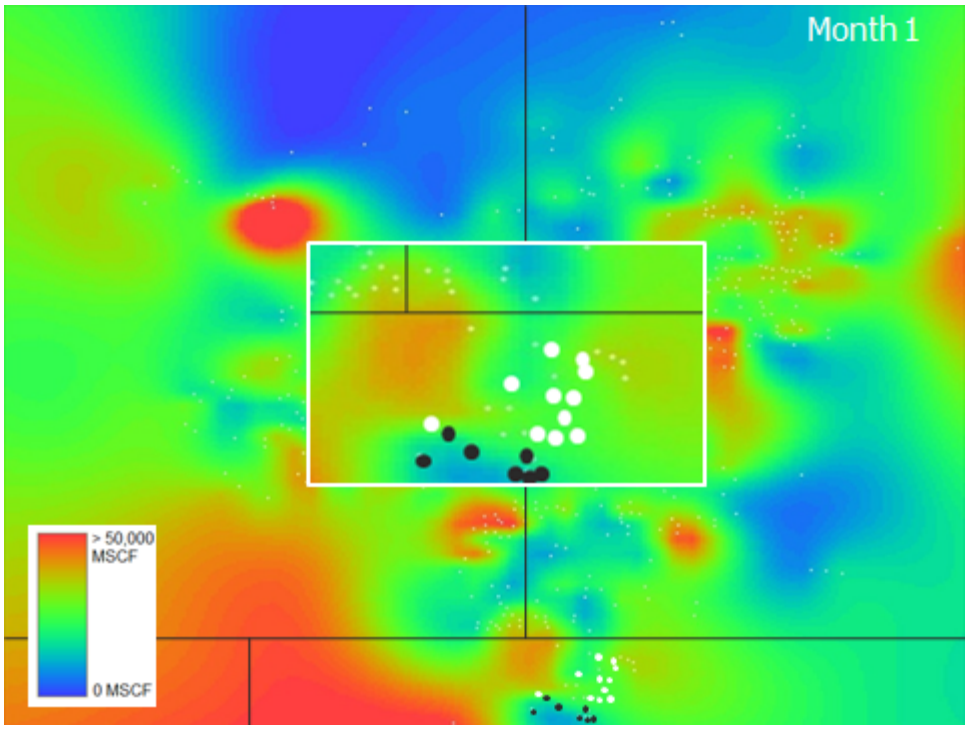

Fig. 3.25: Tarrant wells on first month vertical wells only decline map (white wells: perforating zone 1. Black wells: not perforating zone 1).

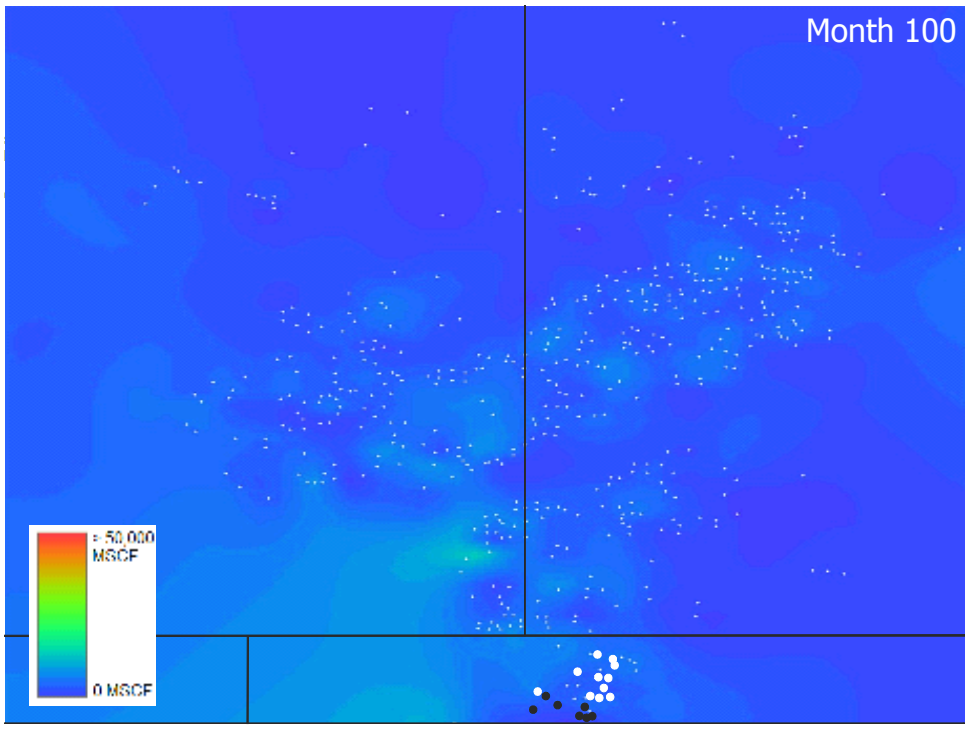

Fig. 3.26: Tarrant wells on 100th month vertical wells only decline map.

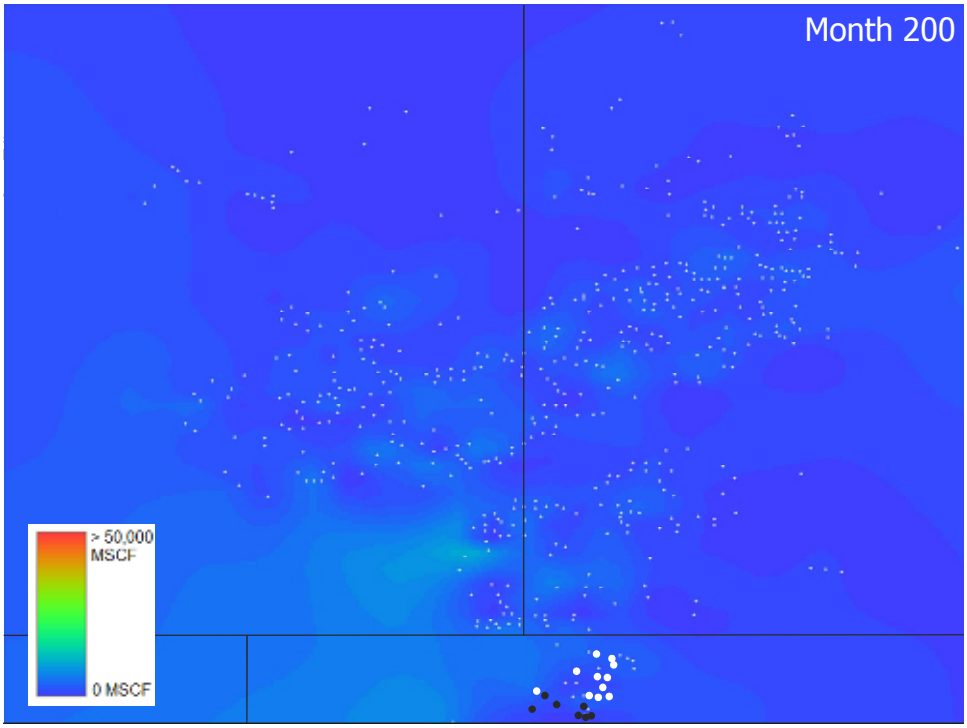

Fig. 3.27: Tarrant wells on 200th month vertical wells only decline map.

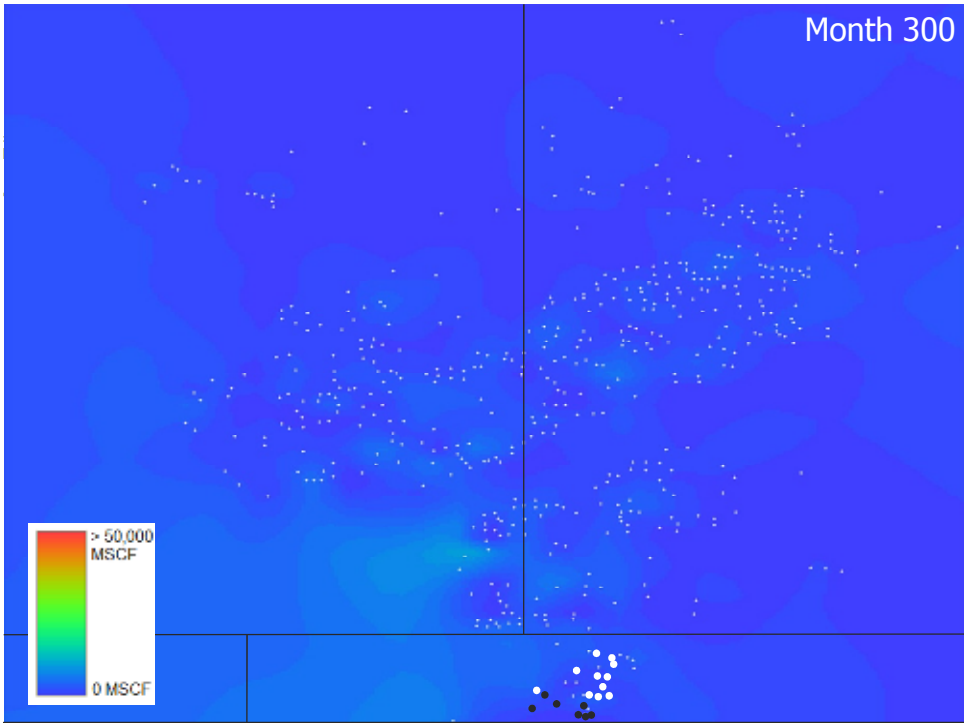

Fig. 3.28: Tarrant wells on 300th month vertical wells only decline map.

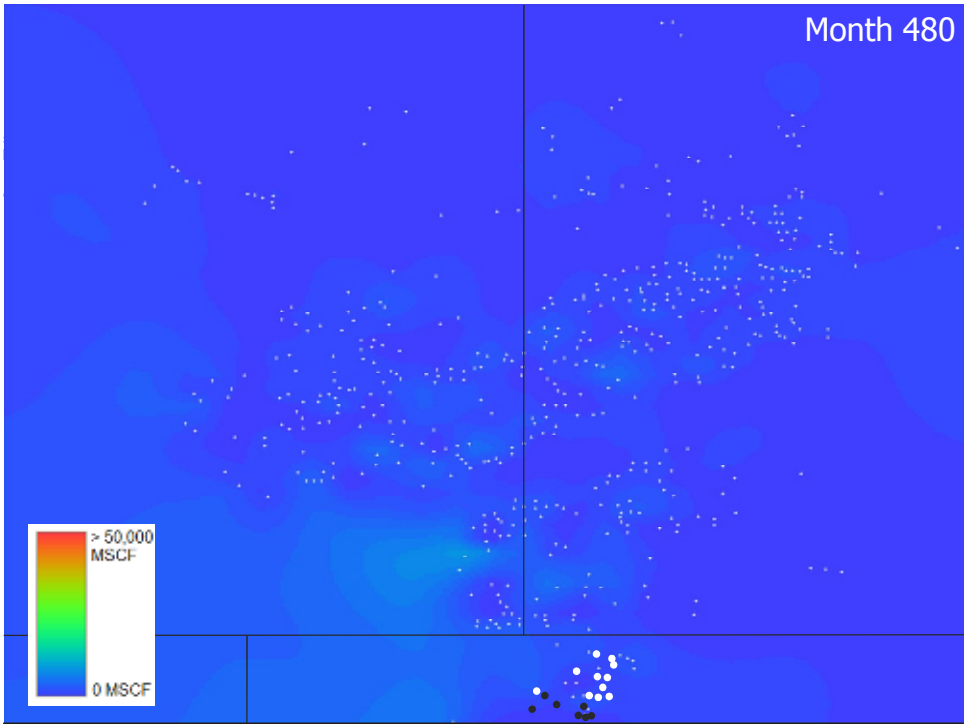

Fig. 3.29: Tarrant wells on 480th month vertical wells only decline map.

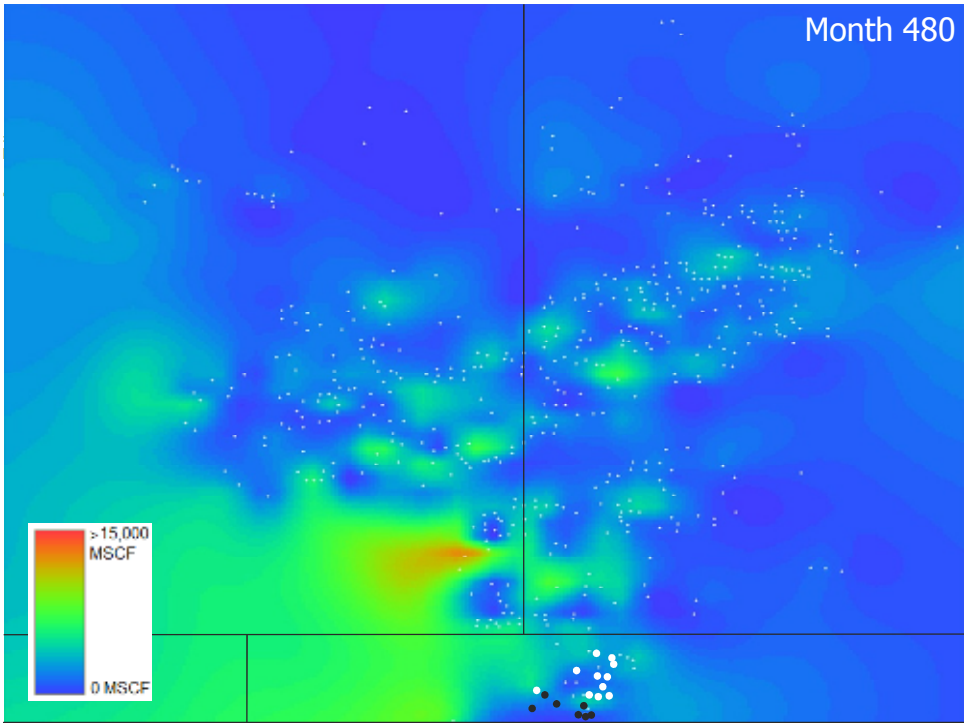

Fig. 3.30: Tarrant wells on 480th month vertical wells only decline map (shifted scale).

Since data sources here do not tell which parts of zones 2, 3, and 4 are perforated, the only way to tell their influence on production is through their thicknesses. Zones thicknesses are read from each individual well log and plotted versus first month productions. **Fig. 3.31** shows the correlation between zone 2 thicknesses in Tarrant wells and corresponding first month production. No definite correlation could be established here. Therefore, contribution of zone 2 to the total production could not be seen through its gross thickness. Zone 3 thicknesses are plotted in the same way versus first month production **(Fig. 3.32).** a possible correlation is observed in Fig 3.32. Wells with thicker zone 3 tend to produce more in the first month of production. Zone 4 thicknesses, Upper Barnett Shale, do not correlate to first month productions, as could be seen in **Fig. 3.33.** This possibly concludes that zones 1 and 3 tend to contribute to total Barnett gas production. However, influence of zones 2 and 4 on production could not be seen through variations in thickness.

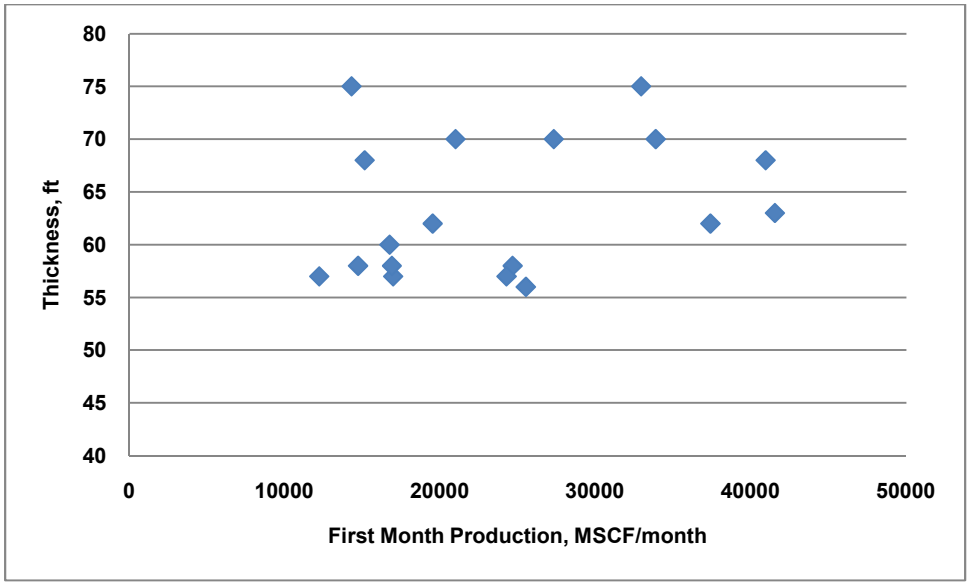

Fig. 3.31: Zone 2 thickness vs. 1st month production rates plot (18 Tarrant wells).

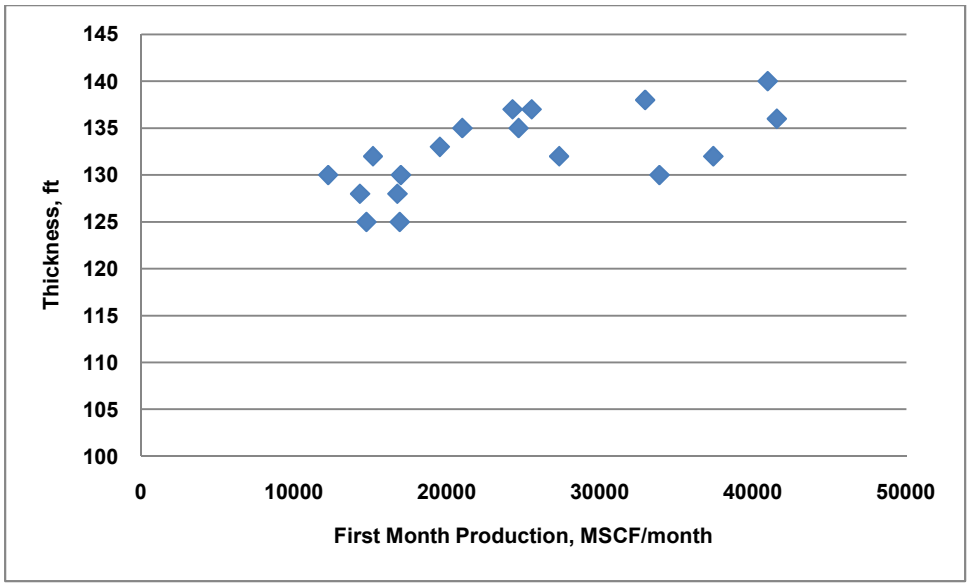

Fig. 3.32: Zone 3 thickness vs. 1st month production rates plot (18 Tarrant wells).

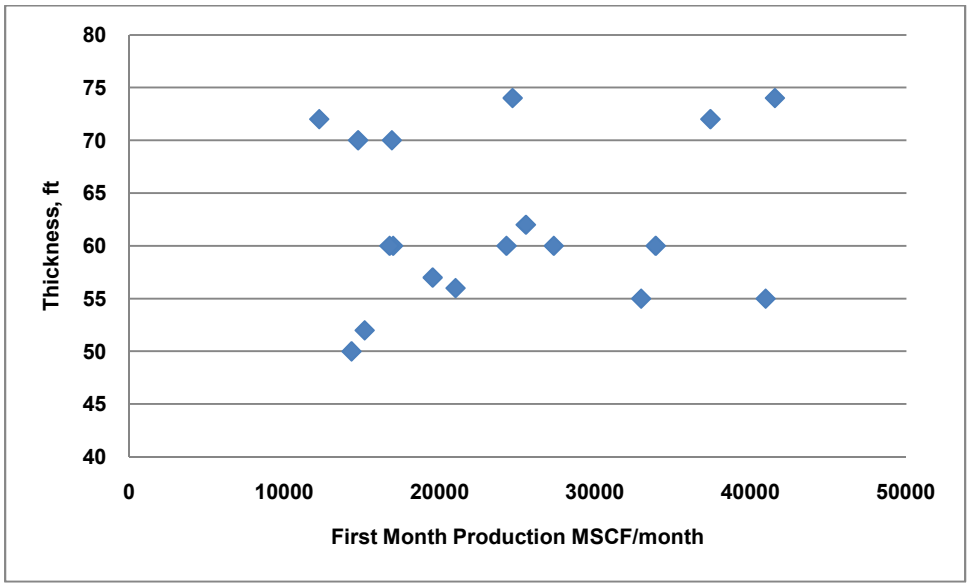

Fig. 3.33: Zone 4 (Upper Barnett) thickness vs. 1st month production rates plot (18 Tarrant wells).

3.6 Limitations

It is worth mentioning that some limitations exist in this study. As mentioned earlier, three data sources only are available and used throughout the study: Scout Tickets, HPDI, and IHS excel sheet. These data sources do not provide any information on the following:

- Reservoir pressure: no data concerning reservoir pressure is available. Therefore, degree of pressure depletions could not be studied or associated with the decline map analysis.
- Well completion: only major perforated sections are available through these data sources. Specified perforated zones are unavailable. These data sources do not provide thorough data regarding completion techniques.
- Horizontal well surveys: in some parts through this study, horizontal wells are excluded. The reason is that no surveys are available. Therefore, reservoir point of entry, lateral lengths, and estimated reservoir exposure could not be specified.
- Well logs: for 560 vertical wells and 221 horizontal wells, 35 vertical well logs are available. Furthermore, these logs include gamma ray and resistivity readings only. No density or neutron logs are available. This shortage limits the extent of petrophysical studies conducted.

CHAPTER IV

CONCLUSIONS AND RECOMMENDATIONS

4.1 Conclusions

Conclusions of this study could be summarized in the following points:

1. According to the forecast process conducted in this study, an average horizontal well production curve declines a little faster than an average vertical well. After 40 years of production, an average horizontal well would produce with a monthly production rate that is 76.4% less than the first month production rate. On the other hand, an average vertical well would produce with a monthly production rate that is 69.4% less than the first month production rate. However, an average horizontal well would still have a higher monthly production rate and higher EUR even though it declines a little faster.
2. Barnett gross reservoir thickness, including the Forestburg formation, does not have a definitive influence on vertical well production decline curves. Therefore, Barnett gross reservoir thickness, including Forestburg formation, does not influence monthly production rates or EUR's in the core area (Denton, Wise, and Tarrant counties)
3. Total perforation footage of each well does not have an effect on monthly production rates. It is seen through this study that no correlation between total perforation footage and monthly production rates or EUR's could be established.

4. Out of Barnett four zones, zone 1 and 3 seem to contribute to Barnett monthly gas production. However, zones 2 and 4 do not show any clear effect on production through variations in gross thickness. This conclusion is determined based on the limited perforation zones data provided from the three data sources included in this study.
5. Decline Map Analysis (DMA) converts decline curves into decline maps. It is a good tool to:
    a. Visualize and compare between decline curves through time easily.
    b. Test the influence of any parameter on all decline curves at the same time and see the results clearly along with each well location on the map.

4.2 Recommendations

To simplify any future work pursued on this study, an excel database is created. This database includes: actual monthly gas production rates, forecasted monthly gas production rates, initial regression plot, and final forecast plot for each individual well. **Fig. 4.1** shows a snapshot of this database interface. By choosing a well API number from the drag-down menu, this interface accesses the database and loads its data on the current sheet. This database contains the 781 wells data included in this study. More wells could be added by one click. This database is available in the Petroleum Department shared folder, along with instructions on adding new wells.

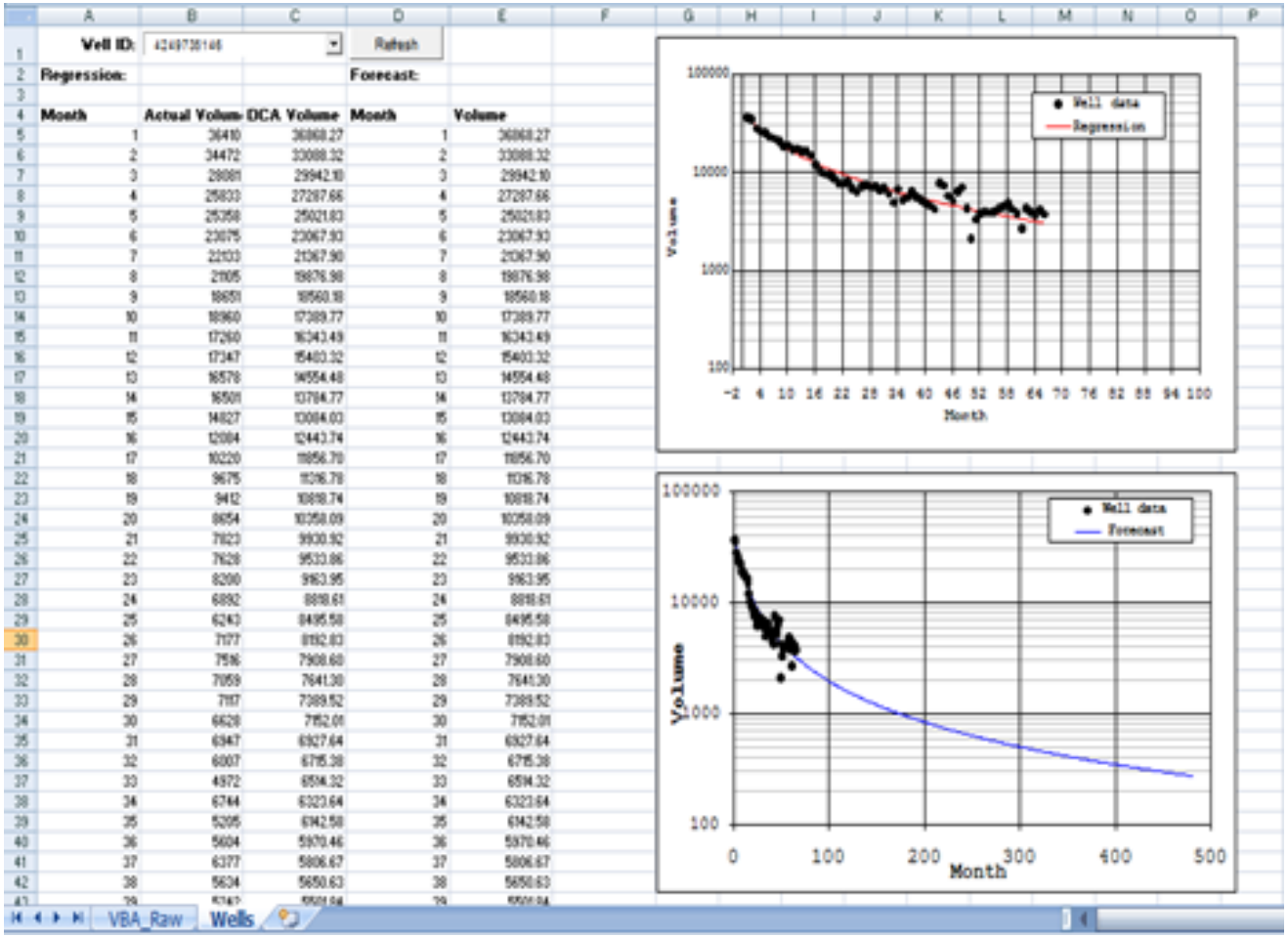

Fig. 4.1: Snapshot of the Barnett production forecasts database.

The following recommendations could be taken into consideration when conducting any further work on this study:

- Integrating well logs with decline maps to study reservoir petrophysical properties and their influence on production rates and decline maps.
- Reservoir pressure data could be used along with decline maps to test its influence on production decline curves behavior.
- Specified perforated zones are needed to see their influence on production rates.
- Any parameter that could possibly affect production rates could be tested on decline maps and see how this parameter correlates to these maps.
- Surveys are needed to include horizontal wells in such studies.
- More Barnett wells could be added and processed similarly to broaden the study.

NOMENCLATURE

AOI	Area of interest
b	Decline exponent
D_i	Initial decline rate
DCA	Decline curve analysis
DMA	Decline map analysis
Q_i	Initial daily gas flow rate
Q_t	Gas flow at “t” time
N_p	Cumulative monthly gas flow

REFERENCES

Ausubel, J.H. 1996. Can Technology Spare the Earth?. *American Scientist* **84**: 166-178.

Barnett Shale History. Barnett Shale Lawsuit, Bamettshalelawsuit.com. Downloaded 27 May 2009.

Bowker, K. A. 2003. Recent Development of the Barnett Shale Play, Fort Worth Basin. *West Texas geological Society Bulletin* **42** (6): 4-11.

Chaouche, A. 2006. Petroleum System Attributes of the Bossier Shale of East Texas and Barnett Shale of North-Central Texas: Evolving Ideas and their Impact on Shale and Tight Sand Gas Resource Assessment. *Gulf Coast Association of Geological Societies Transactions* **56**: 139-149.

Deshpande, V. 2007. General Screening Criteria for Shale Gas Reservoirs and Production Data Analysis of Barnett Shale. M.S Thesis, Texas A&M University, College Station, Texas.

Directional and Horizontal Drilling. Natural Gas, www.naturalgas.org/naturalgas/extraction_directional.asp. Downloaded 5 May 2009.

Flippin, J. W. 1982. The Stratigraphic, Structure, and Economic Aspects of the Paleozoic Strata in Earth County, North-Central Texas. *Dallas Geological Society*: 129-177.

Hayden, J., and Pursell, D. 2005. The Barnett Shale: Visitors Guide to the Hottest Gas Play in the US. Pickering Energy, INC, Houston, Texas (October 2005).

Henry, D. J. 1982. Stratigraphy of the Barnett Shale (Mississippian) and Associated Reefs in the Northern Fort Worth Basin. *Dallas Geological Society*: 157-177.

Hill, D. G., and Nelson, C. R. 2000. Gas Productive Fractured Shales: An Overview and Update. *Gas TIPS* **6** (2): 4-13.

Hill, D. G., Jarvie, D. M., Zumberge, J., Henry, M., and Pollastro, R. M. 2007. Oil and Gas Geochemistry and Petroleum Systems of the Fort Worth Basin. *AAPG Bulletin* **91**: 445-473.

Jarvie, D. M., Claxton, B. L., Henk, F., and Breyer, J. T. 2001. Oil and Shale Gas from the Barnett Shale, Ft. Worth Basin, Texas. *AAPG Annual Meeting Program* **10**: A100.

Lahti, V. R., and Huber, W. F. 1982. The Atoka Group (Pennsylvanian) of the Boonsville Field Area, North-Central Texas. *Dallas Geological Society*: 377-400

Lee, J., and Wattenberger, R. A. 1996. Gas Reservoir Engineering. Textbook Series, SPE, Richardson, Texas **5:** 215-216

Loucks, R. G., and Ruppel, S. C. 2007. Mississippian Barnett Shale: Lithofacies and Depositional Setting of a Deep-water Shale-gas Succession in the Fort Worth Basin, Texas. *AAPG Bulletin* **91** (4): 579-601.

Mohaghegh, S. D., Gaskari, R., and Jalali, J. 2005. New Method for Production Data Analysis to Identify New Opportunities in Mature Fields: Methodology and Application. Paper SPE 98010 presented at the SPE Eastern Regional Meeting. Morgantown, West Virginia, September 14-16.

Montgomery, S. L., Jarvie D. M., Bowker K. A, and Pollastro, R. M. 2005. Mississippian Barnett Shale, Fort Worth Basin, North-Central Texas: Gas-Shale Play with Multi–Trillion Cubic Foot Potential. *AAPG Bulletin* **89** (2): 155-175.

Pollastro, R. M. 2007. Total Petroleum System Assessment of Undiscovered Resources in the Giant Barnett Shale Continuous (Unconventional) Gas Accumulation, Fort Worth Basin, Texas. *AAPG Bulletin* **91** (4): 551-578.

Pollastro, R. M., Jarvie, D. M., Hill, R. J., and Adams, C. W. 2007. Geologic Framework of the Mississippian Barnett Shale, Barnett-Paleozoic Total Petroleum System, Bend Arch-Fort Worth Basin, Texas. *AAPG Bulletin* **91** (4): 405-436.

Rach, N. M. 2004. Drilling Expands in Texas' Largest Gas Field. *Oil & Gas Journal* **102** (3): 45-50.

Tian, Y. 2009. Regional Stratigraphic and Sedimentary Facies Analyses, Barnett Shale, Fort Worth Basin, Texas. Ongoing M.S Thesis, Texas A&M University, College Station, Texas.

Zhao, H., Givens, N. B., and Curtis, B. 2007. Thermal Maturity of the Barnett Shale Determined from Well-log Analysis. *AAPG Bulletin* **91** (4): 535-549.

APPENDIX

DECLINE MAPS OF CURRENT AOI

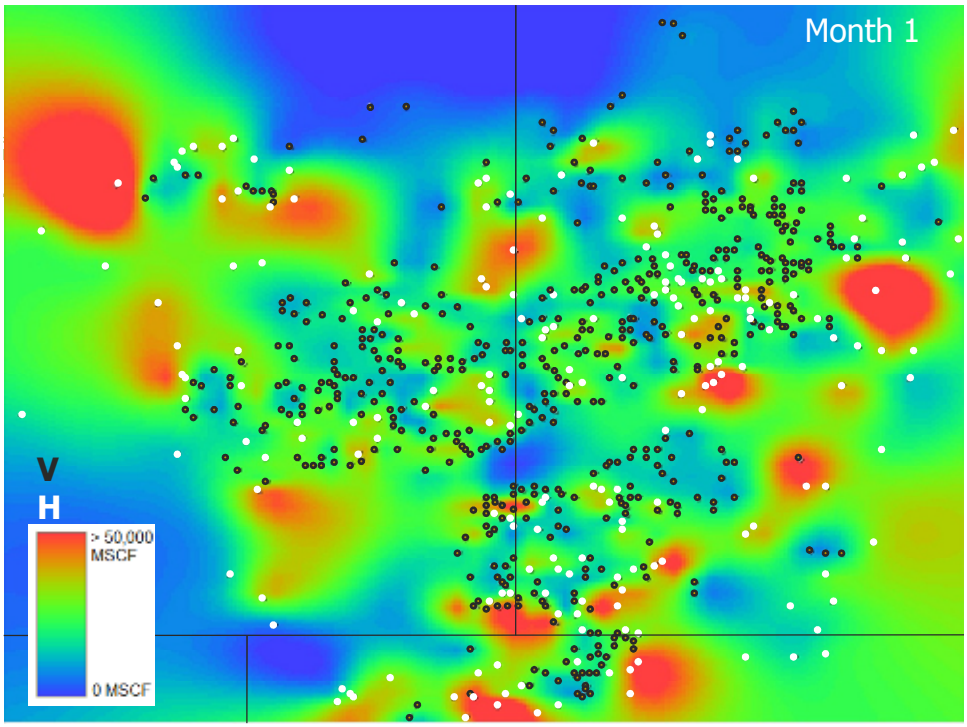

Fig. A-1: First month decline map of the current AOI.

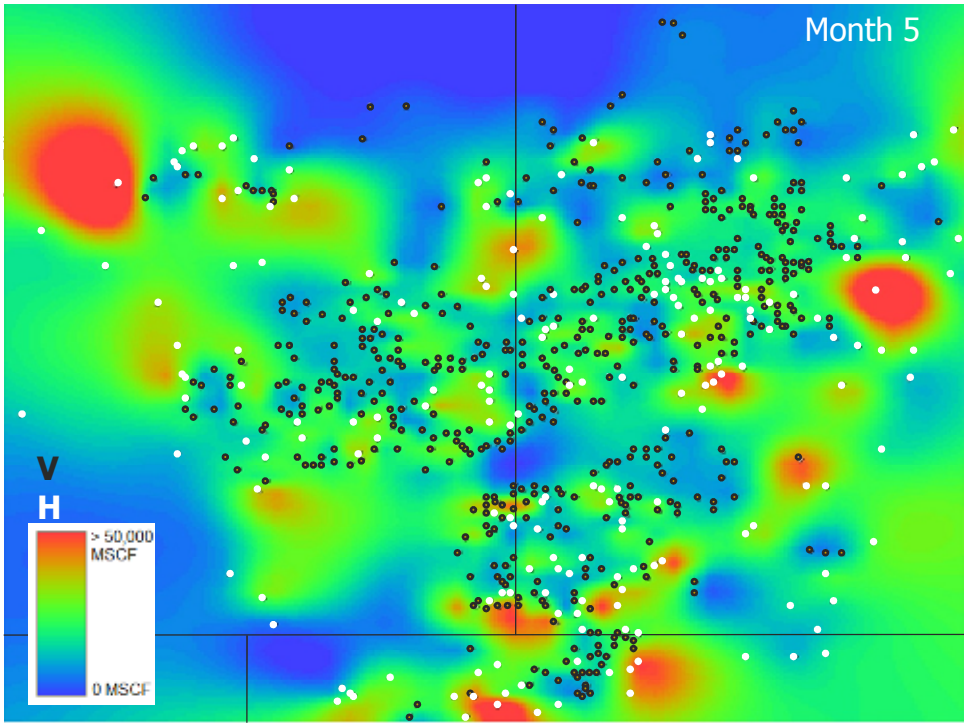

Fig. A-2: 5th month decline map of the current AOI.

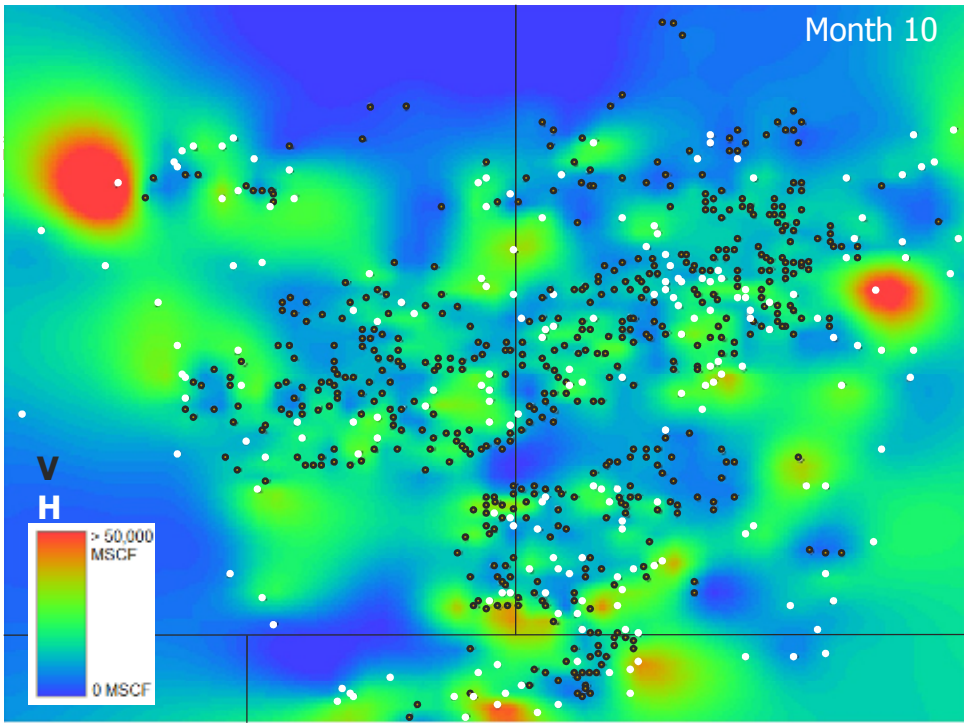

Fig. A-3: 10th month decline map of the current AOI.

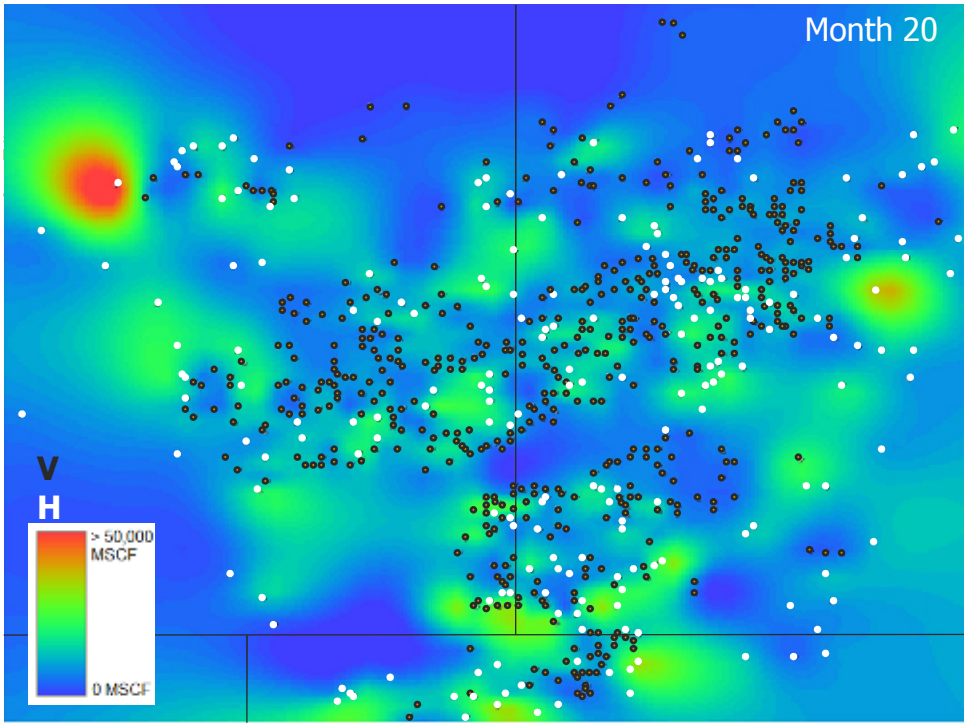

Fig. A-4: 20th month decline map of the current AOI.

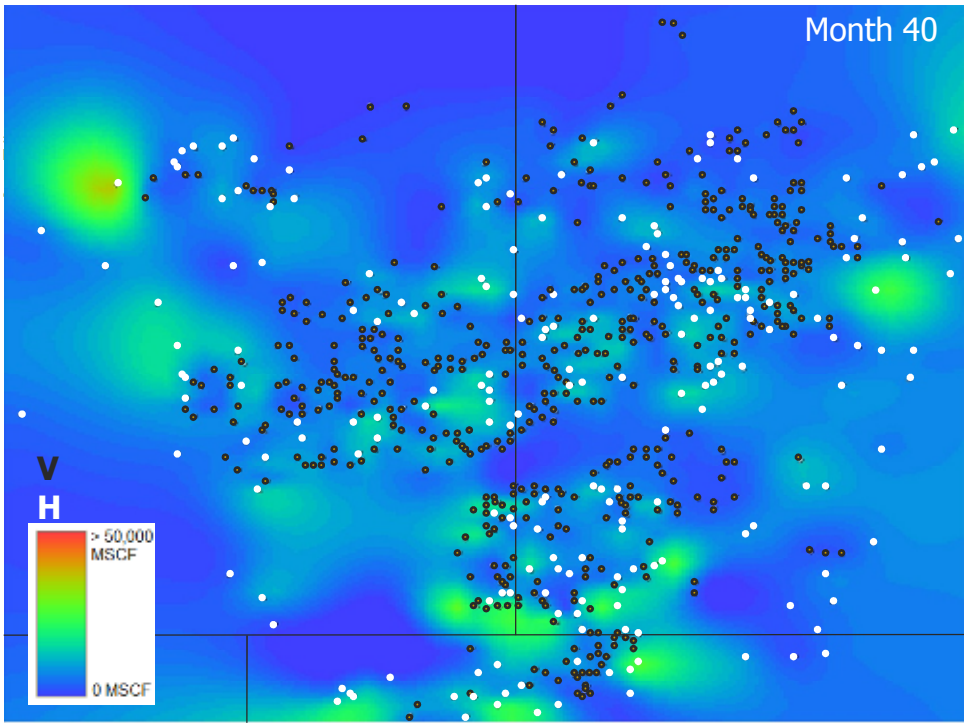

Fig. A-5: 40th month decline map of the current AOI.

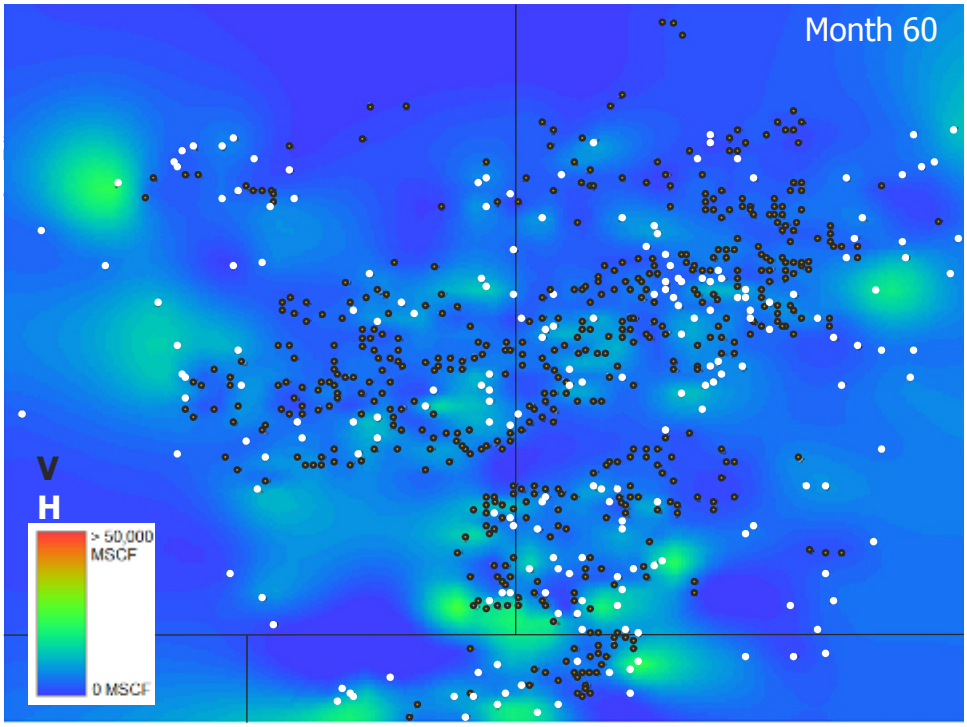

Fig. A-6: 60th month decline map of the current AOI.

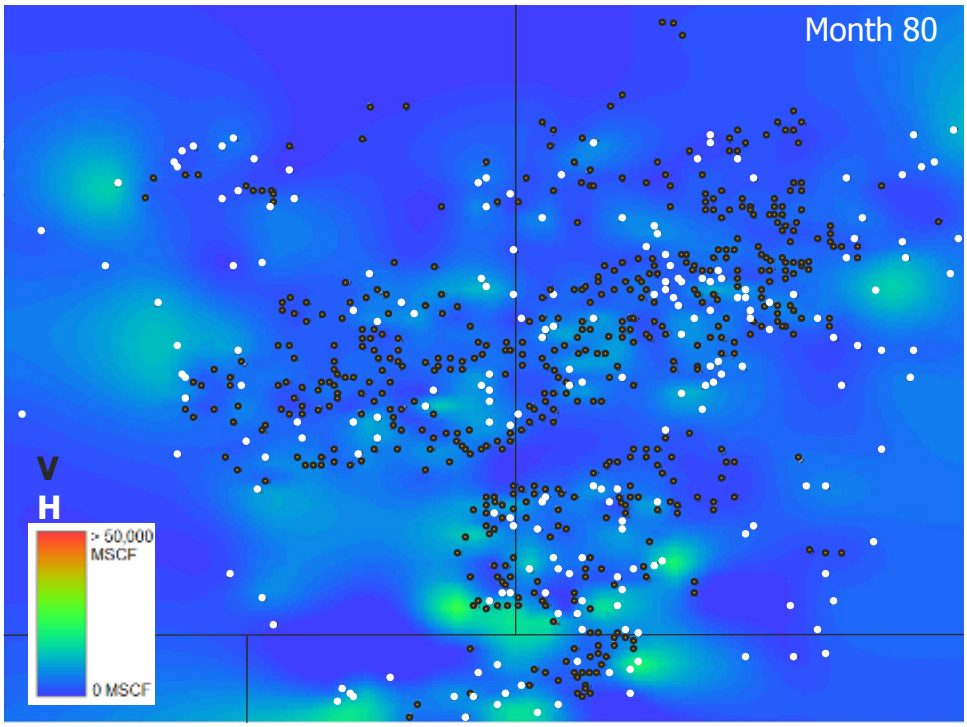

Fig. A-7: 80th month decline map of the current AOI.

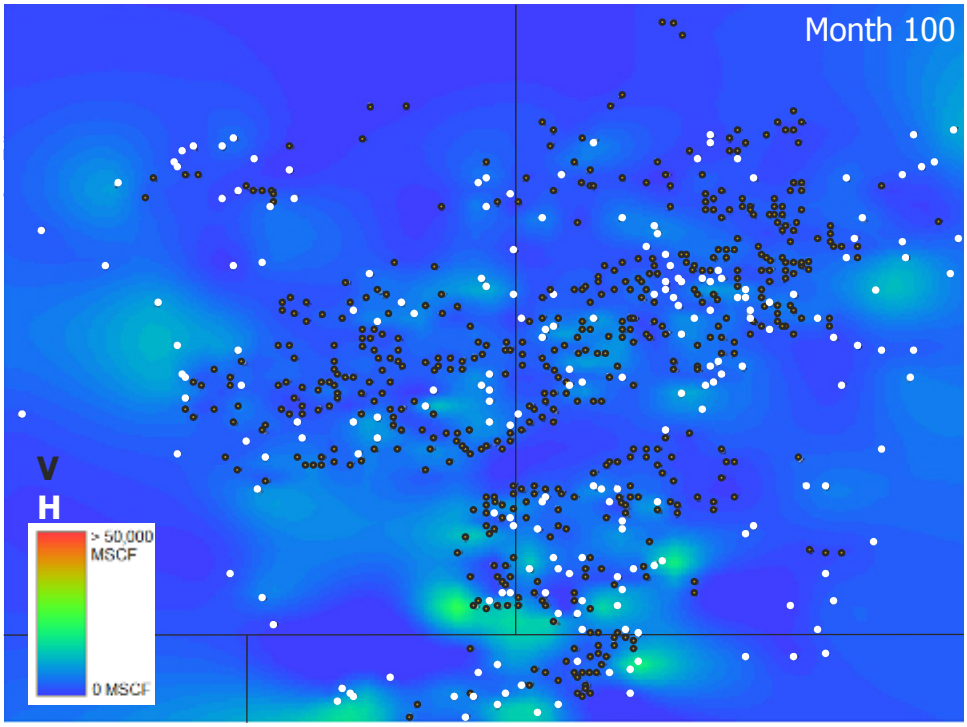

Fig. A-8: 100th month decline map of the current AOI.

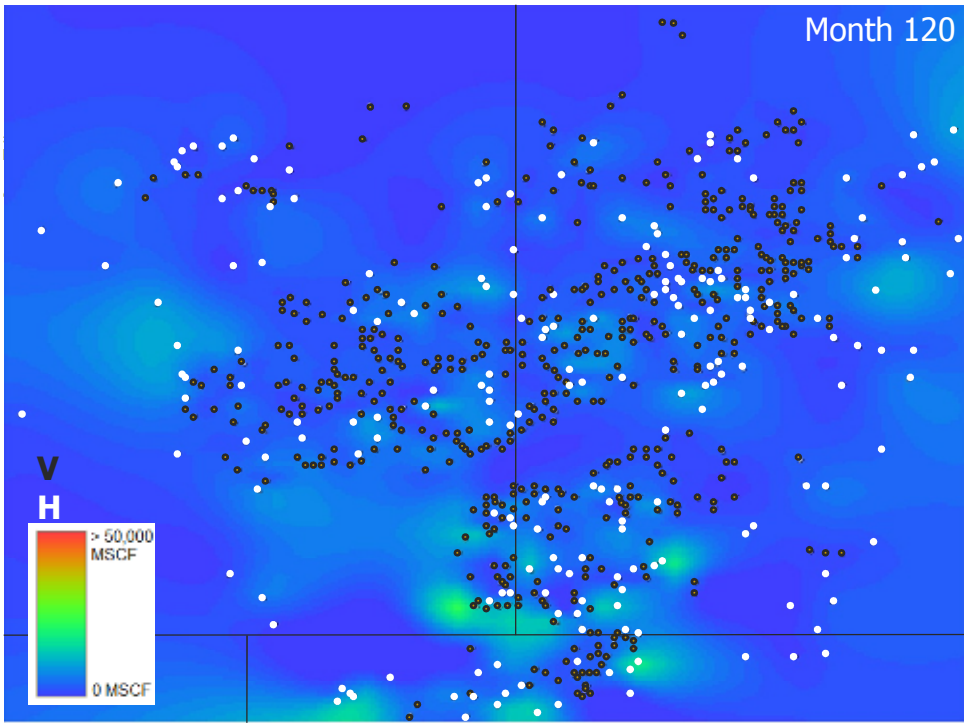

Fig. A-9: 120th month decline map of the current AOI.

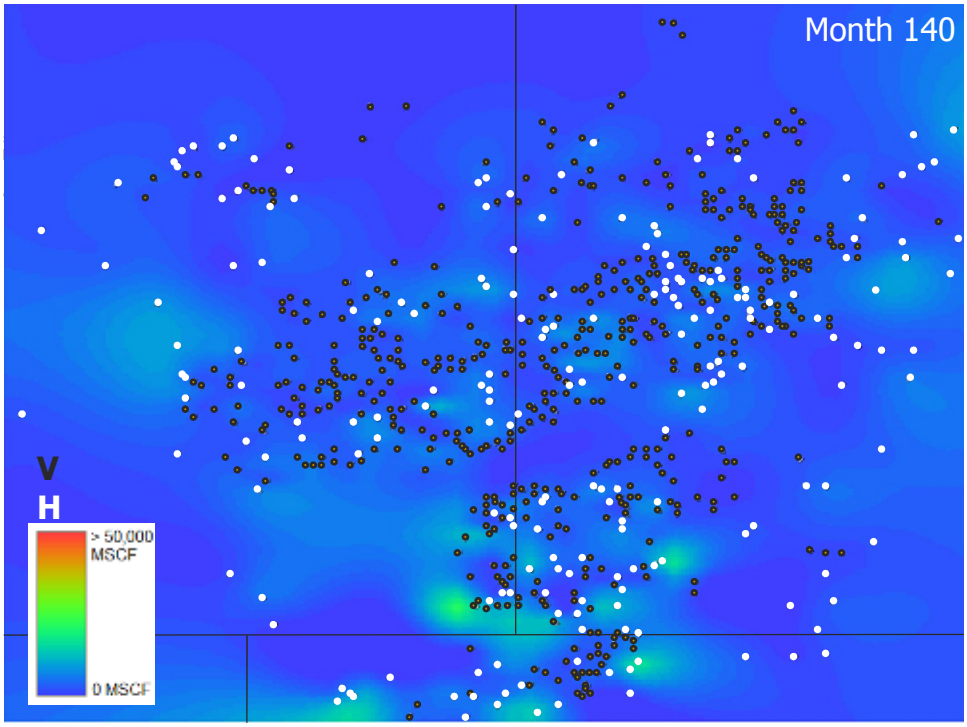

Fig. A-10: 140th month decline map of the current AOI.

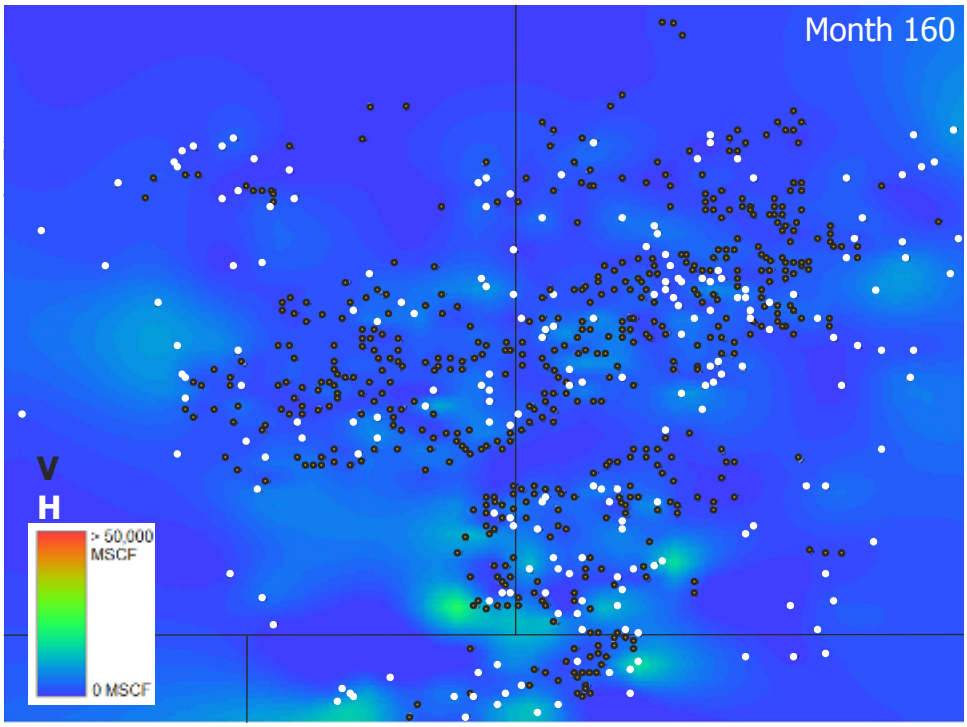

Fig. A-11: 160th month decline map of the current AOI.

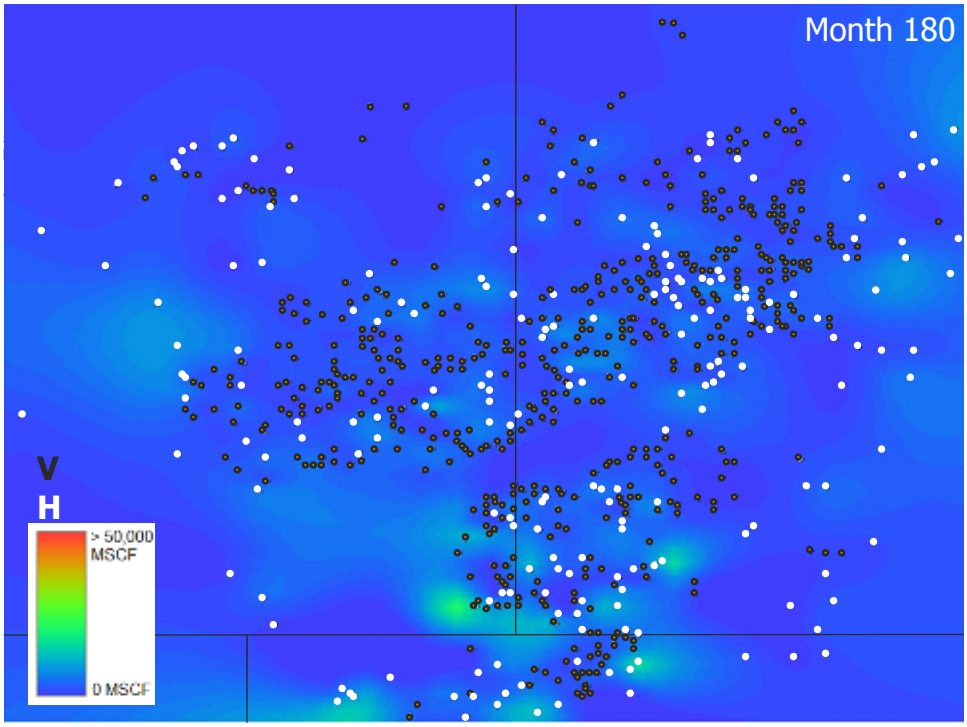

Fig. A-12: 180th month decline map of the current AOI.

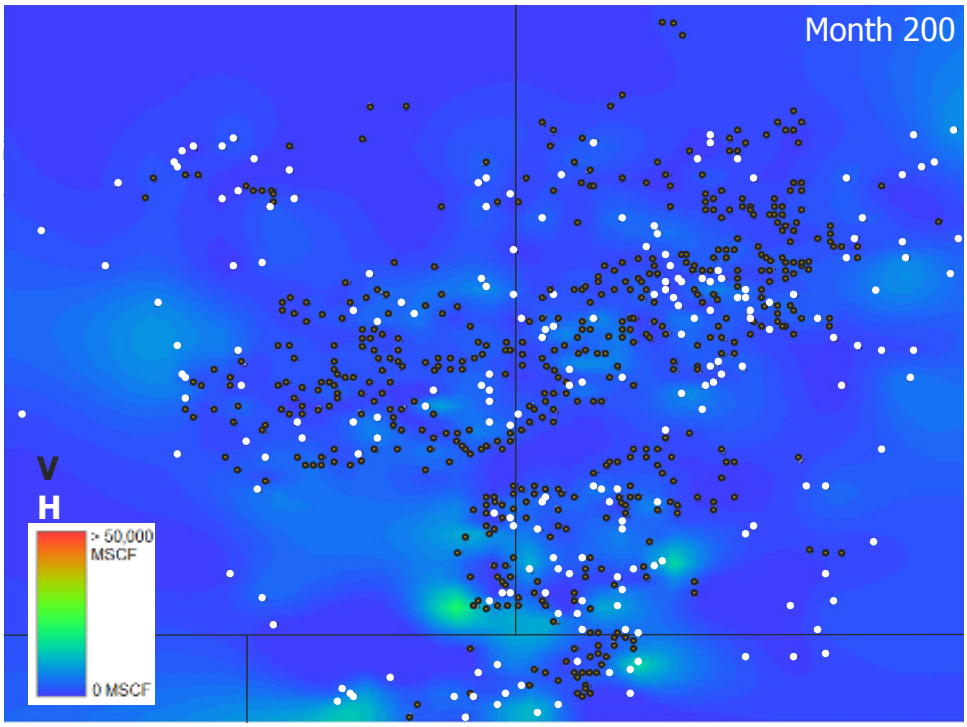

Fig. A-13: 200th month decline map of the current AOI.

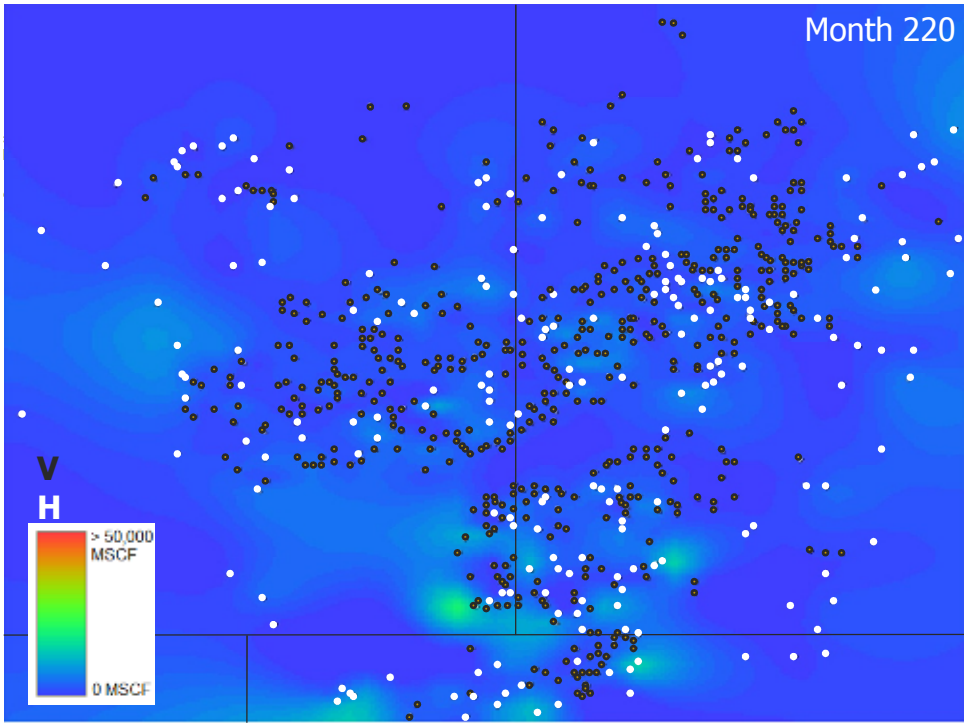

Fig. A-14: 220th month decline map of the current AOI.

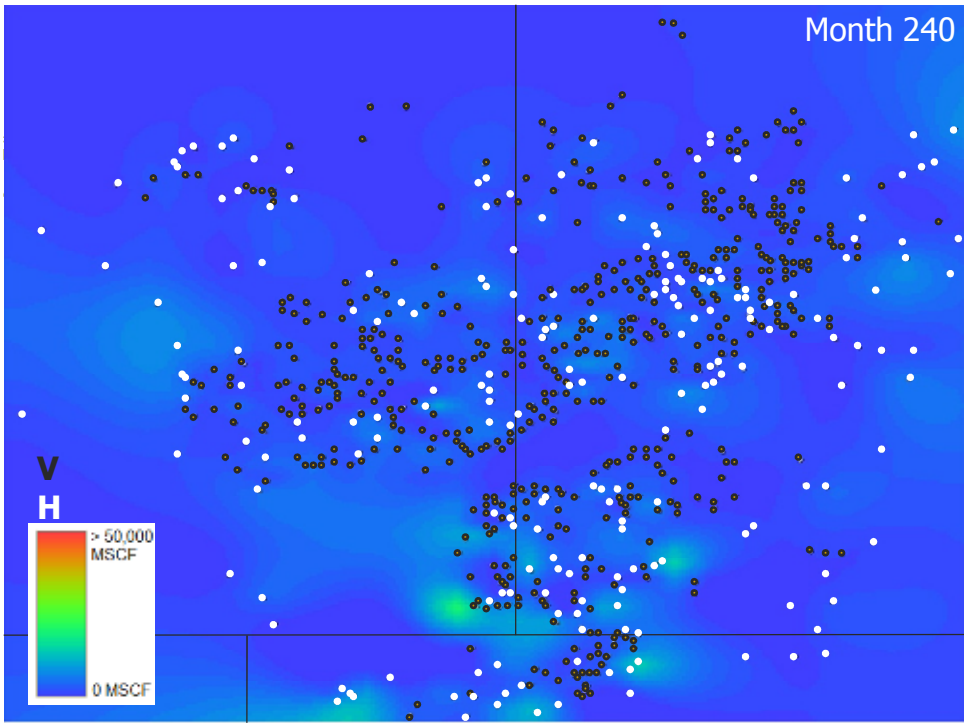

Fig. A-15: 240th month decline map of the current AOI.

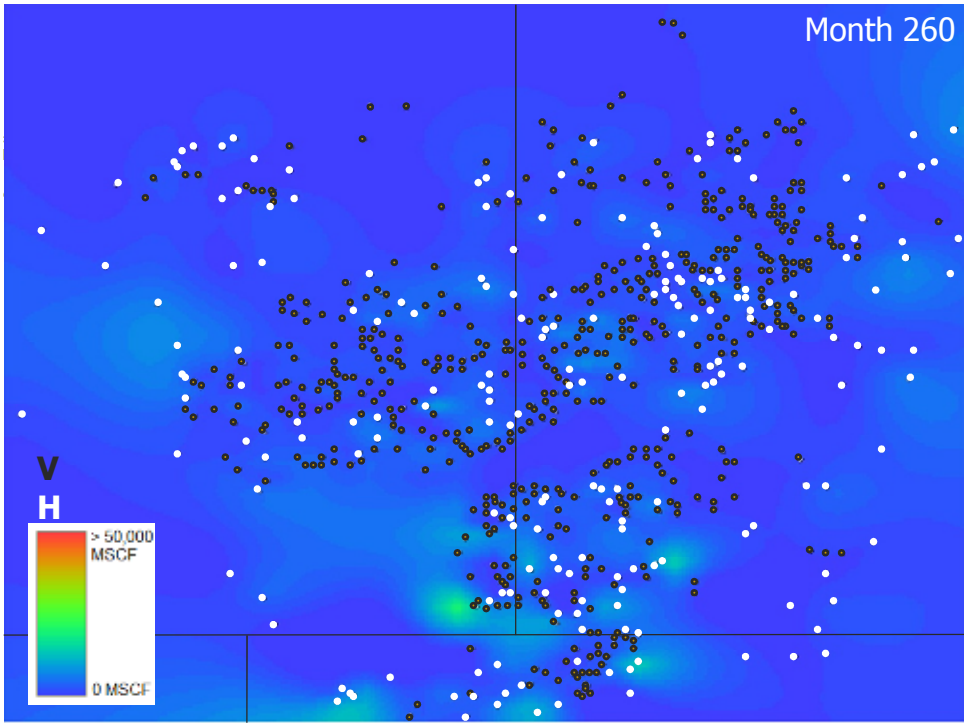

Fig. A-16: 260th month decline map of the current AOI.

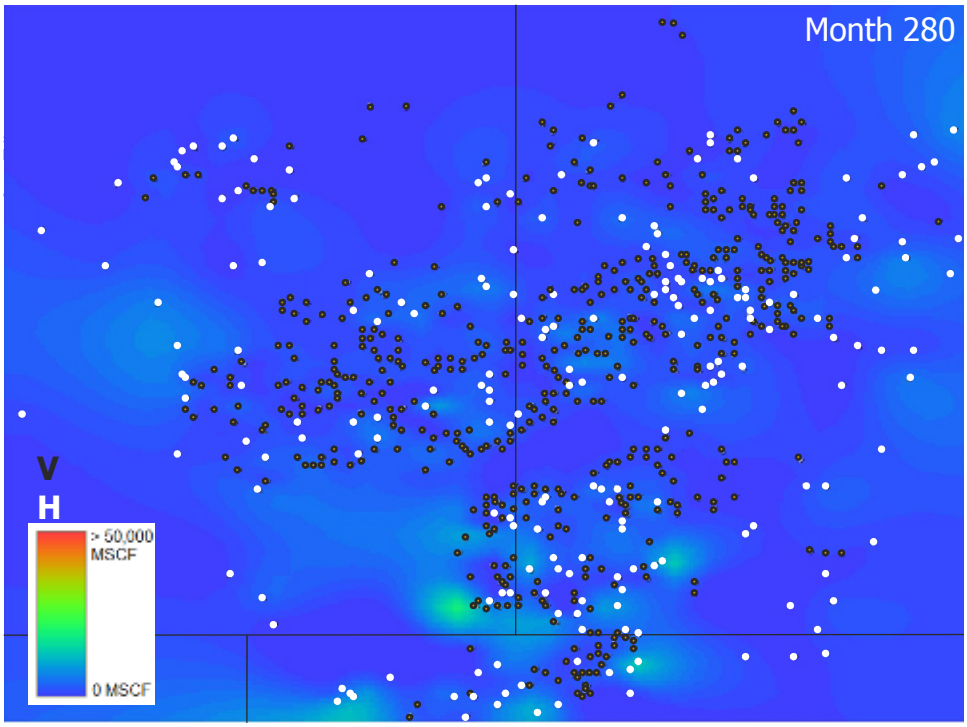

Fig. A-17: 280th month decline map of the current AOI.

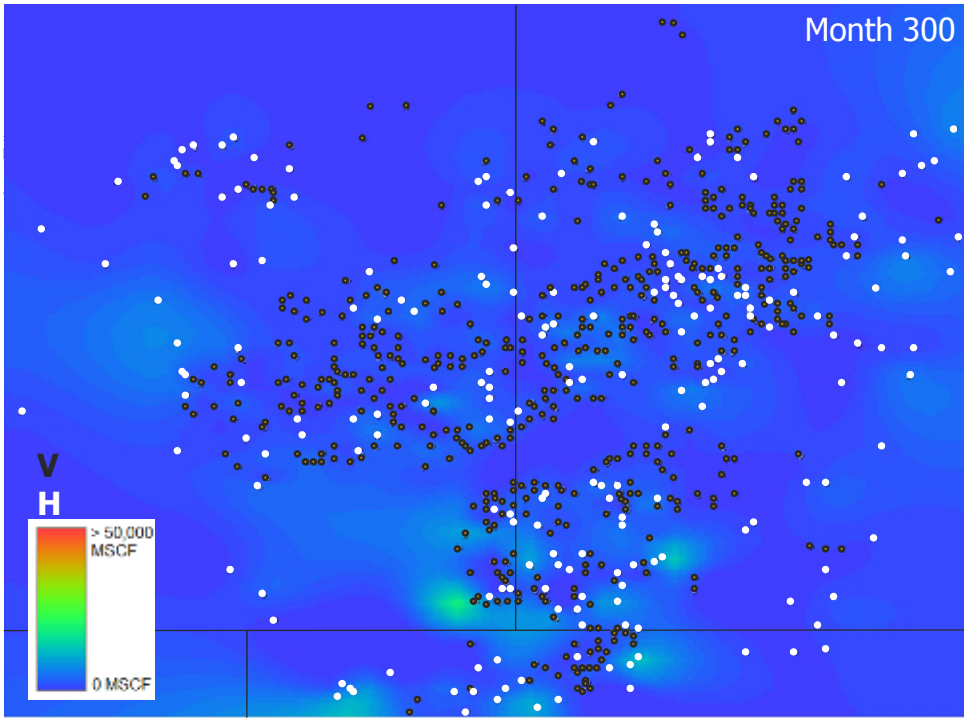

Fig. A-18: 300th month decline map of the current AOI.

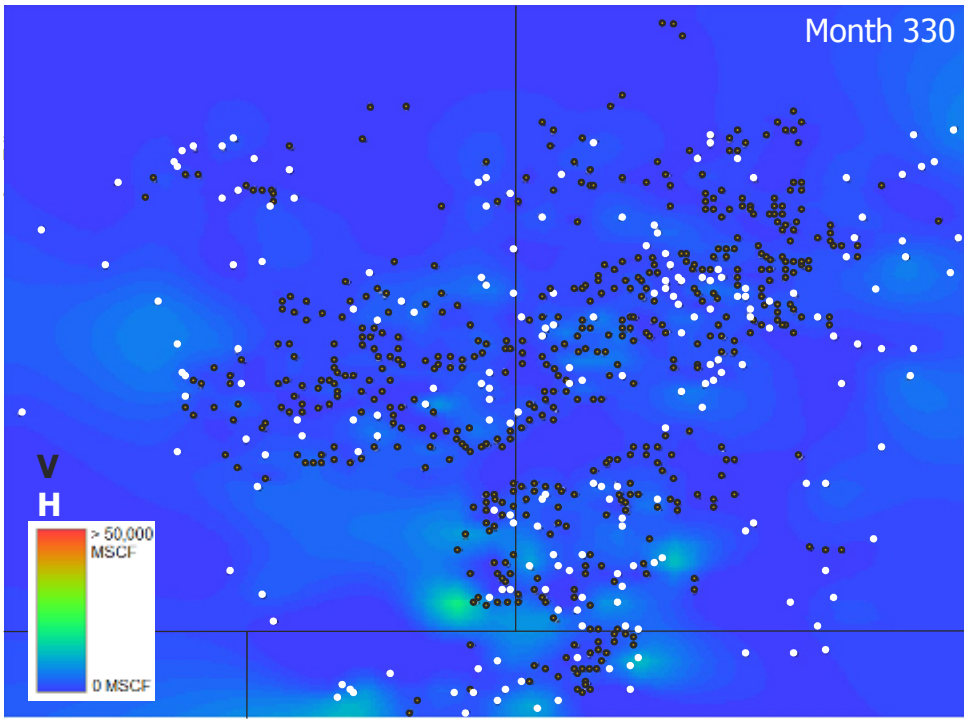

Fig. A-19: 330th month decline map of the current AOI.

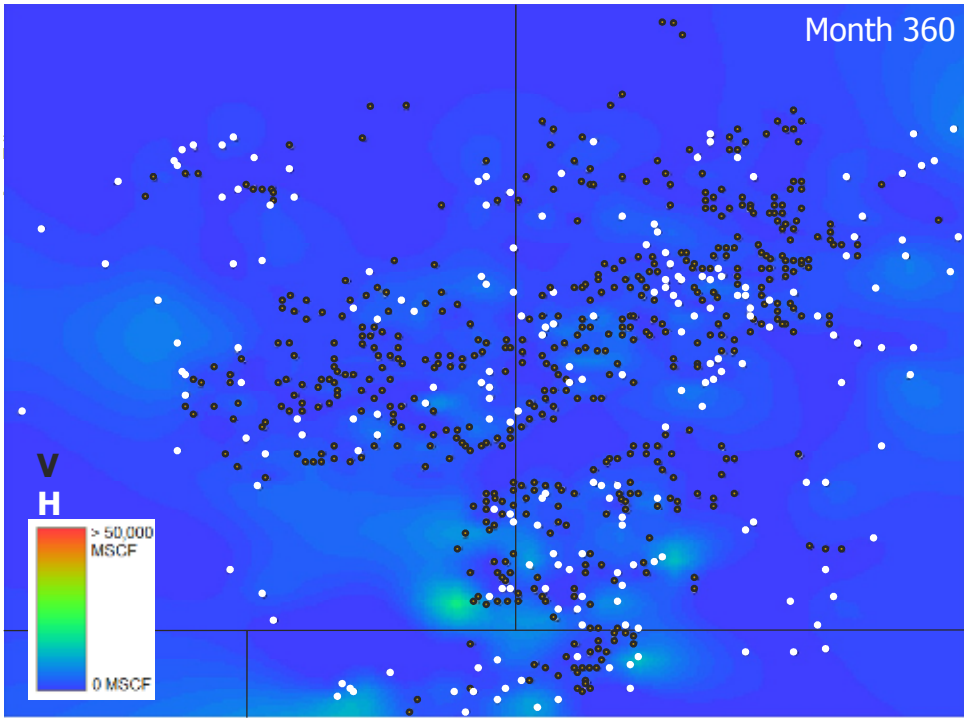

Fig. A-20: 360th month decline map of the current AOI.

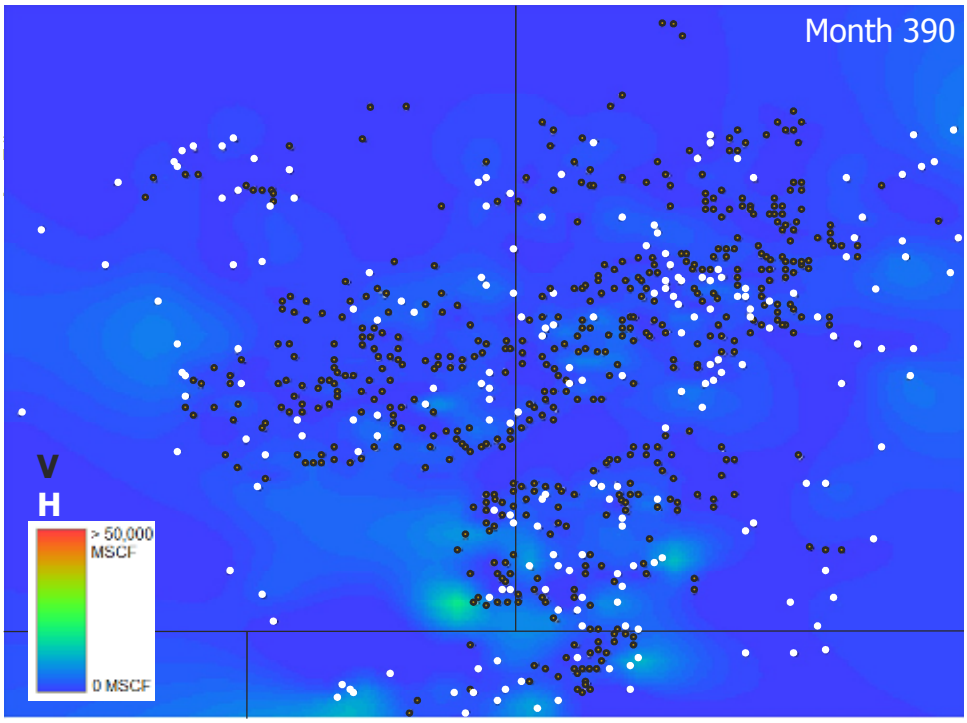

Fig. A-21: 390th month decline map of the current AOI.

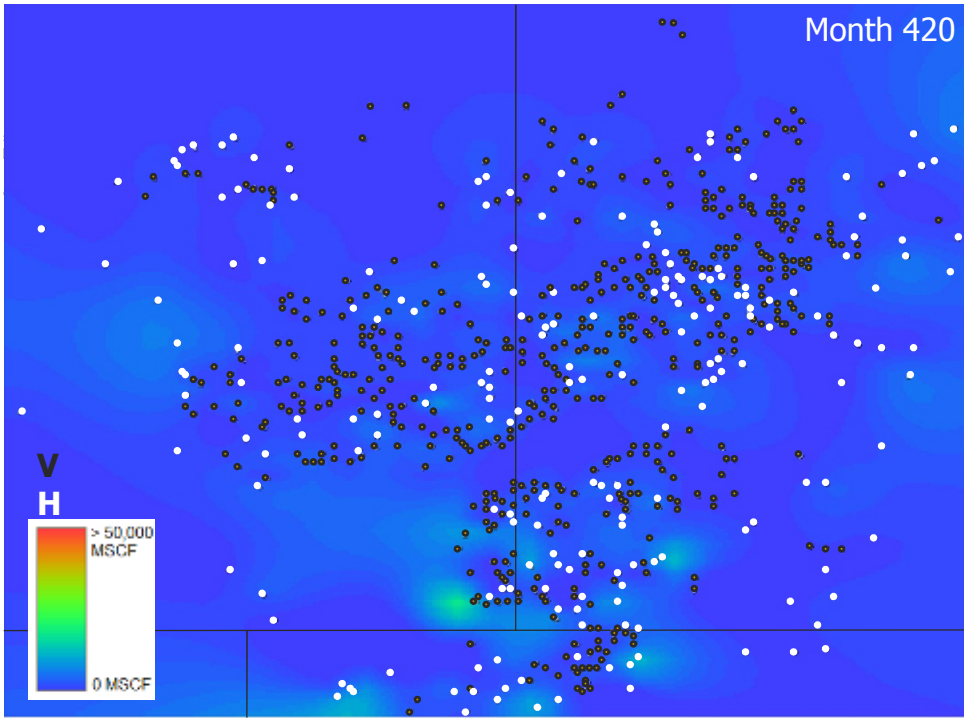

Fig. A-22: 420th month decline map of the current AOI.

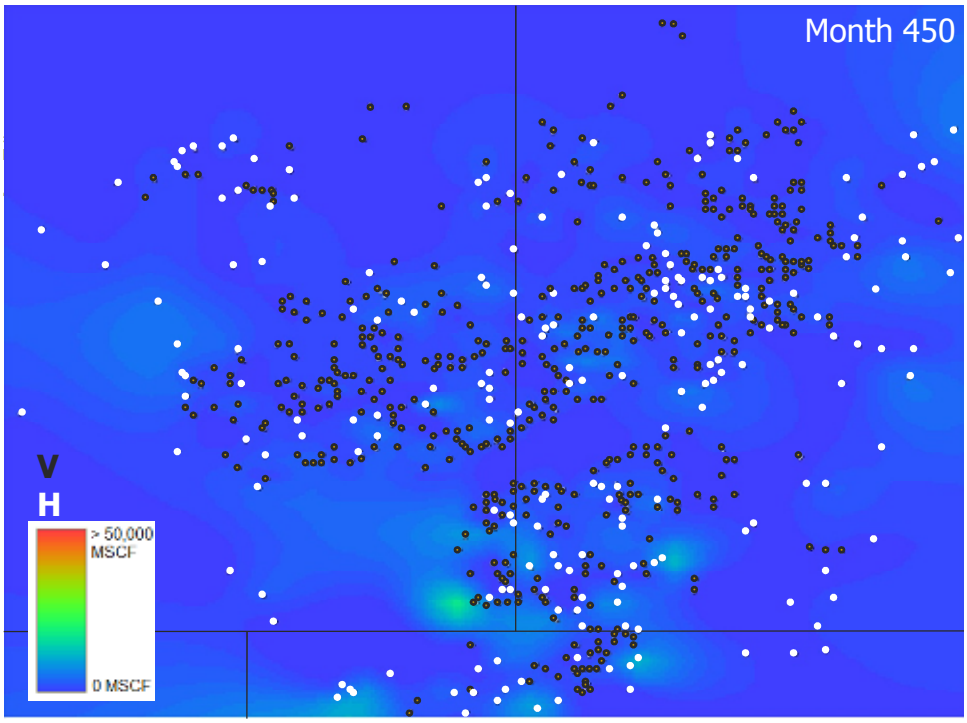

Fig. A-23: 450th month decline map of the current AOI.

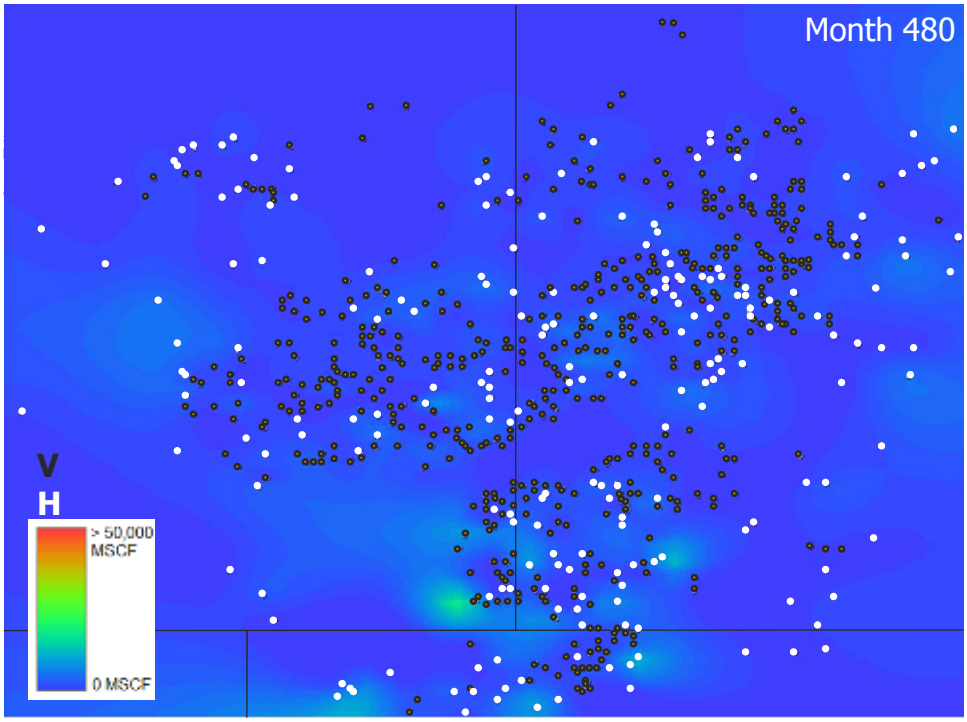

Fig. A-24: 480th month decline map of the current AOI.

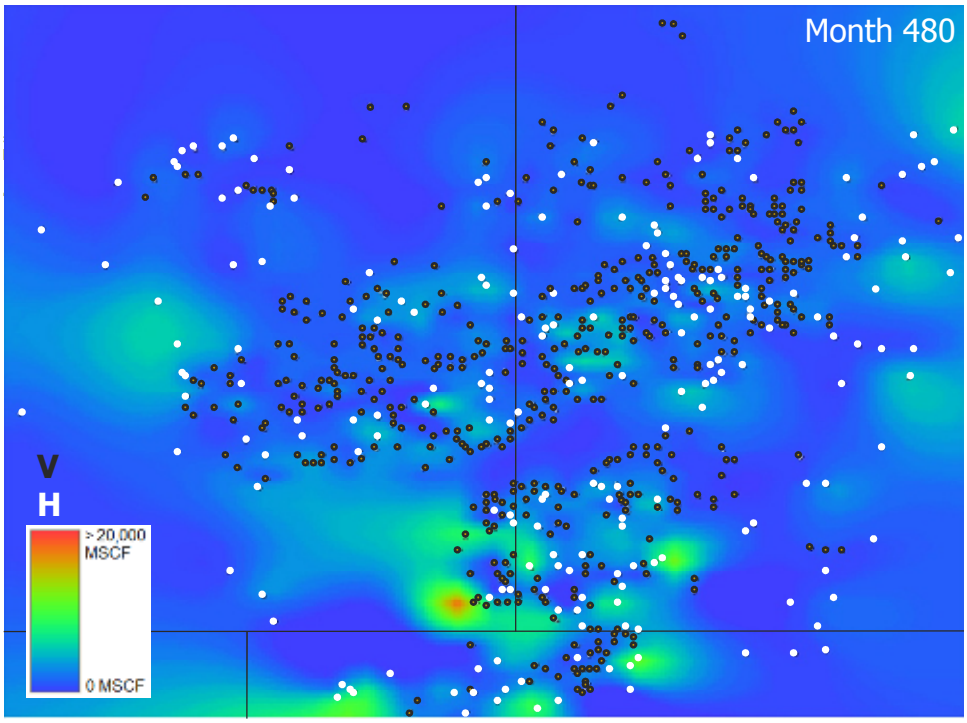

Fig. A-25: 480th month decline map of the current AOI (shifted scale).

VITA

NAME: Ibrahim S. Alkassim

PERMANENT ADDRESS: Saudi Aramco
P.O.Box, 10520
Dhahran, 31311
Saudi Arabia

EDUCATION: B.S., Geology
University of New Orleans,
New Orleans, Louisiana
May, 2005

M.S., Petroleum Engineering
Texas A&M University, August 2009